

AMERICAN UNIVERSITY OF BEIRUT

ASSESSMENT OF COMMON PERSULFATE ACTIVATION
TECHNIQUES FOR THE DEGRADATION OF THEOPHYLLINE
DRUG IN PHARMACEUTICAL PRODUCTION PLANT
WASTEWATER

by
SUHA ADNAN AL HAKIM

A thesis
submitted in partial fulfillment of the requirements
for the degree of Master of Science
to the Department of Chemistry
of the Faculty of Arts and Sciences
at the American University of Beirut

Beirut, Lebanon
September 2019


AMERICAN UNIVERSITY OF BEIRUT

ASSESSMENT OF COMMON PERSULFATE ACTIVATION
TECHNIQUES FOR THE DEGRADATION OF THEOPHYLLINE
DRUG IN PHARMACEUTICAL PRODUCTION PLANT
WASTEWATER

by
SUHA ADNAN AL HAKIM

Approved by:

Dr. Antoine Ghauch, Professor
Department of Chemistry



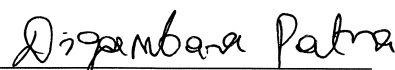
Advisor

Dr. Tarek Ghaddar, Professor
Department of Chemistry



Member of Committee

Dr. Digambara Patra, Professor
Department of Chemistry



Member of Committee

September 5, 2019

ACKNOWLEDGMENTS

I would like to sincerely thank my thesis supervisor and mentor Dr. Antoine Ghauch for his thorough guidance and help. I am also grateful to the members of my thesis committee: Dr. Tarek Ghaddar and Dr. Digambara Patra for their helpful feedback. Also, I would like to thank the staff of the KAS CRSL for their assistance in utilizing the instruments. I would like to extend my gratitude to the academic and nonacademic staff of the Chemistry Department for their support. My research would have been impossible without the aid and support of members of the water treatment lab: Abbas, Sali, Nagham, Maya, Rime, Omar and Zahraa. Finally, I would like to thank my family and friends for their support.

AN ABSTRACT OF THE THESIS OF

Suha Adnan Al Hakim for

Master of Science

Major: Chemistry

Title: Assessment of Common Persulfate Activation Techniques for the Degradation of Theophylline Drug in Pharmaceutical Production Plant Wastewater

Oxidative degradation of emerging waterborne contaminants, particularly pharmaceuticals, by AOPs has gained a major interest in the past decade. The aim of this work was to assess the degradation of theophylline (TP), which is a pharmaceutical, utilizing persulfate (PS) activated by UV₂₅₄, thermally and chemically. The latter two activation techniques were studied both separately and combined. Additionally, TP was eliminated from a simulated and a real industrial effluent.

In the first part of this work UV₂₅₄/PS system was studied for TP degradation. Results showed that TP is strongly resistant to degradation through direct photolysis under UV₂₅₄ irradiation. Effect of [PS]₀ was tested where a positive correlation between [PS]₀ and degradation rate was observed. A [PS]₀ = 0.25 mM achieved total degradation of [TP]₀ = 10 mg L⁻¹ in a period of 20 min with $k_{\text{obs}} = 0.173 (\pm 0.004) \text{ min}^{-1}$, where pseudo-first order reaction kinetics was obtained. To test the effect of different matrix parameters on TP degradation, the pH of the solution, concentrations of chlorides and bicarbonates in addition to dissolved oxygen were varied and tested. Results showed that neutral pH gave the highest improvement in the degradation rate ($k_{\text{obs}} = 0.40 (\pm 0.03) \text{ min}^{-1}$), while chlorides and bicarbonates showed minimal impact, and anoxic conditions hindered TP degradation. Additionally, since pharmaceutical factory effluents can be mixed with different natural water matrices, TP was spiked into natural spring, sea and waste water. The three tested water matrices showed a decrease in the degradation rate, with the waste water causing most significant inhibition ($k_{\text{obs}} = 6.9 (\pm 0.9) \times 10^{-3} \text{ min}^{-1}$). Radical scavenging experiments showed that sulfate radicals had the main contribution in TP degradation. To further test the applicability of the UV₂₅₄/PS system, waste water effluent was obtained from a local pharmaceutical manufacturing facility containing [TP]₀ = 160 mg L⁻¹. Total TP degradation was achieved in the effluent solution over 3 h utilizing [PS]₀ = 25 mM. Reaction stoichiometric efficiency was calculated to be 3.7%.

In the second part of this work Fe²⁺/heat/PS system was studied for TP degradation. Degradation was tested first in heat/PS system and resulted in 60% degradation at t = 60 min for [PS]₀ = 5 mM and T = 60°C. Second, Fe²⁺/PS system was tested at room

temperature and showed minimal effectivity. As a result, the two activation methods were combined into Fe²⁺/heat/PS system. The combination of the two activation methods improved oxidation efficiency, where complete TP degradation was obtained within 60 min for [PS]₀ = [Fe²⁺]₀ = 2 mM at T = 60°C. The reaction followed a pseudo-first order reaction rate with k_{obs} = 7.7 (±0.1) 10⁻² min⁻¹. [PS]₀: [Fe²⁺]₀ ratio was optimized where 1:1 ratio gave best results. Effect of temperature and [PS]₀ were tested where both showed positive correlation with degradation rate. Chlorides present in the reaction medium caused inhibition of the degradation process while nitrates showed a slight enhancing effect. TP was dissolved in natural spring, sea and waste water matrices, where slower degradation rate compared to that in DI water medium was obtained. The waste water matrix caused the greatest inhibition (k_{obs} = 2.6 (±0.6) x 10⁻⁴ min⁻¹). The Fe²⁺/heat/PS system was applied to the same factory effluent containing [TP]₀ = 160 mg L⁻¹. Effective and full TP degradation was obtained within 120 min with the system operating at 60°C and with [PS]₀ = [Fe²⁺]₀ = 50 mM.

Keywords: AOPs, Persulfate, Theophylline, UV-254 nm, Chemical activation, Heat, Water treatment

CONTENTS

ACKNOWLEDGMENTS	V
ABSTRACT	VI
CHAPTER I INTRODUCTION	1
A. Emerging Water Contaminants.....	1
B. Advanced Oxidation Processes	2
C. Theophylline as a Target Molecule.....	3
D. Purpose.....	5
CHAPTER II THEOPHYLLINE DEGRADATION BY UV ₂₅₄ ACTIVATED PERSULFATE.....	10
CHAPTER III THEOPHYLLINE DEGRADATION BY THERMALLY AND CHEMICALLY ACTIVATED PERSULFATE	41
CHAPTER IV CONCLUSION	67

CHAPTER I INTRODUCTION

A. Emerging Water Contaminants

The increase in human population in addition to the increase in consumption of various products and utilities accompanied by the advancement of the lifestyle has raised alarms concerning the quality of water, air and soil. Water contamination by various emerging and unregulated products has caused a major concern in the scientific community over the last two decades [1,2]. This increased attention for water contamination is aided by the advanced methods used for trace detection of pharmaceuticals and other organic contaminants in water, such as the advanced mass spectrometry (MS) coupled to high performance chromatographic techniques [3].

Pharmaceuticals and personal care products (PPCPs) are a group of compounds that gained a great interest in the scientific community. PPCPs include a variety of organic groups, such as hormones, antibiotics, antimicrobial agents, in addition to fragrances, cosmetics, sun-screen agents, etc. [4,5]. PPCPs constitute a major concern due to their potential effect on the human health and the environment. Accordingly, PPCPs are considered as emerging contaminants [5].

Water pollution by PPCPs occurs through several routes. A major cause of water pollution by PPCPs is the release of sewage water, where it is released untreated or treated using conventional methods that are not efficient in their removal [6]. PPCPs were detected in waste water in several regions around the world [7–9]. Another important reason is the release of untreated factory effluent into the environment, as effluents from

pharmaceutical production plants that could contain several pharmaceutical active ingredients. Additionally, the direct disposal of several drugs and personal care products into the environment contributes to the latter's contamination [10].

Presence of PPCPs in water, even at trace concentrations, pose an environmental and a health risk. First, there is a risk of bioaccumulation, as the accumulation of lipophilic PPCPs in aquatic organisms, where a study showed that 92 out of 275 drugs found in the environment are potentially bioaccumulative [4,11,12]. Second, the presence of antibiotics in water causes the development of antibiotic resistance, which poses a threat to human and animal health [13]. Additionally, there exists uncertain synergistic/antagonistic effect of long term exposure to mixtures of pharmaceuticals at low concentrations [14].

B. Advanced Oxidation Processes

Due to the mentioned concern on water pollution, water treatment is integrated to treat discharged water from domestic, agricultural and industrial sources. The conventional treatment methods include, but are not limited to, chemical precipitation, carbon absorption, evaporation and ion exchange [15]. It has been shown that conventional methods do not treat PPCPs efficiently, and PPCPs are consequently resistant to such treatments [16–18]. This necessitates the development and application of novel treatment methods effective in degrading PPCPs.

Advanced Oxidation Processes (AOPs) are novel techniques that have proved their efficiency in the treatment of various organic contaminants. AOPs generally work by the generation of powerful reactive oxidative species (ROS) such as hydroxyl,

hydroperoxyl, sulfate and superoxide radicals which have high redox potentials and act to degrade the contaminant in question [19]. AOPs can be divided into four main categories as follows [20]:

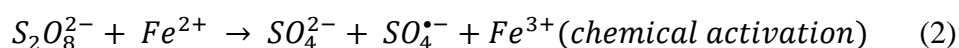
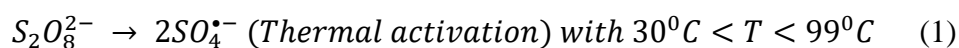
i. Chemical-based AOPs including the use of chemical reagents solely. An example is the Fenton process which is the oldest AOP method. Fenton utilizes iron(III) salt in addition to hydrogen peroxide (H₂O₂).

ii. Photochemical-based AOPs requiring the use of a light source such as the use of UV or solar light and is generally coupled to oxidants.

iii. Sonochemical-based AOPs demanding the use of ultrasounds and usually coupled to the use of oxidants.

iv. Electrochemical-based AOPs utilizing electrochemistry to generate hydroxyl radicals.

One of the recent technologies of AOPs is the use of activated Persulfate (PS). PS shows an advantage over peroxide, since it is more stable. PS was proved to be efficient in degrading several categories of organic contaminants. PS can be activated thermally [21–24], chemically [25,26], by UV [27,28], or through a combination of activation techniques to generate highly reactive sulfate radicals (SRs) species (Eq. 1-3) [25,27–30].



C. Theophylline as a Target Molecule

Theophylline (TP) is one of the drugs that is largely consumed and disposed into the environment. TP is a xanthine, similar in structure to caffeine and theobromine, and used in the treatment of lung diseases such as asthma, shortness of breath and wheezing [31]. TP is found in a normal diet such as in tea and in cacao beans in trace amounts [32,33].

TP enters the environment through several routes. First, the discharge of untreated waste water effluents from pharmaceutical production plants can contain TP. Second, domestic waste water might contain TP from urine excretion due to consumption of pharmaceuticals and natural compounds [10,34]. Additionally, TP could be directly disposed into the environment as by throwing away TP-containing drugs. Unfortunately, TP was detected in spring water in Lebanon, which is possibly due to the release of untreated municipal waste water and industrial effluents [35].

In the past decade, several methods were tested on TP degradation. Liang et al. [36] studied Pd@MIL-100(Fe), a metal organic framework, for visible light ($\lambda \geq 420$ nm) driven photodegradation of TP and other PPCPs, with H₂O₂ added to reaction mixture to achieve full degradation. On the other hand Kim Ilho et al. [37,38] used UV and UV/H₂O₂ systems to study the degradation of TP in a mixture of 30 PPCPs. The former system showed that TP was highly resistant to UV and was classified as slowly-degrading compared to other studied PPCPs. With initial [H₂O₂] of 8.2 mg L⁻¹ in a medium of pure water, UV/H₂O₂ system resulted in a pseudo first order reaction for TP degradation with $k_{\text{obs}} = 1.7 \times 10^{-3} \text{ s}^{-1}$ at 20 °C and pH 7. Also, M. M. Sunil Paul et. al. worked on UV/H₂O₂ system to assess kinetics and by-products of TP oxidation by hydroxide radicals utilizing high resolution mass spectrometric analysis [39]. They concluded that the studied

compound is vulnerable against oxidizing radicals and demonstrated two reaction pathways induced by hydrogen addition and hydrogen abstraction. Additionally, a UV/TiO₂ system [40], as well as a ferrate system [41] were tested.

D. Purpose

PS-based AOPs showed great effectivity in degrading pharmaceuticals, but, to our knowledge, was not tested for TP degradation. Accordingly, a set of experiments were designed and applied to study the degradation of TP in simulated effluents and in a real highly charged industrial waste from a local pharmaceutical factory. Activation of PS was tested using UV-254 nm, thermally, and chemically, where the latter two techniques were tested separately as well as combined. Several parameters were assessed in both systems of UV activated PS as well as combined chemically and thermally activated PS. This allowed the optimization of the degradation process in both systems yielding full TP degradation at an affordable cost. It was shown that UV activated PS system is of lower cost, performs better at neutral pH and is resistant to quenching by chlorides. However, the combined chemical and thermal system is optimum at acidic pH and in media of low chloride content.

Bibliography

- [1] K. Noguera-Oviedo, D.S. Aga, Lessons learned from more than two decades of research on emerging contaminants in the environment, *J. Hazard. Mater.* 316 (2016) 242–251. doi:<http://dx.doi.org/10.1016/j.jhazmat.2016.04.058>.
- [2] R. Hirsch, T. Ternes, K. Haberer, K.-L. Kratz, Occurrence of antibiotics in the aquatic environment, *Sci. Total Environ.* 225 (1999) 109–118. doi:[http://dx.doi.org/10.1016/S0048-9697\(98\)00337-4](http://dx.doi.org/10.1016/S0048-9697(98)00337-4).
- [3] W.W. Buchberger, Current approaches to trace analysis of pharmaceuticals and personal care products in the environment, *J. Chromatogr. A.* 1218 (2011) 603–618. doi:<http://dx.doi.org/10.1016/j.chroma.2010.10.040>.
- [4] J.B. Ellis, Pharmaceutical and personal care products (PPCPs) in urban receiving waters, *Environ. Pollut.* 144 (2006) 184–189. doi:<https://doi.org/10.1016/j.envpol.2005.12.018>.
- [5] J.-L. Liu, M.-H. Wong, Pharmaceuticals and personal care products (PPCPs): A review on environmental contamination in China, *Environ. Int.* 59 (2013) 208–224. doi:<https://doi.org/10.1016/j.envint.2013.06.012>.
- [6] C.G. Daughton, T.A. Ternes, Pharmaceuticals and personal care products in the environment: agents of subtle change?, *Environ. Health Perspect.* 107 (1999) 907–938. doi:10.1289/ehp.99107s6907.
- [7] N. Nakada, T. Tanishima, H. Shinohara, K. Kiri, H. Takada, Pharmaceutical chemicals and endocrine disruptors in municipal wastewater in Tokyo and their removal during activated sludge treatment, *Water Res.* 40 (2006) 3297–3303. doi:<https://doi.org/10.1016/j.watres.2006.06.039>.
- [8] D. Ashton, M. Hilton, K. V Thomas, Investigating the environmental transport of human pharmaceuticals to streams in the United Kingdom, *Sci. Total Environ.* 333 (2004) 167–184. doi:<https://doi.org/10.1016/j.scitotenv.2004.04.062>.
- [9] G.R. Boyd, J.M. Palmeri, S. Zhang, D.A. Grimm, Pharmaceuticals and personal care products (PPCPs) and endocrine disrupting chemicals (EDCs) in stormwater canals and Bayou St. John in New Orleans, Louisiana, USA, *Sci. Total Environ.* 333 (2004) 137–148. doi:<https://doi.org/10.1016/j.scitotenv.2004.03.018>.
- [10] T. Heberer, Occurrence, fate, and removal of pharmaceutical residues in the aquatic environment: a review of recent research data, *Toxicol. Lett.* 131 (2002) 5–17. doi:[http://dx.doi.org/10.1016/S0378-4274\(02\)00041-3](http://dx.doi.org/10.1016/S0378-4274(02)00041-3).
- [11] A. Wennmalm, S.C. Council, Pharmaceuticals : Environmental Effects, in: *Environ. Heal.*, 2011: pp. 462–471. doi:<http://dx.doi.org/10.1016/B978-0-444-52272-6.00714-5>.
- [12] A. Zenker, M.R. Cicero, F. Prestinaci, P. Bottoni, M. Carere, Bioaccumulation and biomagnification potential of pharmaceuticals with a focus to the aquatic environment, *J. Environ. Manage.* (2014). doi:10.1016/j.jenvman.2013.12.017.
- [13] T.U. Berendonk, C.M. Manaia, C. Merlin, D. Fatta-Kassinos, E. Cytryn, F. Walsh, H. Bürgmann, H. Sørum, M. Norström, M.N. Pons, N. Kreuzinger, P. Huovinen, S. Stefani, T. Schwartz, V. Kisand, F. Baquero, J.L. Martinez, Tackling antibiotic resistance: The environmental framework, *Nat. Rev. Microbiol.* (2015). doi:10.1038/nrmicro3439.

- [14] O.A. Jones, J.N. Lester, N. Voulvoulis, Pharmaceuticals: A threat to drinking water?, *Trends Biotechnol.* (2005). doi:10.1016/j.tibtech.2005.02.001.
- [15] P. Rajasulochana, V. Preethy, Comparison on efficiency of various techniques in treatment of waste and sewage water – A comprehensive review, *Resour. Technol.* 2 (2016) 175–184. doi:10.1016/j.reffit.2016.09.004.
- [16] Y. Luo, W. Guo, H.H. Ngo, L.D. Nghiem, F.I. Hai, J. Zhang, S. Liang, X.C. Wang, A review on the occurrence of micropollutants in the aquatic environment and their fate and removal during wastewater treatment, *Sci. Total Environ.* 473–474 (2014) 619–641. doi:10.1016/j.scitotenv.2013.12.065.
- [17] Y. Yang, Y.S. Ok, K.-H. Kim, E.E. Kwon, Y.F. Tsang, Occurrences and removal of pharmaceuticals and personal care products (PPCPs) in drinking water and water/sewage treatment plants: A review, *Sci. Total Environ.* 596–597 (2017) 303–320. doi:https://doi.org/10.1016/j.scitotenv.2017.04.102.
- [18] S.A. Snyder, Occurrence, treatment, and toxicological relevance of EDCs and pharmaceuticals in water, in: *Ozone Sci. Eng.*, 2008: pp. 65–69. doi:10.1080/01919510701799278.
- [19] D.A. Armstrong, R.E. Huie, S. Lyman, W.H. Koppenol, G. Merényi, P. Neta, D.M. Stanbury, S. Steenken, P. Wardman, Standard electrode potentials involving radicals in aqueous solution: Inorganic radicals, *Bioinorg. React. Mech.* (2013). doi:10.1515/irm-2013-0005.
- [20] M.A. Oturan, J.-J. Aaron, Advanced Oxidation Processes in Water/Wastewater Treatment: Principles and Applications. A Review, *Crit. Rev. Environ. Sci. Technol.* 44 (2014) 2577–2641. doi:10.1080/10643389.2013.829765.
- [21] A. Ghauch, A.M. Tuqan, N. Kibbi, Naproxen abatement by thermally activated persulfate in aqueous systems, *Chem. Eng. J.* 279 (2015) 861–873. doi:10.1016/j.cej.2015.05.067.
- [22] A. Ghauch, A.M. Tuqan, N. Kibbi, S. Geryes, Methylene blue discoloration by heated persulfate in aqueous solution, *Chem. Eng. J.* 213 (2012) 259–271. doi:http://dx.doi.org/10.1016/j.cej.2012.09.122.
- [23] A. Ghauch, A.M. Tuqan, N. Kibbi, Ibuprofen removal by heated persulfate in aqueous solution: A kinetics study, *Chem. Eng. J.* 197 (2012) 483–492. doi:10.1016/j.cej.2012.05.051.
- [24] A. Ghauch, A.M. Tuqan, Oxidation of bisoprolol in heated persulfate/H₂O systems: Kinetics and products, *Chem. Eng. J.* (2012). doi:10.1016/j.cej.2011.12.048.
- [25] S. Naim, A. Ghauch, Ranitidine abatement in chemically activated persulfate systems: Assessment of industrial iron waste for sustainable applications, *Chem. Eng. J.* (2016). doi:10.1016/j.cej.2015.11.101.
- [26] A. Ghauch, G. Ayoub, S. Naim, Degradation of sulfamethoxazole by persulfate assisted micrometric Fe⁰ in aqueous solution, *Chem. Eng. J.* (2013). doi:10.1016/j.cej.2013.05.045.
- [27] A. Ghauch, A. Baalbaki, M. Amasha, R. El Asmar, O. Tantawi, R. El Asmar, O. Tantawi, Contribution of persulfate in UV-254 nm activated systems for complete degradation of chloramphenicol antibiotic in water, *Chem. Eng. J.* 317 (2017) 1012–1025. doi:10.1016/j.cej.2017.02.133.

- [28] M. Amasha, A. Baalbaki, S. Al Hakim, R. El Asmar, A. Ghauch, Degradation of a Toxic Molecule o-Toluidine in Industrial Effluents using UV254/PS System, *J. Adv. Oxid. Technol.* 21 (n.d.) 261–273.
<https://www.ingentaconnect.com/content/sycamore/jaot/2018/00000021/00000001/art00023>.
- [29] M. Amasha, A. Baalbaki, A. Ghauch, A comparative study of the common persulfate activation techniques for the complete degradation of an NSAID: The case of ketoprofen, *Chem. Eng. J.* 350 (2018) 395–410.
 doi:<https://doi.org/10.1016/j.cej.2018.05.118>.
- [30] G. Mark, M.N. Schuchmann, H.P. Schuchmann, C. von Sonntag, The photolysis of potassium peroxodisulphate in aqueous solution in the presence of tert-butanol: a simple actinometer for 254 nm radiation, *J. Photochem. Photobiol. A Chem.* (1990). doi:10.1016/1010-6030(90)80028-V.
- [31] I. American Society of Health-System Pharmacists, Theophylline, (2017).
<https://medlineplus.gov/druginfo/meds/a681006.html>.
- [32] C.A. Shively, S.M. Tarka, Methylxanthine composition and consumption patterns of cocoa and chocolate products, *Prog. Clin. Biol. Res.* 158 (1984) 149–178. <http://europepmc.org/abstract/MED/6396642>.
- [33] D.D. Tang-Liu, R.L. Williams, S. Riegelman, Disposition of caffeine and its metabolites in man., *J. Pharmacol. Exp. Ther.* 224 (1983) 180–185.
<http://jpet.aspetjournals.org/content/224/1/180>.
- [34] M.E. Rybak, M.R. Sternberg, C.-I. Pao, N. Ahluwalia, C.M. Pfeiffer, Urine excretion of caffeine and select caffeine metabolites is common in the US population and associated with caffeine intake, *J. Nutr.* 145 (2015) 766–774.
- [35] J. DOUMMAR, K. NÖDLER, T. GEYER, M. SAUTER, Assessment and Analysis of Micropollutants (2010-2011), n.d.
- [36] R. Liang, S. Luo, F. Jing, L. Shen, N. Qin, L. Wu, A simple strategy for fabrication of Pd@MIL-100(Fe) nanocomposite as a visible-light-driven photocatalyst for the treatment of pharmaceuticals and personal care products (PPCPs), *Appl. Catal. B Environ.* 176–177 (2015) 240–248.
 doi:10.1016/j.apcatb.2015.04.009.
- [37] I. Kim, N. Yamashita, H. Tanaka, Photodegradation of pharmaceuticals and personal care products during UV and UV/H₂O₂ treatments, *Chemosphere.* 77 (2009) 518–525. doi:<https://doi.org/10.1016/j.chemosphere.2009.07.041>.
- [38] I. Kim, H. Tanaka, Photodegradation characteristics of PPCPs in water with UV treatment, *Environ. Int.* 35 (2009) 793–802.
 doi:<https://doi.org/10.1016/j.envint.2009.01.003>.
- [39] M.M. Sunil Paul, U.K. Aravind, G. Pramod, A. Saha, C.T. Aravindakumar, Hydroxyl radical induced oxidation of theophylline in water: a kinetic and mechanistic study, *Org. Biomol. Chem.* 12 (2014) 5611–5620.
 doi:10.1039/C4OB00102H.
- [40] R. Liang, A. Hu, W. Li, Y.N. Zhou, Enhanced degradation of persistent pharmaceuticals found in wastewater treatment effluents using TiO₂ nanobelt photocatalysts, *J. Nanoparticle Res.* 15 (2013) 1990. doi:10.1007/s11051-013-1990-x.

- [41] S. Sun, J. Jiang, S. Pang, J. Ma, M. Xue, J. Li, Y. Liu, Y. Yuan, Oxidation of theophylline by Ferrate (VI) and formation of disinfection byproducts during subsequent chlorination, *Sep. Purif. Technol.* 201 (2018) 283–290.
doi:<https://doi.org/10.1016/j.seppur.2018.03.014>.

CHAPTER II

THEOPHYLLINE DEGRADATION BY UV_{254} ACTIVATED PERSULFATE

Since PS showed promising results in the treatment of pharmaceuticals in water effluents, it was chosen as an oxidant to treat TP in a simulated and real pharmaceutical effluent solution. UV_{254} in a batch setup integrating commercial disinfection lamps was used to activate PS. A thorough study was conducted including the effect of $[PS]_0$ and several matrix parameters. The UV/PS system was applied to treat a real pharmaceutical effluent solution containing a high [TP].

Results of this project are presented below in the form of a research paper published in Chemical Engineering Journal (Volume 380, 15 January 2020).



Degradation of theophylline in a UV₂₅₄/PS system: Matrix effect and application to a factory effluent



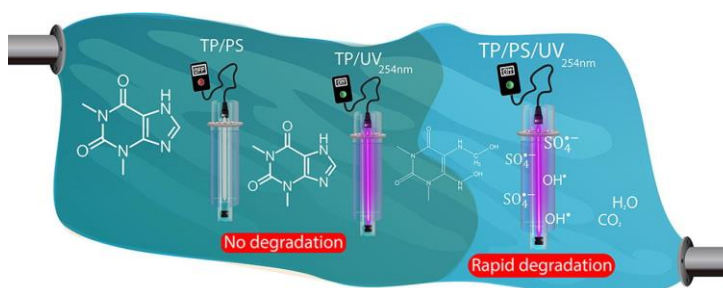
Suha Al Hakim, Saly Jaber, Nagham Zein Eddine, Abbas Baalbaki, Antoine Ghauch*

American University of Beirut, Faculty of Arts and Sciences, Department of Chemistry, P.O. Box 11-0236 Riad El Solh, 1107-2020 Beirut, Lebanon

HIGHLIGHTS

- UV₂₅₄/PS system fully degraded Theophylline (TP) in an aqueous medium.
- Neutral pH was optimum for TP degradation.
- Chlorides and bicarbonates had low impact on TP degradation.
- UV₂₅₄/PS system totally degraded TP in a concentrated pharmaceutical effluent.
- Pharmaceutical excipients showed slight effect on TP degradation process.

GRAPHICAL ABSTRACT



ARTICLE INFO

Keywords:

AOPs
Persulfate
Theophylline
UV-254 nm
Pharmaceutical effluent treatment

ABSTRACT

Oxidative degradation of emerging waterborne contaminants, particularly pharmaceuticals, is currently an extensively studied field of research. In this study, a UV-254 nm activated persulfate (PS) system (UV₂₅₄/PS) was used to eliminate Theophylline (TP) from simulated and real industrial effluents. Results showed that TP is strongly resistant to degradation through direct photolysis under UV-254 nm irradiation. UV₂₅₄/PS system showed efficient degradation, in which [PS]₀ = 0.25 mM achieved total degradation of [TP]₀ = 10 mg L⁻¹ in a period of 20 min and followed a pseudo-first order reaction kinetics ($k_{\text{obs}} = 0.173 (\pm 0.004) \text{ min}^{-1}$). Effect of several matrix parameters were tested to study the robustness of TP degradation in real-life cases such as pH, chlorides, bicarbonates, and dissolved oxygen, in which neutral pH gave the highest degradation rate ($k_{\text{obs}} = 0.40 (\pm 0.03) \text{ min}^{-1}$), chlorides and bicarbonates showed minimal impact, and anoxic conditions inhibited TP degradation with a significant decrease in k_{obs} , e.g. $0.817 (\pm 0.41) \times 10^{-1} \text{ min}^{-1}$. Additionally, TP was spiked into natural spring, sea and wastewater, where the three tested matrices showed a decrease in the degradation rate, with the latter being the most significant ($k_{\text{obs}} = 6.9 (\pm 0.9) \times 10^{-3} \text{ min}^{-1}$). Radical scavenging experiments showed that sulfate radicals were the main contributors in TP degradation. Furthermore, wastewater effluent obtained from a local pharmaceutical manufacturing facility and containing [TP]₀ = 160 mg L⁻¹ was also tested and showed successful full degradation over 3 h in 25 mM PS-spiked medium with an average reaction stoichiometric efficiency of about 3.7% and at an estimated cost of 17.2 \$ m⁻³.

1. Introduction

Environmental contamination by pharmaceuticals and personal care

products (PPCPs) has raised a major concern among the scientific community over the last two decades [1,2]. This is mainly due to the advancements in analytical chemistry techniques which allowed

* Corresponding author.

E-mail address: antoine.ghauch@aub.edu.lb (A. Ghauch).

<https://doi.org/10.1016/j.cej.2019.122478>

Received 31 March 2019; Received in revised form 8 August 2019; Accepted 9 August 2019

Available online 12 August 2019

1385-8947/ © 2019 Elsevier B.V. All rights reserved.

scientists to discover the presence of PPCPs at previously undetectable concentrations in surface and ground water around the world [3]. One of the drugs largely consumed and disposed into the environment is Theophylline (TP), a xanthine used in the treatment of lung diseases such as asthma, shortness of breath and wheezing [4]. TP is similar in structure to caffeine and theobromine and found in a normal diet as in tea and cacao beans in trace amounts [5,6]. Routes of TP entry into the environment include the discharge of untreated wastewater effluents from pharmaceutical production plants and domestic wastewater; where the latter contains TP from urine excretion due to consumption of pharmaceuticals and natural compounds, as well as direct disposal of TP-containing drugs [7,8]. TP was detected in spring water in Lebanon, possibly due to the release of untreated municipal wastewater and industrial effluents [9]. The presence of TP in nature increases concern of bioaccumulation which could result in undesirable health effects to humans and various animals, where it has been found that TP is moderately toxic to mammals ($LD_{50} > 200 \text{ mg kg}^{-1}$) [10,11]. It is estimated that over 80% of the global wastewater is released to the environment without any prior treatment [12]. This factor, in addition to the resistance of PPCPs to conventional wastewater treatment methods [13] raises a great concern regarding the safety of natural aquatic systems.

Advanced Oxidation Processes (AOPs) have shown efficiency in the treatment of organic compounds. During the past decade, several research groups studied the degradation of TP using different methods. For instance, TP degradation was studied using Pd@MIL-100(Fe), a metal organic framework, for visible light ($\lambda \geq 420 \text{ nm}$) driven photodegradation [14]. Another study used UV and UV/H₂O₂ systems to study the degradation of TP in a mixture of 30 PPCPs [15,16]. Additionally, a UV/TiO₂ system [17], as well as a ferrate system [18] were tested for TP degradation.

Persulfate (PS) technology is one of the recent technologies of AOPs. PS can be activated thermally, chemically, by UV, or through a combination of activation techniques to generate highly reactive sulfate radicals ($SO_4^{\cdot-}$) species [19–22].

Of the activation methods, UV-activated PS has shown efficient degradation of several pharmaceuticals [21,23–25], but, to our knowledge, was not tested for TP degradation. Accordingly, a set of experiments were designed and applied to study the degradation of TP in simulated effluents and in a real highly charged industrial waste from a local pharmaceutical factory. Several parameters were assessed so as to optimize the degradation process yielding full TP degradation with an acceptable reaction stoichiometric efficiency (RSE) at an affordable cost.

2. Materials and methods

2.1. Chemicals

Theophylline ($C_7H_8N_4O_2 \geq 99\%$), sodium persulfate (PS) ($Na_2S_2O_8, \geq 99.0\%$), and phosphate buffer (monobasic and dibasic), all used in conducting the degradation experiments, were purchased from Sigma-Aldrich (China, France, and Germany, respectively). Potassium iodide (KI) (puriss, 99.0–100.5%, Switzerland), was used for the quantification of PS in solution. Methanol (CH_4O) of HPLC grade (Germany) was used for the chromatographic elution process as mobile phase in combination with deionized water. Methanol and tertiary butyl alcohol ($C_4H_{10}O$) obtained from Sigma-Aldrich (Germany), were used in the quenching experiments. To assess the ionic additives effect, sodium chloride (NaCl) and sodium bicarbonate ($NaHCO_3$) were purchased from Fluka (Netherlands). Hydrogen Peroxide, used as an oxidant for a comparative study against PS, was obtained from Sigma Aldrich (Germany). Deionized water (DI) was used in the preparation of all solutions used in this work.

2.2. Chemical analyses

2.2.1. TP quantification

To quantify TP, high performance liquid chromatography (HPLC, Agilent 1100 series) equipped with a quaternary pump, a vacuum degasser, an autosampler unit with cooling maintained at 4 °C, and a thermally controlled column compartment set at 30 °C was used. For TP separation from its byproducts and other organic additives, a Discovery® HS C-18 reverse phase column (5 µm; 4.6 mm internal diameter × 250 mm in length) connected to a security guard column HS C-18 (5 µm; 4.0 mm internal diameter 20 mm long) (Pennsylvania, USA) was used. The HPLC was equipped with two detectors placed in series, a diode-array detector (DAD) for the quantification of TP, and an ion-trap mass spectrometry detector (MSD) for the identification of TP's transformation products. The mobile phase consisted of water and methanol (70:30 ratio) kept under isocratic flowrate of 0.5 mL min^{-1} . The injection volume was set at 80 µL. All samples were pre-filtered through a 0.45 µm PTFE 13 mm disc filters (Jaytee Biosciences Ltd., UK). Theophylline retention time (R_t) was observed at 12 min using the abovementioned conditions. TP calibration curve and LINESIT output giving all statistical parameters required to determine the uncertainty on all quantified TP in UV₂₅₄/PS treated samples are summarized in Fig. 1S.

2.2.2. PS quantification

To quantify PS, an in-house validated analytical method developed by Baalbaki et al. [26] was used. The method relied on modifying the configuration of an HPLC unit allowing the formation of I_3^- complex which is detected by the DAD at a wavelength of 352 nm.

2.3. Experimental setup: UV reactors

A bench-scale setup was assembled using 6 low-pressure mercury lamps (LPHgLS) fitted in quartz inserts that are submerged in home-made borosilicate cylinders. These lamps are commercially available and used in principle for water disinfection. The reactors are placed in a water bath connected to a chiller to keep constant the reaction temperature. The reactor is the same as the one used by Amasha et al. [20,21] of our research group. A scheme of the reactor (Fig. 2S) along with its components' origins are further elaborated in text S2 of the supplementary material.

2.4. Experimental procedure

Stock solutions of TP and PS were prepared on a daily basis and mixed with the required volumes of DI and/or matrix solutions in the 400 mL borosilicate reactors. After which the quartz protected LPHgLS were immersed in the reactors. 2 mL samples were then withdrawn at specific time intervals using appropriate syringes and injected through 0.45 µm PTFE 13 mm disc filters into the HPLC vials for analysis. Preparation of the stock solutions, the order of addition of reactants and further details of the experimental procedure are presented in text S3 of the supplementary material.

3. Results and discussion

3.1. UV₂₅₄ exposure effect: PS-free solution vs PS-spiked solution

To test for the possibility of direct and indirect photolysis of TP by LPHgLS, [TP] was monitored under the effect of UV-light, with and without PS addition. Fig. 1 shows that UV-254 nm only had no significant degradation effect on TP, where $\frac{[TP]}{[TP]_0}$ after 60 min of exposure was higher than 88% for all [TP]₀ tested. It can also be noticed that as [TP]₀ increases, the % degradation under UV-254 nm alone decreases reaching, at 60 min of reaction time, 12, 8 and 2% for [TP]₀ = 10, 20

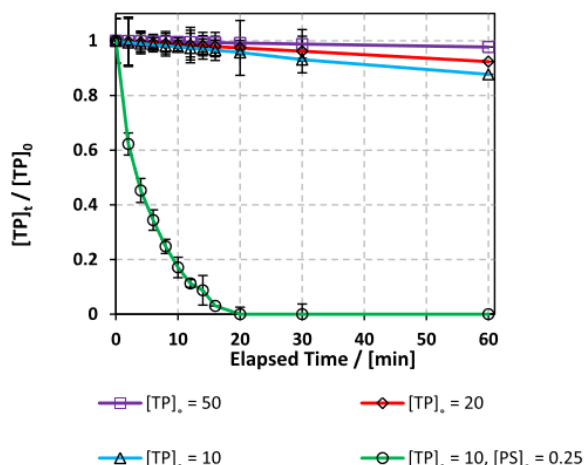


Fig. 1. Effect of UV fluence on TP degradation in PS-free and PS-spiked solutions. Control experiments (upper curves): $[TP]_0 = 50, 20$ and 10 mg L^{-1} in PS-free solutions under UV 254 nm irradiation. The lowest curve represents the time course degradation of TP in PS spiked system under UV 254 nm irradiation ($[TP]_0 = 10 \text{ mg L}^{-1}$ and $[PS]_0 = 0.25 \text{ mM}$). Error bars are calculated as $\frac{ts}{\sqrt{n}}$, where absent bars fall within the symbols.

and 50 mg L^{-1} , respectively. This decrease in the % degradation at higher $[TP]_0$ can be attributed to the inner filter effect, where TP absorption spectrum (Fig. 1Sc) shows that absorption easily occurs at the wavelength emitted by the used LPHGLs mainly 254 nm. Inner filter effect is more prominent at higher $[TP]_0$ where more absorbing molecules are present causing the solution to be less transmissible to UV-254 nm radiation and photon penetration. Inner filter effect was also noticed by Ao et al. (2017) during sulfamethoxazole photolysis [27]. Moreover, Fig. 1 shows that, in the presence of persulfate (0.25 mM) under UV-254 nm irradiation, $[TP]$ ($[TP]_0 = 10 \text{ mg L}^{-1}$) reached a level below the detection limit after only 20 min of reaction. Thus, even though TP absorbs at UV-254 nm, its direct photolysis is not significant, which necessitates the use of oxidizing agents for effective degradation. The study of Pereira et al. (2007) showed that other pharmaceuticals such as naproxen and carbamazepine were resistant, or showed slight degradation, upon direct photolysis using only LPHGLs in oxidants-free solutions [28].

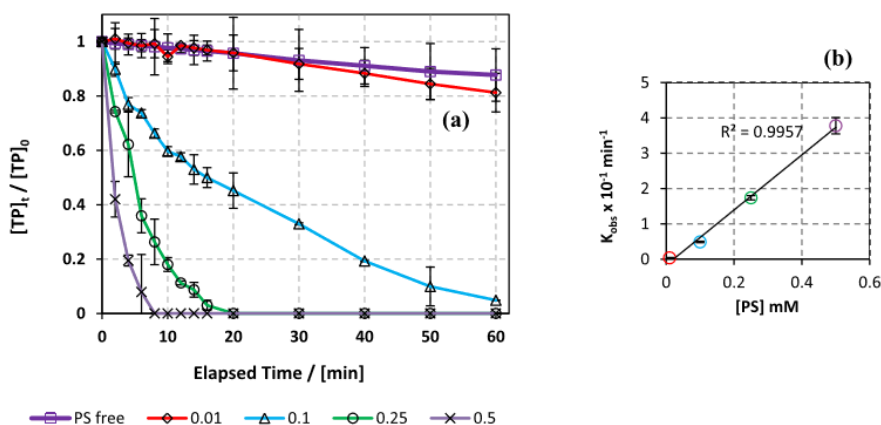


Fig. 2. Degradation of $[TP]_0 = 10 \text{ mg L}^{-1}$ at $[PS]_0 = 0.01\text{--}0.5 \text{ mM}$. (a) Time course showing $\frac{[TP]_t}{[TP]_0}$ variation in UV₂₅₄/PS system. Error bars are calculated as $\frac{ts}{\sqrt{n}}$, where absent bars fall within the symbols. (b) A fitting of k_{obs} obtained for plots of $\ln \frac{[TP]_t}{[TP]_0}$ versus time (min) for tested conditions upon first order fitting versus $[PS]$ showing high correlation ($R^2 = 0.9957$).

3.2. Kinetic study

The rate of degradation of TP was studied at four different $[PS]_0$ (Fig. 2). Pseudo-first-order kinetics model showed good fittings for TP degradation, where R^2 obtained for the plot of $\ln \frac{[TP]_t}{[TP]_0}$ versus time (min) showed good linearity (Table S1). Thus Eq. (1) can be followed, with k_{obs} being the pseudo-first-order rate constant, and t representing time (min). The obtained data showed also that k_{obs} increased linearly with increasing $[PS]_0$ (Fig. 2b), thus k_{obs} is found to be proportional to $[PS]_0$ in the studied range. In fact, pseudo-first order is frequently considered for degradation reactions of organic compounds in PS-activated systems [25,29–31].

$$\ln \frac{[TP]_t}{[TP]_0} = -k_{obs}t \quad (1)$$

3.3. Choice of $[PS]_0$ for control experiment

The initial $[TP]$ tested was 10 mg L^{-1} , which is in the expected range for wastewater effluent of a pharmaceutical production facility after dilution within the factory discharge. However, samples taken from a local plant revealed higher values of $[TP]$ reaching 160 mg L^{-1} (Section 3.9); moreover, sustainable technical practices yielding less water consumption for cleaning reactors are rarely adopted and thus a more diluted effluent is expected. Accordingly, $[PS]_0$ was varied experimentally to reach full TP degradation in a period of 20 min at 0.01, 0.1, 0.25 and 0.5 mM. As it can be noticed from Fig. 2, results showed that as $[PS]_0$ increased the degradation rates increased, and thus the time needed for total TP degradation decreased. One can assume that higher density of $SO_4^{\cdot -}$ is achieved with higher $[PS]_0$ and that without significant radical-radical quenching reactions. For example, at $[PS]_0 = 0.25$ and 0.5 mM, total TP degradation was reached within a range of 20 and 8 min, respectively (Fig. 2a). Accordingly, $[PS]_0 = 0.25 \text{ mM}$ was chosen as an ideal oxidant concentration in order to conduct matrix effect experiments over an acceptable reaction time. In fact, this specific concentration showed rapid degradation of TP and is technically feasible in terms of sample withdrawal and tracking of $[TP]$ as well as $[PS]$ in solution for kinetics study.

3.4. Additives and matrix effects

3.4.1. pH effect

Several studies tested the pH effect on the degradation of various

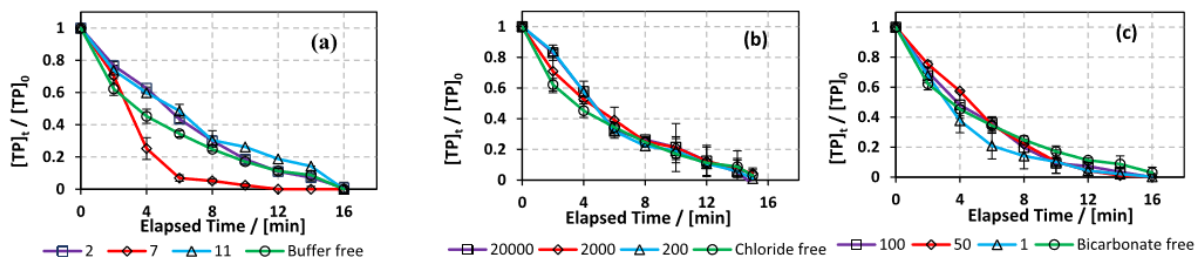


Fig. 3. Degradation of TP under effect of (a) pH, (b) salinity ($[\text{NaCl}] = 0\text{--}20,000 \text{ mg L}^{-1}$), and (c) bicarbonates ($0\text{--}100 \text{ mM}$). Experimental conditions: $[\text{TP}]_0 = 10 \text{ mg L}^{-1}$, $[\text{PS}]_0 = 0.25 \text{ mM}$. Error bars are calculated as $\frac{\sigma}{\sqrt{n}}$, where absent bars fall within the symbols.

organic compounds and diverse results were obtained. It was found that frequently acidic pH conditions improved the degradation rate of the tested pollutants however, improved degradation was also observed at neutral and slightly basic pHs [32].

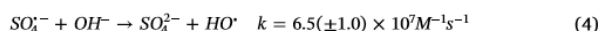
TP degradation was studied in non-buffered and in 10 mM buffered solutions of different pHs imitating extreme cases of acidic, basic as well as neutral conditions (Fig. 3a). For the case of non-buffered (DI) solution, an acidic pH is obtained upon PS addition ($\text{pHi} = 5.4$). The acidification of the medium by PS is very well known and can be explained by Eqs. (2) and (3) [33].



The results obtained, for buffered solutions, showed that pH changes had significant impact on TP degradation. For example, neutral ($\text{pH} = 7$) conditions gave the highest degradation rate constant ($k_{\text{obs}} = 0.40 (\pm 0.03) \text{ min}^{-1}$) compared to buffer-free solutions ($k_{\text{obs}} = 0.173 (\pm 0.004) \text{ min}^{-1}$), whereas acidic ($\text{pH} = 2$) and basic ($\text{pH} = 11$) pH conditions inhibited TP degradation to some extent with $k_{\text{obs}} = 0.19 (\pm 0.01) \text{ min}^{-1}$ and $0.139 (\pm 0.005) \text{ min}^{-1}$, respectively (Table 1). k_{obs} were calculated using pseudo-first order model. Moreover, phosphate species of different concentrations (10 and 20 mM) used for buffering TP solutions showed slight effect on the degradation of TP as reported in Fig. 3S of the supporting information.

The decrease in the rate of the oxidation reaction at $\text{pH} = 11$ compared to that at neutral pH could be attributed to the quenching effect of hydroxide ions (OH^-) on $\text{SO}_4^{\cdot-}$; in fact, at significant alkaline pH, OH^- reacts with $\text{SO}_4^{\cdot-}$ and generates sulfate anion (SO_4^{2-}) (Eq. (4)) [34]. The obtained HO^\cdot is of a shorter lifetime and lower selectivity than that of $\text{SO}_4^{\cdot-}$ which could be contributing to the decrease in the rate constant of TP degradation in a basic medium compared to that in an acidic medium [35]. To further investigate base activation of PS, the same conditions as for the already studied buffers were applied for TP

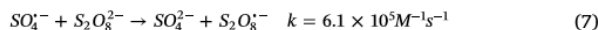
solution at $\text{pH} = 11$, however, in the absence of UV. The results showed that no TP degradation was obtained. Thus, the base activation of PS was not prominent (Fig. 4S).



On the other hand at acidic pH, a rapid transformation of PS into $\text{SO}_4^{\cdot-}$ is favored due to acid catalysis upon formation of HS_2O_8^- which improves TP degradation more than that at basic pH (Eqs. (5) and (6)) [36]. This observation corroborates the results obtained by Ghauch et al. [37] on the degradation of ibuprofen in thermally activated PS systems under acidic conditions.



However, the additional formation of $\text{SO}_4^{\cdot-}$ generates a high concentration of radicals and cause quenching mechanism between $\text{SO}_4^{\cdot-}$ (Eqs. (7) and (8)) [34,38]. Thus, the presence of TP in an acidic medium allows the PS-induced radicals in the medium to be partially quenched.



Additionally, the variance in TP degradation rate in water media of different pH values could be associated with its pKa (8.81) [39]. At the tested acidic $\text{pH} = 2$, protonated TP (TPH^+) is prevalent while at the basic $\text{pH} = 11$, non-protonated TP is the major species. However, at neutral $\text{pH} = 7$ both species are present with $\frac{[\text{TPH}^+]}{[\text{TP}]} \approx 10^{1.81}$, based on the use of the Henderson equation. The presence of both species could result in two different degradation mechanisms simultaneously and thus better degradation kinetics [40]. Therefore, circumneutral pH showed the best pH range to consider for the studied degradation of TP, due to the presence of both HO^\cdot and $\text{SO}_4^{\cdot-}$, and the protonated and non-protonated forms of TP [41].

3.4.2. Chloride effect

Pharmaceutical factory effluent might contain chlorides from different sources. Factories along the coast might domestically use brackish water that could be mixed with the pharmaceutical flushing water before exiting the factory. Additionally, detergents used to clean the factory's reactors as well as some pharmaceutical excipients used might contain chlorides. To test for the applicability of the studied oxidation method on water having different salinity levels (ionic strengths), experiments were conducted under four different matrix conditions simulating conditions of distilled, fresh, brackish and saline water having $[\text{NaCl}]$ of about 0, 200, 2000 and 20000 mg L^{-1} , respectively. These $[\text{NaCl}]$ values were chosen based on Gorrell et al. and on EPA data [42,43]. As it can be noticed from Fig. 3b, the degradation of TP was only slightly affected by NaCl presence. Table 1 showed that k_{obs} changed slightly from $0.173 (\pm 0.004) \text{ min}^{-1}$ at $[\text{NaCl}] = 0 \text{ mg L}^{-1}$ to $0.198 (\pm 0.001) \text{ min}^{-1}$ at $[\text{NaCl}] = 20,000 \text{ mg L}^{-1}$. Hence, it is expected that PS in the presence

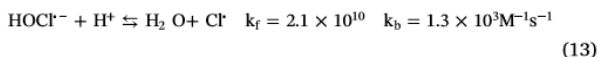
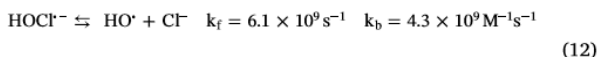
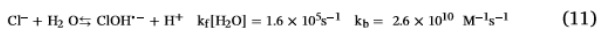
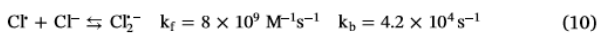
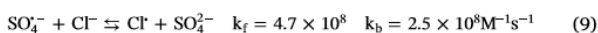
Table 1

Values of pH and the observed degradation rate constants obtained for different matrix conditions. Experimental conditions: $[\text{TP}]_0 = 10 \text{ mg L}^{-1}$ and $[\text{PS}]_0 = 0.25 \text{ mM}$.

Additive	Concentration	(unit)	pHi/pHf	$k_{\text{obs}} \times 10^{-1} (\text{min}^{-1})$
Additive free	–	–	5.4/3.8	1.73 (± 0.04)
Buffer	10	mM	2	1.9 (± 0.1)
			7	4.0 (± 0.3)
			11	1.39 (± 0.05)
NaCl	20,000	mg L^{-1}	4.0/3.5	1.98 (± 0.01)
			4.1/3.6	1.79 (± 0.01)
			4.6/3.6	2.0 (± 0.1)
HCO_3^-	100	mM	8.7/8.4	2.4 (± 0.1)
			8.5/8.2	3.0 (± 0.1)
			7.1/4.3	2.6 (± 0.1)
Methanol	100	mM	6.3/3.7	$5.4 (\pm 0.3) \times 10^{-2}$
			5.4/4.1	$1.5 (\pm 0.1) \times 10^{-1}$

of NaCl be partially consumed upon quenching by Cl^- to form chlorine radical (Cl_2^-) (Eqs. 9–10). At the same time, one can predict that the remaining unquenched SO_4^- radicals along with the formed chlorine radicals were enough to degrade TP in solution at a similar rate close to that of TP degradation experiments carried out in NaCl-free solution.

A quick review on the effect of chlorides on the oxidation reaction in PS-based AOPs systems showed diverse results which varied between, enhancing, inhibiting, and negligible effect, where the effect of Cl^- on the degradation rate depends on its concentration, the probe, and the PS activation mechanism utilized (Table S2) [21,25,30,44–55]. Enhancement of the oxidative degradation reaction rate can be explained by the formation of Cl^\cdot having a redox potential ($E^0 = 2.432 (\pm 0.018)$) close to that of SO_4^- ($E^0 = 2.437 (\pm 0.019)$) [14], in addition to the formation of HO^\cdot (Eqs. (9), (11) and (12)) [56–58]. It is well known that HO^\cdot acts by H^\cdot abstraction, thus providing an enhancement in the oxidation rate for compounds susceptible to such degradation mechanism. Inhibition of the degradation process, however, can be explained mainly by the quenching of SO_4^- by Cl^- producing Cl^\cdot which in turn reacts to produce Cl_2^- of lower redox potential ($E^0 = 2.126 (\pm 0.017)$) [14] than that of SO_4^- (Eqs. (9) and (10)) [56,57]. Additionally, the quenching of HO^\cdot by Cl^- is also expected, where HO^\cdot is more prevalent at basic pH [34,59]. For the case of negligible effect, as in current TP case, Cl^\cdot formed compensates for the lost effectivity of SO_4^- consumed (Eqs. (9)–(13)) [56–58].



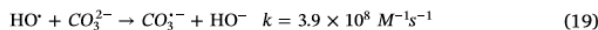
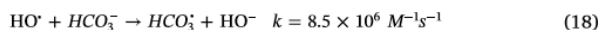
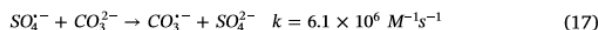
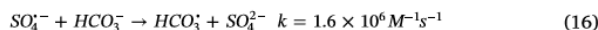
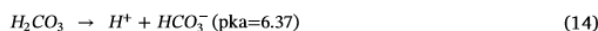
3.4.3. Bicarbonate effect

The effect of NaHCO_3 on TP degradation was also studied at different concentrations: 1, 50 and 100 mM. Addition of NaHCO_3 increased pH_i from 5.6 to a range between 7.1 and 8.7 depending on $[\text{NaHCO}_3]$ in the medium. HCO_3^- added to the solution results in the formation of H_2CO_3 and CO_3^{2-} (Eqs. (14) and (15)) [30]. As it can be noticed (Table 1, Fig. 3c), k_{obs} increased by 50% for the case of 1 mM ($k_{\text{obs}} = 0.26 (\pm 0.01) \text{min}^{-1}$) compared to the control case (bicarbonate-free solution; $k_{\text{obs}} = 0.173 (\pm 0.004) \text{min}^{-1}$). However, this trend is supported until greater concentration of bicarbonate (up to 50 mM) for which an increase of about 74% in k_{obs} is obtained ($0.300 (\pm 0.001) \text{min}^{-1}$). As for bicarbonate concentration close to 100 mM, one can notice a decrease in k_{obs} of about 20% compared to that of 50 mM (e.g. $0.240 (\pm 0.001) \text{min}^{-1}$ vs $0.300 (\pm 0.001) \text{min}^{-1}$). As a result, one can deduce that the improved efficiency of the oxidation reaction of TP is limited to a certain range of bicarbonate concentration mainly between 1.0 and 50 mM.

A mini-review on the effect of bicarbonate on the degradation of different probes in PS-based AOPs systems showed that HCO_3^- may have an enhancing or an inhibiting effect on the degradation of an organic probe (Table S3) [21,25,53,54,30,44,46–51]. Enhancement in the degradation rate of an organic contaminant is generally attributed to the working neutral/basic pH conditions that contribute to the increase in HO^\cdot upon reaction of SO_4^- with HO^- (Eq. (4)) which in its turn enhances the degradation rate of the probe [34].

In the case of TP, an increase in the pH of the solution is noticed with increasing $[\text{NaHCO}_3]$. Section 3.4.1 shows that neutral pH, obtained by using phosphate buffer solution, enhances the degradation reaction ($k_{\text{obs}} = 0.40 (\pm 0.03) \text{min}^{-1}$). However, for the case of neutral pH obtained by adding HCO_3^- (1 mM), lesser improvement in the

degradation reaction rate constant (k_{obs} of $0.26 (\pm 0.01) \text{min}^{-1}$) is obtained. Thus, even though the neutral pH is favored, there is some inhibition caused by bicarbonate species present. This inhibition can be explained by an increase in the ionic strength of the solution yielding SO_4^- quenching mainly by HCO_3^- as well as CO_3^{2-} (Eqs. (16) and (17)), in addition to slower kinetics because of more difficult collision between reactive species in the medium [56]. Also, increasing $[\text{HCO}_3^-]$ and $[\text{CO}_3^{2-}]$ may react to quench HO^\cdot , when present in the medium (Eqs. (18) and (19)) [60,61]. The carbonate radical $\text{CO}_3^{\cdot-}$ produced from quenching of SO_4^- , and possibly HO^\cdot , is of a lower redox potential ($E^0 = 1.57 (\pm 0.03)$) [14], and thus is less potent to oxidize the organic probe. For instance, TP, as well as 17 β -estradiol showed that an increase in $[\text{NaHCO}_3]$ changed its effect on their degradation rate from enhancement to inhibition [44]. This is because the additional increase in the pH would cause the quenching of SO_4^- to outweigh the gain obtained by the formation of HO^\cdot . It is expected that probes more susceptible to H^\cdot abstraction have improved degradation, whereas probes that are mostly susceptible to electron transfer have inhibited degradation upon addition of HCO_3^- . In conclusion, the effect of addition of HCO_3^- is dependent on its concentration, the probe studied, and the pH change in the medium.



3.4.4. Effect of dissolved oxygen

Dissolved oxygen (DO) is a crucial parameter for optimizing degradation processes based on the use of AOPs. In order to address this parameter, similar experiments, as previously described, were performed however in the absence of DO. DO was removed by bubbling the TP solution with nitrogen gas over a period of 1 h. This purge time was enough to consider almost complete DO depletion in the solution as previously reported by Ghauch et al. [33]. The results showed a net decrease in k_{obs} by almost half of its value obtained under oxic conditions e.g. $(0.817 (\pm 0.41) \times 10^{-1} \text{min}^{-1})$ vs $1.73 (\pm 0.04) \times 10^{-1} \text{min}^{-1}$ (Fig. 4). In fact, powerful ROS such as $\text{O}_2^{\cdot-}$ might be formed and contribute greatly to the oxidation of organic compounds toward mineralization [62]. Fig. 5S presents the use of chloroform as a superoxide quencher [63]. Results showed that slower degradation is obtained in the presence of chloroform for the first 6 min after which degradation rate increases possibly due to the generation of chlorine-based active radicals that might contain in addition of chlorine, carbon and hydrogen. Accordingly, these generated chlorine-based radicals are different than chlorine radicals produced from chloride ions in water in terms of chemical reactivity (Section 3.4.2). Thus, $\text{O}_2^{\cdot-}$ is expected to be formed in the $\text{UV}_{254\text{nm}}/\text{PS}$ system studied.

3.5. Case of spring, sea and wastewater

Since pharmaceutical effluents are in general mixed to different water matrices upon their discharge in the surroundings, the effectivity of the degradation process was studied in real water samples. Spring, sea and wastewater samples were taken from 33°44'17.9"N 35°34'12.5"E, 33°54'11.1"N 35°28'44.8"E and 33°54'08.2"N 35°29'05.0"E locations, respectively. These samples were spiked with an appropriate volume of TP and PS stock solutions so as to obtain the following starting concentrations: $[\text{PS}]_0 = 0.25 \text{mM}$ and $[\text{TP}]_0 = 10 \text{mg L}^{-1}$. As it can be noticed from the obtained results

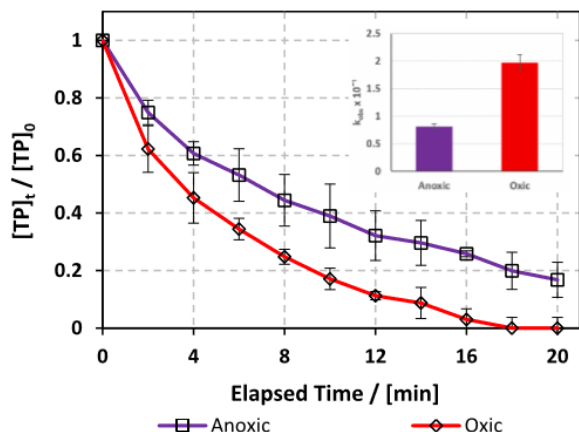


Fig. 4. Effect of the presence of dissolved oxygen on TP degradation in UV₂₅₄/PS system. Anoxic conditions are obtained upon N_{2(g)} bubbling for 20 min. Oxic conditions are obtained without any N₂ bubbling with [DO] = 8 mg L⁻¹ at room temperature. Experimental conditions: [TP]₀ = 10 mg L⁻¹ and [PS]₀ = 0.25 mM. Error bars are calculated as $\frac{t_n}{\sqrt{n}}$, where absent bars fall within the symbols. The inset shows k_{obs} values for anoxic and oxic conditions.

(Fig. 5a,b), TP degradation was hindered in the three water matrices tested, where k_{obs} decreased from $1.73 (\pm 0.04) \times 10^{-1} \text{ min}^{-1}$ in DI matrix to $8.5 (\pm 0.7) \times 10^{-2} \text{ min}^{-1}$, $7.2 (\pm 0.8) \times 10^{-2} \text{ min}^{-1}$, and $6.9 (\pm 0.9) \times 10^{-3} \text{ min}^{-1}$ in sea, spring and wastewater matrices, respectively. k_{obs} was the lowest in the case of wastewater, where total and fecal coliforms, chlorides, sulfates, bicarbonates, chemical oxygen demand (COD) and turbidity were the highest. This decrease in the oxidation rate can be explained by the competing reactions occurring in solution, where PS would react with organic compounds present in the medium leading to a decrease in its concentration and therefore its conversion rate into $\text{SO}_4^{\cdot-}$ participating in the TP oxidative degradation reaction. Another factor that most probably contributed to the decrease in the degradation rate constant of the oxidative reaction is the drop in the penetration capacity of the UV-254 nm rays reaching the entire solution due to increased turbidity. This is in accordance with previous work done on wastewater by Ghauch group on the degradation of chloramphenicol and ketoprofen in similar UV/PS systems, where in both cases, degradation in wastewater had the lowest rate [19,21]. As for sea and spring water, k_{obs} were very close which can be explained by the minor effect of chloride ions as demonstrated in the previous section. One can also notice from Table 2 that TC and TFC decreased in sea water upon treatment due most probably to the use of the UV-254 nm germicidal lamps, in addition to the possible effect of PS oxidation

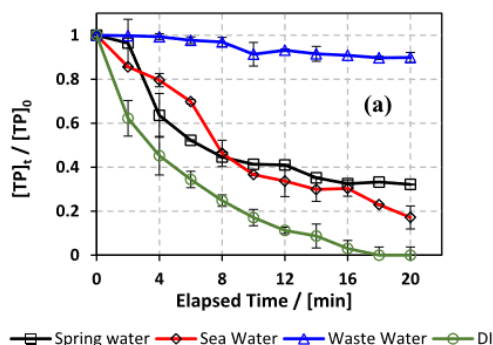


Fig. 5. (a) Degradation of TP in real water samples: spring, sea and wastewater, and (b) calculated degradation rate constants k_{obs} . Error bars are calculated as $\frac{t_n}{\sqrt{n}}$, where absent bars fall within the symbols.

acting on the various micro-organisms present. However, in the case of wastewater, TC and TFC were still significantly present even after treatment (Table 2). Thus, when dealing with complex polluted water media, AOPs are more significant for implementation as a tertiary treatment technique, where fewer particles are present in the medium and limited competing reactions are favored so that oxidation is thus more effective [64].

3.6. Effectivity of sulfate and hydroxyl radicals

Upon activation of PS in water, $\text{SO}_4^{\cdot-}$ as well as HO^{\cdot} are expected to be formed. To test for relative effectiveness of the $\text{SO}_4^{\cdot-}$ and HO^{\cdot} produced on TP degradation, quenching experiments were performed upon adding methanol (MeOH) and *tert*-Butyl-alcohol (TBA) separately. Experiments were conducted in TP solutions (10 mg L⁻¹) with MeOH and TBA concentrations of about 100 mM which is 400 times greater than the concentration of PS used (e.g. 0.25 mM) to ensure proper quenching of radicals. Eqs. (20)–(23) [19] and the analyses of the reaction rate ratio $\left(\frac{k_{HO^{\cdot}}}{k_{\text{SO}_4^{\cdot-}}}\right)$ show that MeOH and TBA are respectively 88 and 1,500 times kinetically more reactive toward HO^{\cdot} than $\text{SO}_4^{\cdot-}$, thus it can be said that TBA mainly quenches HO^{\cdot} while MeOH quenches both mentioned radicals.

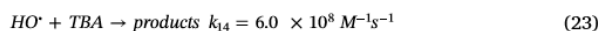
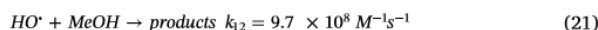
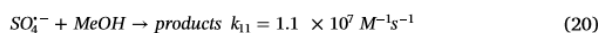


Fig. 6 and Table 1 show clearly that the spiked scavengers decreased the rate constants of TP oxidation reaction. For example, k_{obs} decreased from $1.73 (\pm 0.04) \times 10^{-1} \text{ min}^{-1}$, to $1.5 (\pm 0.01) \times 10^{-1} \text{ min}^{-1}$ and $5.4 (\pm 0.3) \times 10^{-2} \text{ min}^{-1}$ for the cases of no quencher, TBA and MeOH, respectively (Table 1). The % degradation at $t = 16 \text{ min}$ was 95% for the case of no quencher and decreased to 92% and 57% for the cases of TBA and MeOH, respectively.

Tracking the % contribution of every radical and considering Eqs. (20)–(23), $\text{SO}_4^{\cdot-}$ is shown to be the main contributor (% contribution average $\geq 84\%$) to the oxidation process in the medium. In fact, $\text{SO}_4^{\cdot-}$ is the prominent contributor in the first 6 min which resulted in a similar degradation trend for the case of TBA and MeOH at the beginning of the reaction. After that, HO^{\cdot} contribution increases from null to reach $\leq 28\%$ at $t = 16 \text{ min}$. The method used to determine the % contribution of radicals is explained in Text S4, where it utilizes and compares the values of $\frac{[TP]_t}{[TP]_0}$ in cases of MeOH and TBA presence.

This can be related to the initial pH of the reaction medium, where pH_i was acidic (pH_i = 5.3, 6.3 and 5.4 for quencher-free, MeOH and

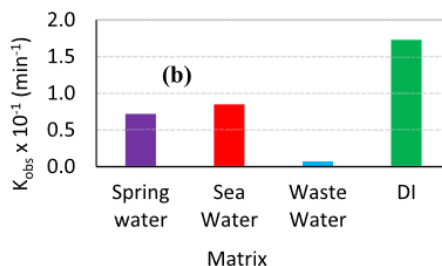


Table 2

Physical parameters of the natural water matrices before and after treatment in UV₂₅₄/PS system. Experimental conditions: [TP]₀ = 10 mg L⁻¹ and [PS]₀ = 0.25 mM.

Parameters	units	Spring Water		Sea Water		Waste Water	
		Before treatment	After treatment	Before treatment	After treatment	Before treatment	After treatment
pH	–	7	6.86	8	7.45	8.2	7.93
Total Coliforms	CFU ^a	NA	NA	76	NA	TNTC ^c	TNTC
Fecal Coliforms	NA	NA	NA	4	NA	TNTC	TNTC
Turbidity	NTU ^b	0.63	0.38	1	0.17	95	69
TSS	mg L ⁻¹	9	2	88	126	425	38
TDS		350	332	32,500	47,400	4400	3840
Sulfate		16	30	3500	3500	420	490
Chloride		42.6	1.85	25,250	21,500	3375	2090
Bicarbonate		230	210	177	156	280	250
COD ^d		132	43	970	930	1106	426

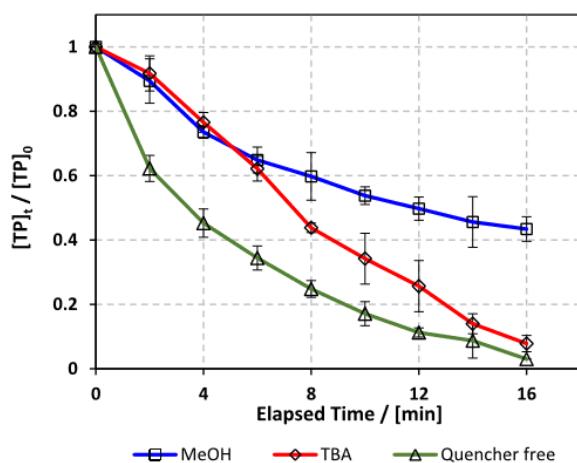
^a Colony forming unit.^b Nephelometric turbidity unit.^c Too numerous to count.^d Chemical oxygen demand.

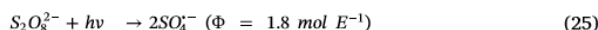
Fig. 6. Identification of the reactive species for TP degradation in UV₂₅₄/PS system. Time course degradation of TP in the absence and in the presence of MeOH and TBA quenchers. Experimental conditions: [MeOH] = [TBA] = 100 mM, [TP]₀ = 10 mg L⁻¹, and [PS]₀ = 0.25 mM. Error bars are calculated as $\frac{\Delta x}{x}$, where absent bars fall within the symbols.

TBA experiments, respectively) which inhibits the formation of HO[•] [34]. HO[•] is known to perform as H[•] abstractor, while SO₄²⁻ is known to act selectively by electron transfer (ET) [65]. As a result, one can deduce that TP, in the tested case, is mainly degraded by ET. This can be explained by the presence of the atoms N and O in TP prone to ET reactions. SO₄²⁻ was the main reactive species in several other AOPs studies utilizing either UV₂₅₄/PS [25,44,48] or heat/PS [47,50,51,53–55] systems especially in slightly acidic media.

3.7. Comparative study: UV₂₅₄/H₂O₂; UV₂₅₄/PS and UV₂₅₄/H₂O₂/PS systems

In order to assess the performance of the PS-based AOP systems tested throughout this work, additional experiments were done so as to evaluate the oxidation power of such a system in the presence of H₂O₂ oxidant alone ([H₂O₂] = 0.25 mM) or in combination with PS ([H₂O₂] = [PS] = 0.125 mM) at [TP]₀ = 10 mg L⁻¹. Fig. 6Sa,b shows that systems utilizing (H₂O₂ + PS) or H₂O₂ alone were slightly better performing than PS-alone system. In fact homolytic cleavage of H₂O₂ and PS by UV-C activation allows the formation of two SO₄^{•-} and two HO[•] respectively, and the consecutive formation of HO[•] from SO₄^{•-} is pH

dependent and more prominent at basic pH (Eq. (4)) [34]. Although a higher quantum yield is expected for S₂O₈²⁻ activation (Eqs. (24) and (25)) [22,66], greater effectivity of H₂O₂ system than that of PS system may be explained by the higher effectivity of HO[•] in the degradation process. For the case of (H₂O₂ + PS) system, high k_{obs}, close to k_{obs} obtained for H₂O₂ system was found due to the formation of both effective SO₄^{•-} and HO[•] where the resulting pH_f is higher than that of PS case allowing HO[•] to be more prominent. Thus, more HO[•] is formed in the hybrid case than in the case of PS alone. The pH_f in the current three studied cases ranged between 5.2 and 5.7. For this same pH range, Yang et al. (2017) [67] also found H₂O₂ to be more effective than PS in degrading sulfamethoxazole, however, at around neutral pH, PS was more effective in its degradation. Olmez-Hanci et al. [34] also obtained larger k_{obs} for H₂O₂/UV-C (0.175 ± 0.003 min⁻¹) than for PS/UV-C (0.106 ± 0.001 min⁻¹) system in the degradation of 48 mg L⁻¹ aqueous phenol solution at fixed acidic pH value (pH = 3.0). Yang et al. (2017) [67] and Yang et al. (2019) [68] showed that efficiency of H₂O₂ is not significantly affected by pH change, whereas, PS degradation activity decreases at extreme acidic pH and in basic media as well. Thus, the preference of the oxidant to be used would depend on the pH of the corresponding medium, as well as the cost and stability of the oxidant. A comparison between the two oxidants shows that H₂O₂ degrades into water and oxygen, whereas PS results in sulfate ions in the treated water which poses an environmental concern. On the other side, PS shows an advantage over H₂O₂ in terms of transportation, storage, shelf-life and requiring much less safety conditions. The sulfates produced, when utilizing PS, can be removed by well-known methods, such as ion exchange and nanofiltration [69], or else they can stay in the treated effluent and will get diluted once discharged into the sea containing around 2,700 mg L⁻¹ SO₄²⁻ [70]. Even for the use of high concentration of PS, e.g. 25 mM as it is the case for TP effluent (Section 3.9.1), the maximum produced sulfate concentration will not exceed 4,800 mg L⁻¹ for a small treated volume that is potent for further dilution upon discharge.



3.8. Mass spectrometry and suggested mechanism

HPLC/MS(-ESI) analysis was done on samples taken at t = 0, 6, 12 and 20 min for [TP]₀ = 10 mg L⁻¹ and [PS]₀ = 0.25 mM. The total ion chromatograms (TIC) obtained showed a main peak corresponding to TP at R_t = 12.2 min, in addition to two peaks corresponding to an identified (BP_i) and an unidentified (BP_u) by-product observed at R_t = 5.2 and 5.8 min, respectively as it can be depicted in Fig. 7a. TP

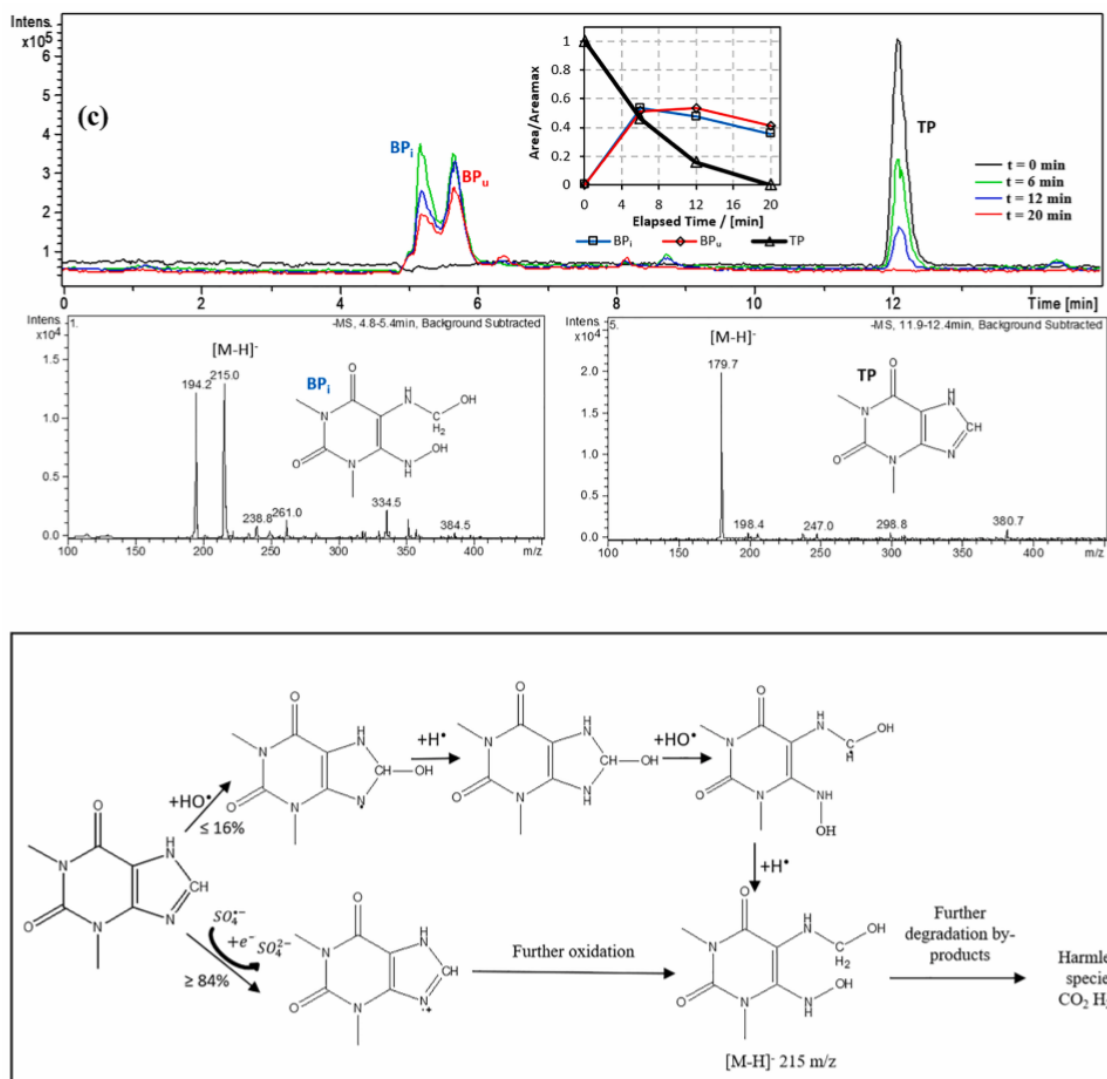


Fig. 7. (a) (-) ESI LC-MS total ion chromatogram of TP degradation at different reaction times in UV₂₅₄/PS system, containing a graph showing relative peak areas of the identified and unidentified by-products (BP₁ and BP_u), in addition to TP. (b) Mass spectrum of degradation by-product at $R_t = 5.2$ min and of TP ($R_t = 12.2$ min). (c) Proposed TP degradation mechanism by $SO_4^{\bullet -}$ and HO^{\bullet} . Experimental conditions: $[TP]_0 = 10 \text{ mg L}^{-1}$ and $[PS]_0 = 0.25 \text{ mM}$.

peak showed total degradation where a maximum peak area is observed at $t = 0$ min to vanish completely after 20 min of reaction time (Fig. 7a). For both BP₁ and BP_u no peaks were initially observed however maximum detector responses were obtained at 6 min of reaction to decrease again with time as shown in the inset of Fig. 7a. Thus, by-products are successively formed and degraded in the UV₂₅₄/PS system. This might be due to direct photolysis or to the oxidative role of produced HO^{\bullet} and/or $SO_4^{\bullet -}$ in the reactive medium. The mass spectrum of BP₁ showed two main peaks at $m/z = 194.2$ and 215.0 . The former peak is a non-identified fragment while the latter corresponded to the identified transformation TP by-product BP₁ at its $[M-H]^-$ molecular ion (Fig. 7b)). The mass spectrum of TP showed a major peak of $m/z = 179.7$ corresponding to TP molecular ion of $[M-H]^-$. The suggested degradation mechanism is presented in Fig. 7c, showing probable initiation of the degradation process by the attack of either HO^{\bullet} or $SO_4^{\bullet -}$ on TP molecule. As previously suggested, TP has more chances to undergo $SO_4^{\bullet -}$ attack with a contribution of about 86% at the beginning

of the oxidation reaction as shown in Section 3.6. Both attacks result in the formation of an unstable molecule, possessing an unpaired electron ready for rapid reaction to reach stability. Hydroxyl additions might occur increasing thereby the internal energy of the molecule more specifically the five-membered ring for potential ring opening. In fact, it is well known that five-membered rings are less stable than six-membered rings and in the case of TP, the molecule showed some hindrance in its six-membered ring part leaving structure changes at the five-member part. The transformation products are not neutral in the reactive medium and can undergo further oxidation toward full mineralization as reported in previous work using comparable UV₂₅₄/PS systems [19,21]. The formed species also contribute to a drop in the solution's pH ($\Delta\text{pH} = 1.6$, $\text{pH}_f = 3.8$) affecting thereby all possible oxidation reactions in the reactive medium. Such a drop in pH could be attributed to low molecular weight acids that are the ultimate organic molecules to be formed in a common AOP system just before total mineralization [71,72].

3.9. Case study: Pharmaceutical effluent

3.9.1. Optimization of [PS]₀ for efficient degradation

In order to assess the applicability of the studied UV₂₅₄/PS system on real pharmaceutical effluents, a field study was conducted. Wastewater was collected from a Lebanese pharmaceutical production plant that produces a syrup containing TP in addition to several excipients. All ingredients are added to a 1000 L 316 SS L mixing container, after which the mixture is pumped through a filter press into a 100 L 316 SS L container. Wastewater samples were collected from the washing effluent obtained upon cleaning the 1000 L 316 SS L mixing container and the filter press (Fig. 7Sa,c). DI water is used in the pharmaceutical factory for cleaning and washing all utensils used for any drug production including the mixing reactors. The resulting wastewater mixture was analyzed and showed high concentration of TP of about 160 mg L⁻¹ supposed to be discarded directly into the municipal sewer system without prior treatment

The pharmaceutical effluent mixture was treated using the UV₂₅₄/PS system with [PS]₀ = 25, 50, 75 and 100 mM. Results showed that almost total degradation was reached in the four cases, with minor decrease in the efficiency of the oxidation reaction for the lower [PS]₀ used e.g. 25 mM (Fig. 8). As it can be seen, the degradation rate constant *k*_{obs} decreased by almost 57% from 2.20 (± 0.08) × 10⁻² min⁻¹ for [PS]₀ = 100 mM to 1.4 (± 0.1) × 10⁻² min⁻¹ for [PS]₀ = 25 mM (Table 3).

The UV₂₅₄/PS treatment caused a drop in pH, with a maximum of ΔpH = 2.35 (Eqs. (2) and (3)). The COD value of the effluent was 28000 mg L⁻¹ which is typical of a highly charged industrial effluent. After treatment, COD values in cases of [PS]₀ = 75 and 100 mM were corrected using calibration curve method in order to eliminate the overestimation caused by PS remained in the solution (Text S5, Table S5)[73,74]. The treatment showed a decrease in the biological oxygen demand (BOD₅) proportional to [PS]₀ used demonstrating that PS is effective in targeting organic contaminants (Table 3). The addition of high concentration of sodium persulfate salt resulted in a sharp increase in the total dissolved solids with the increase in [PS]₀ (Table 3).

Moreover, the [PS] was tracked throughout the reaction time and the % RSE was determined for the four studied cases following Eq. (26). The RSE is defined as the ratio of the number of moles of the degraded organic contaminant divided by the number of moles of oxidant (PS) consumed in the process.

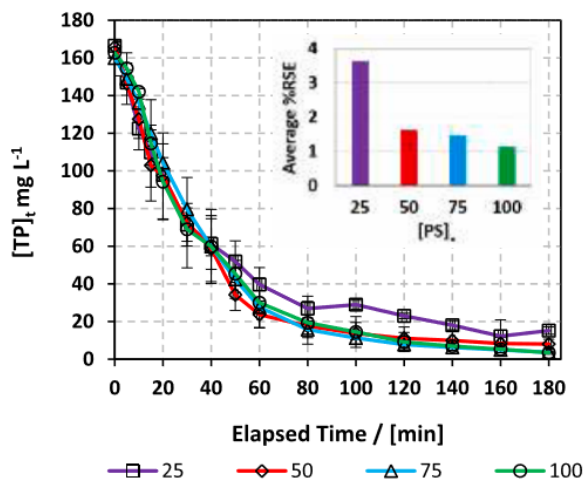


Fig. 8. Degradation of TP in a real pharmaceutical effluent. Experimental conditions: [TP]₀ = 160 mg L⁻¹ and [PS]₀ = 25–100 mM. The inset shows the average % RSE values determined at each PS concentration. Error bars are calculated as $\frac{\sigma}{\bar{x}}$, where absent bars fall within the symbols.

Table 3

Physical parameters of the pharmaceutical effluent before and after treatment in the UV₂₅₄/PS system at initial (t = 0 min) and final (t = 180 min) time. Experimental conditions: [TP]₀ = 160 mg L⁻¹ and [PS]₀ = 25–100 mM.

[PS] mM	0	25	50	75	100
<i>k</i> _{obs} min ⁻¹ (× 10 ⁻²)	–	1.4 (± 0.1)	1.8 (± 0.1)	2.2 (± 0.1)	2.20 (± 0.08)
pH _i /pH _f	–	3.43/1.53	3.43/1.15	4.15/1.89	4.15/1.80
COD ^a (mg L ⁻¹)	28,000	27,390	27,130	23,824	22,474
BOD ₅ ^b (mg L ⁻¹)	11,505	10,620	10,020	7530	8850
TDS ^c (g L ⁻¹)	0.394	6.095	8.578	14.06	17.47

^a Chemical oxygen demand.

^b Biological oxygen demand in five days.

^c Total dissolved solid.

$$\% \text{ RSE} = \frac{n(\text{TP})_{\text{degraded}}}{n(\text{PS})_{\text{consumed}}} \times 100 \quad (26)$$

The % RSE showed the highest value of 3.7% at [PS]₀ = 25 mM (Fig. 8). Thus, this concentration is considered the optimum case to adopt for the degradation of high TP's content effluent e.g. 160 mg L⁻¹. A higher % RSE (52%) was obtained by Ghauch et al. upon degradation of Chloramphenicol (CAP) in DI medium in a similar UV₂₅₄/PS systems [19]. This observation is not surprising for three reasons: (1) the lesser is the concentration of PS used in the medium (0.25 mM for CAP against 25 mM for TP), the greater is the % RSE obtained as previously demonstrated; (2) competitive reactions of PS with most of the excipients (e.g. sorbitol, potassium sorbate, ethanol, vanillin and saccharine, as provided by manufacturer) can cause a decrease in the production of SO₄⁻ (because of radical quenching with ethanol for example) and in the efficiency of SO₄⁻ to only hit the selected TP probe; and (3) direct photolysis which is not significant in the current case (~10% on average, Fig. 1) compared to that of CAP (65%).

3.9.2. Economic feasibility

Economic feasibility was assessed utilizing electric energy per order (E_{EO}) and the prices of chemicals used. E_{EO} (kWh/m³/order) is defined as the electric energy in kilowatt hours required to degrade contaminants by one order of magnitude, for example from 10 mg L⁻¹ to 1 mg L⁻¹, in one cubic meter of contaminated air or water, and is calculated using Eq. (27) for a batch system [75].

$$E_{EO} = \frac{P \times t \times 1000}{V \times \log(C_i/C_f)} \quad (27)$$

where P is the power supplied to the system in kW, t is the duration of treatment in hour, V is the volume treated in L, C_i and C_f are the respective initial and final concentrations, and 1000 is a conversion factor from L to m³.

To simplify Eq. (27), the first-order reaction rate is used Eq. (28). Changing unit of t and substitution of Eq. (28) in Eq. (27), the following simplification is done (Eqs. (28)–(30)).

$$\log \frac{C_i}{C_f} = 0.4343 \times k_{\text{obs}} \times t \quad (28)$$

$$E_{EO} = \frac{P \times t \times 1000}{V \times 0.4343 \times k_{\text{obs}} \times t \times 60} \quad (29)$$

$$E_{EO} = \frac{38.4 \times P}{V \times k_{\text{obs}}} \quad (30)$$

In the simplified Eq. (30), P is in kW, V in L, *k*_{obs} in min⁻¹, and EEO is in kWh/m³/order [75]. The total cost is calculated for the case of [PS]₀ = 25 mM since it was chosen as the optimum concentration yielding almost full TP degradation in the pharmaceutical effluent. In our studied UV₂₅₄/PS system, each 0.4 L reactor used required an 11 Watts lamp. *k*_{obs} for the case of [PS]₀ = 25 mM is 1.4

Table 4
Total system cost based on electricity price rates in Lebanon and in the US.

E_{EO} (kWh/m ³ / order)	Electricity cost (\$/m ³)		Reagent price	Total cost (\$/m ³)	
	Lebanon	US	(\$/m ³)	Lebanon	US
75	12.8	5.35	11.9	24.7	17.2

(± 0.1) $\times 10^{-2} \text{ min}^{-1}$. Thus, the E_{EO} for the studied case is 75 kWh/m³/order. Finally, in order to determine the total cost of the proposed pharmaceutical effluent treatment in batch system, Eq. (31) was used as it follows:

$$\text{Total system cost} (\$/\text{m}^3) = \text{Electrical Energy Cost} + \text{Reagent Cost} \quad (31)$$

The electrical energy cost is estimated based on the actual electricity cost in Lebanon and in the United States. In the former, Electricité du Liban (EDL) average rate of 255 LBP/kWh is equivalent to 0.169 \$/kWh at the current conversion rate [76,77], while in the latter, the average electricity cost for the industrial sector is about 0.0709 \$/kWh. As for reagent cost, it is calculated using wholesale prices available on-line through the local distributors (Table S4). The total system cost is presented in detail in Table 4, where, based on prices of electricity in the US, a total of 17.2 \$ is enough to treat 1 m³ of a highly charged pharmaceutical effluent with the reagent price being the main contributor to the total price. If the treatment is to be done in Lebanon, however, it is expected to cost more (24.7% m⁻³) since electricity prices are higher.

3.9.3. Effect of successive PS spiking

The effect of successive versus simultaneous addition of PS was tested in order to find the better way of improving the oxidation process by avoiding potential radical-radical quenching that might decrease the reaction efficiency. The results presented in Text S6 and Fig. 8S of supplementary information showed the same outcomes in terms of complete degradation of TP along with total PS consumption. Accordingly, oxidation reaction can be performed in solutions of high concentration and ionic strength through elevated [PS] and without decreasing significantly the degradation yield of the pharmaceutical compounds in question. Moreover, one can notice that the % RSE, calculated for each cycle separately, was about 3.6%. However, it dropped with every cycle to reach 0.6% in the fifth cycle, which can be explained by the competitive reactions between active radicals e.g. $\text{SO}_4^{\cdot-}$, HO^{\cdot} to degrade the accumulated by-products versus initial [TP] present in solution.

3.9.4. Test of the system robustness

The robustness of the UV₂₅₄/PS system was tested upon spiking the reaction medium with concentrated effluent solution, where lower degradation was observed with each spiking accompanied with lesser % RSE as depicted in Fig. 8S. For example, a drop in the % RSE from 4.5 to 0.5 after 3 h of reaction was noticed with 90% of the initial [PS] consumed in the first cycle of 60 min. Accordingly, it is suggested that the system used is thus of low tolerance to major fluctuations in effluent concentration.

As a result, one can deduce that in cases of varying and increasing effluent concentrations upon characterization, it is recommended that PS be spiked successively (Section 3.9.3) with [PS] range consistent with that of [TP] fluctuation. More details are provided in Text S6 of supplementary information.

4. Conclusions

TP degradation was tested in an assembled UV₂₅₄/PS lab scale batch system for simulated and real concentrated industrial effluents. The

effect of various experimental parameters on TP degradation was studied. Results showed that UV₂₅₄ alone could not efficiently degrade TP through photolysis only phenomenon, while the addition of [PS]₀ = 0.25 mM totally degraded [TP]₀ = 10 mg L⁻¹ within 20 min following a pseudo-first order reaction kinetics ($k_{obs} = 0.173 (\pm 0.004) \text{ min}^{-1}$). The degradation process was inhibited in acidic and basic media, while neutral pH showed improved degradation ($k_{obs} = 0.40 (\pm 0.03) \text{ min}^{-1}$). Bicarbonate as well as chloride presence had minimal effect on TP degradation rate. In spring, sea and wastewater matrices TP showed slower degradation than that in DI confirming thereby the necessity of treating pharmaceutical factory effluents independently before mixing them with natural water. The studied system was successfully applied to treat TP in a real industrial effluent highly charged in TP (e.g. 160 mg L⁻¹) dissolved in a DI water matrix. The UV₂₅₄/PS system resulted in the complete degradation of TP in a real pharmaceutical production facility effluent over 180 min however using 25 mM of PS and reaching an optimum % average RSE of about 3.7%. The economic feasibility study estimated the cost of the chosen AOP to be close to 17.2 \$ m⁻³ in highly charged effluents. The results showed also that adding PS to the effluent mixture simultaneously at $t = 0 \text{ min}$ or successively over the reaction course (e.g. 180 min) resulted in full TP degradation accompanied with a total consumption of the initial PS added. However, it was demonstrated that the system was not robust against [TP] fluctuation, where a sudden increase in effluent concentration requires a relative increase of [PS] added. It was concluded that oxidant dosage should be determined based on temporal monitoring of the pharmaceutical active ingredient concentration under degradation. Based on ROS quenching experiments, it was demonstrated that the UV₂₅₄/PS system put in advance $\text{SO}_4^{\cdot-}$ as the main contributors to TP degradation especially at the beginning of the oxidation reaction. Although full TP degradation was reached, however LC/MS analysis depicted the presence of non-persistent TP transformation products that vanished with time. Finally, this work has reported for the first time the feasibility of the UV₂₅₄/PS systems in degrading persistent PAIs at very high concentration in batch systems and opened the way toward continuous additional investigation for effluent treatment in a continuous system.

Acknowledgements

This research was funded in part by the Lebanese National Council for Scientific Research (Award Number 103250), the K Shair CRSL fund (Award Number 103191), and the University Research Board (Award Number 103186) of the American University of Beirut and USAID-Lebanon through The National Academy of Sciences under PEER project 5-18 (Award number 103262). Prof. Antoine Ghauch greatly appreciates the help of M. Ramez Lotfi, the GM of MEPHICO, allowing access to the production line for samples collection. The author is thankful to Joan Younes, Samer Khalil, Simon Al-Ghawy, and Boutros Sawaya for their technical assistance and the personnel of the K. Shair CRSL for their kind help. The author is also grateful to graphic designer Zaynab Mayladan for her help in drawing the graphical abstract.

Appendix A. Supplementary data

Supplementary data to this article can be found online at <https://doi.org/10.1016/j.cej.2019.122478>.

References

- [1] K. Noguera-Oviedo, D.S. Aga, Lessons learned from more than two decades of research on emerging contaminants in the environment, J. Hazard. Mater. 316 (2016) 242–251, <https://doi.org/10.1016/j.jhazmat.2016.04.058>.
- [2] R. Hirsch, T. Ternes, K. Haberer, K.-L. Kratz, Occurrence of antibiotics in the aquatic environment, Sci. Total Environ. 225 (1999) 109–118, [https://doi.org/10.1016/S0048-9697\(98\)00337-4](https://doi.org/10.1016/S0048-9697(98)00337-4).
- [3] W.W. Buchberger, Current approaches to trace analysis of pharmaceuticals and

- personal care products in the environment, *J. Chromatogr. A* 1218 (2011) 603–618, <https://doi.org/10.1016/j.chroma.2010.10.040>.
- [4] I. American, Society of health-system pharmacists, Theophylline (2017).
- [5] C.A. Shively, S.M. Tarka, Methylxanthine composition and consumption patterns of cocoa and chocolate products, *Prog. Clin. Biol. Res.* 158 (1984) 149–178 <http://europepmc.org/abstract/MED/6396642>.
- [6] D.D. Tang-Liu, R.L. Williams, S. Riegelman, Disposition of caffeine and its metabolites in man, *J. Pharmacol. Exp. Ther.* 224 (1983) 180–185 <http://jpet.aspetjournals.org/content/224/1/180>.
- [7] M.E. Rybak, M.R. Sternberg, C.-I. Pao, N. Ahluwalia, C.M. Pfeiffer, Urine excretion of caffeine and select caffeine metabolites is common in the US population and associated with caffeine intake, *J. Nutr.* 145 (2015) 766–774.
- [8] T. Heberer, Occurrence, fate, and removal of pharmaceutical residues in the aquatic environment: a review of recent research data, *Toxicol. Lett.* 131 (2002) 5–17, [https://doi.org/10.1016/S0378-4274\(02\)00041-3](https://doi.org/10.1016/S0378-4274(02)00041-3).
- [9] J. Doummar, K. Nödler, T. Geyer, M. Sauter, Assessment and Analysis of Micropollutants 2010–2011 n.d.
- [10] K.V. Blake, A. Neims, D. Nickerson, K.L. Massey, L. Hendeles, Relative efficacy of phenytoin and phenobarbital for the prevention of theophylline-induced seizures in mice, *Ann. Emerg. Med.* 17 (2005) 1024–1028, [https://doi.org/10.1016/s0196-0644\(88\)80439-6](https://doi.org/10.1016/s0196-0644(88)80439-6).
- [11] J.D. Journey, T.P. Bentley, Theophylline Toxicity, StatPearls Publishing, Treasure Island (FL), n.d. <http://europepmc.org/books/NBK532962>.
- [12] S.M.Z. Connor, Richard, Angela Renata, Cordeiro Ortigara, Engin Koncagil, Stefan Uhlenbrook, Birguy M. Lamizana-Diallo, The United Nations World Water Development Report (2017), 2017.
- [13] Y. Luo, W. Guo, H.H. Ngo, L.D. Nghiem, F.I. Hai, J. Zhang, S. Liang, X.C. Wang, A review on the occurrence of micropollutants in the aquatic environment and their fate and removal during wastewater treatment, *Sci. Total Environ.* 473–474 (2014) 619–641, <https://doi.org/10.1016/j.scitotenv.2013.12.065>.
- [14] R. Liang, S. Luo, F. Jing, L. Shen, N. Qin, L. Wu, A simple strategy for fabrication of Pd/MIL-100(Fe) nanocomposite as a visible-light-driven photocatalyst for the treatment of pharmaceuticals and personal care products (PPCPs), *Appl. Catal. B Environ.* 176–177 (2015) 240–248, <https://doi.org/10.1016/j.apcatb.2015.04.009>.
- [15] I. Kim, N. Yamashita, H. Tanaka, Photodegradation of pharmaceuticals and personal care products during UV and UV/H₂O₂ treatments, *Chemosphere* 77 (2009) 518–525, <https://doi.org/10.1016/j.chemosphere.2009.07.041>.
- [16] I. Kim, H. Tanaka, Photodegradation characteristics of PPCPs in water with UV treatment, *Environ. Int.* 35 (2009) 793–802, <https://doi.org/10.1016/j.envint.2009.01.003>.
- [17] R. Liang, A. Hu, W. Li, Y.N. Zhou, Enhanced degradation of persistent pharmaceuticals found in wastewater treatment effluents using TiO₂ nanobelt photocatalysts, *J. Nanoparticle Res.* 15 (2013) 1990, <https://doi.org/10.1007/s11051-013-1990-x>.
- [18] S. Sun, J. Jiang, S. Pang, J. Ma, M. Xue, J. Li, Y. Liu, Y. Yuan, Oxidation of theophylline by Ferrate (VI) and formation of disinfection byproducts during subsequent chlorination, *Sep. Purif. Technol.* 201 (2018) 283–290, <https://doi.org/10.1016/j.seppur.2018.03.014>.
- [19] A. Ghauch, A. Baalbaki, M. Amasha, R. El Asmar, O. Tantawi, R. El Asmar, O. Tantawi, Contribution of persulfate in UV-254 nm activated systems for complete degradation of chloramphenicol antibiotic in water, *Chem. Eng. J.* 317 (2017) 1012–1025, <https://doi.org/10.1016/j.cej.2017.02.133>.
- [20] M. Amasha, A. Baalbaki, S. Al Hakim, R. El Asmar, A. Ghauch, Degradation of a Toxic Molecule o-Toluidine in Industrial Effluents using UV254/PS System, *J. Adv. Oxid. Technol.* 21 (n.d.) 261–273, <https://www.ingentaconnect.com/content/sycamore/jaot/2018/00000021/00000001/art00023>.
- [21] M. Amasha, A. Baalbaki, A. Ghauch, A comparative study of the common persulfate activation techniques for the complete degradation of an NSAID: the case of ketoprofen, *Chem. Eng. J.* 350 (2018) 395–410, <https://doi.org/10.1016/j.cej.2018.05.118>.
- [22] G. Mark, M.N. Schuchmann, H.P. Schuchmann, C. von Sonntag, The photolysis of potassium peroxydisulphate in aqueous solution in the presence of tert-butanol: a simple actinometer for 254 nm radiation, *J. Photochem. Photobiol. A Chem.* (1990), [https://doi.org/10.1016/1010-6030\(90\)80028-V](https://doi.org/10.1016/1010-6030(90)80028-V).
- [23] Y. Gao, N. Gao, Y. Deng, Y. Yang, Y. Ma, Ultraviolet (UV) light-activated persulfate oxidation of sulfamethazine in water, *Chem. Eng. J.* 195 (2012) 248–253, <https://doi.org/10.1016/j.cej.2012.04.084>.
- [24] L. Bu, S. Zhou, Z. Shi, L. Deng, G. Li, Q. Yi, N. Gao, Degradation of oxcarbazepine by UV-activated persulfate oxidation: kinetics, mechanisms, and pathways, *Environ. Sci. Pollut. Res.* 23 (2016) 2848–2855, <https://doi.org/10.1007/s11356-015-5524-1>.
- [25] C. Tan, N. Gao, S. Zhou, Y. Xiao, Z. Zhuang, Kinetic study of acetaminophen degradation by UV-based advanced oxidation processes, *Chem. Eng. J.* (2014), <https://doi.org/10.1016/j.cej.2014.05.013>.
- [26] Abbas Baalbaki, Nigham Zein Eddine, Saly Jaber, Maya Amasha, Antoine Ghauch, Rapid quantification of persulfate in aqueous systems using a modified HPLC unit, *Talanta* 178 (2018) 237–245, <https://doi.org/10.1016/j.talanta.2017.09.036>.
- [27] X. Ao, W. Liu, Degradation of sulfamethoxazole by medium pressure UV and oxidants: peroxymonosulfate, persulfate, and hydrogen peroxide, *Chem. Eng. J.* 313 (2017) 629–637, <https://doi.org/10.1016/j.cej.2016.12.089>.
- [28] V.J. Pereira, K.G. Linden, H.S. Weinberg, Evaluation of UV irradiation for photolytic and oxidative degradation of pharmaceutical compounds in water, *Water Res.* 41 (2007) 4413–4423, <https://doi.org/10.1016/j.watres.2007.05.056>.
- [29] C. Qi, X. Liu, C. Lin, X. Zhang, J. Ma, H. Tan, W. Ye, Degradation of sulfamethoxazole by microwave-activated persulfate: Kinetics, mechanism and acute toxicity, *Chem. Eng. J.* 249 (2014) 6–14, <https://doi.org/10.1016/j.cej.2014.03.086>.
- [30] X. Lu, Y. Shao, N. Gao, J. Chen, Y. Zhang, H. Xiang, Y. Guo, Degradation of diclofenac by UV-activated persulfate process: Kinetic studies, degradation pathways and toxicity assessments, *Ecotoxicol. Environ. Saf.* 141 (2017) 139–147, <https://doi.org/10.1016/j.ecoenv.2017.03.022>.
- [31] S. Dhaka, R. Kumar, M.A. Khan, K.-J. Paeng, M.B. Kurade, S.-J. Kim, B.-H. Jeon, Aqueous phase degradation of methyl paraben using UV-activated persulfate method, *Chem. Eng. J.* 321 (2017) 11–19, <https://doi.org/10.1016/j.cej.2017.03.085>.
- [32] L.W. Matzek, K.E. Carter, Activated persulfate for organic chemical degradation: a review, *Chemosphere* 151 (2016) 178–188, <https://doi.org/10.1016/j.chemosphere.2016.02.055>.
- [33] A. Ghauch, G. Ayoub, S. Naim, Degradation of sulfamethoxazole by persulfate assisted micrometric Fe⁰ in aqueous solution, *Chem. Eng. J.* (2013), <https://doi.org/10.1016/j.cej.2013.05.045>.
- [34] T. Olmez-Hanci, I. Arslan-Alaton, Comparison of sulfate and hydroxyl radical based advanced oxidation of phenol, *Chem. Eng. J.* 224 (2013) 10–16, <https://doi.org/10.1016/j.cej.2012.11.007>.
- [35] J. Rodríguez-Chueca, S. Giannakis, M. Marjanovic, M. Kohantorabi, M.R. Gholami, D. Grandjean, L.F. de Alencastro, C. Pulgarin, Solar-assisted bacterial disinfection and removal of contaminants of emerging concern by Fe²⁺-activated HSO⁻ < inf > 5 < /inf > - vs. S < inf > 2 < /inf > O < inf > 8 < /inf > 2⁻ in drinking water, *Appl. Catal. B Environ.* (2019), <https://doi.org/10.1016/j.apcatb.2019.02.018>.
- [36] D.A. House, Kinetics and mechanism of oxidations by peroxydisulfate, *Chem. Rev.* (1962), <https://doi.org/10.1021/cr60217a001>.
- [37] A. Ghauch, A.M. Tuqan, N. Kibbi, Ibuprofen removal by heated persulfate in aqueous solution: a kinetics study, *Chem. Eng. J.* 197 (2012) 483–492, <https://doi.org/10.1016/j.cej.2012.05.051>.
- [38] C.-W. Wang, C. Liang, Oxidative degradation of TMAH solution with UV persulfate activation, *Chem. Eng. J.* 254 (2014) 472–478, <https://doi.org/10.1016/j.cej.2014.05.116>.
- [39] Dissociation constants of organic acids in aqueous solution, *Pure Appl. Chem.* 1 (1960) 187, <http://dx.doi.org/10.1351/pac196001020187>.
- [40] L. Chen, T. Cai, C. Cheng, Z. Xiong, D. Ding, Degradation of acetamiprid in UV/H₂O₂ and UV/persulfate systems: a comparative study, *Chem. Eng. J.* 351 (2018) 1137–1146, <https://doi.org/10.1016/j.cej.2018.06.107>.
- [41] C. Liang, H.-W. Su, Identification of sulfate and hydroxyl radicals in thermally activated persulfate, *Ind. Eng. Chem. Res.* 48 (2009) 5558–5562, <https://doi.org/10.1021/ie9002848>.
- [42] H.A. Gorrell, Classification of formation waters based on sodium chloride content: geological notes, *Am. Assoc. Pet. Geol. Bull.* 42 (1958) 2513.
- [43] Environment Protection Authority (EPA) in South Australia, Salinity, *Environ. Info.* (n.d.). http://www.epa.sa.gov.au/environmental_info/water_quality/threats/salinity (accessed June 15, 2017).
- [44] A. Angkaew, C. Sakulthaew, T. Satapanajaru, C. Chokejaroenrat, UV-activated persulfate oxidation of 17β-estradiol: Implications for discharge water remediation, *J. Environ. Chem. Eng.* (2018) 102858, <https://doi.org/10.1016/j.jece.2018.102858>.
- [45] Z. Fang, P. Chelme-Ayala, Q. Shi, C. Xu, M. Gamal El-Din, Degradation of naphthenic acid model compounds in aqueous solution by UV activated persulfate: influencing factors, kinetics and reaction mechanisms, *Chemosphere* (2018), <https://doi.org/10.1016/j.chemosphere.2018.07.132>.
- [46] X. Gu, S. Lu, L. Li, Z. Qiu, Q. Sui, K. Lin, Q. Luo, Oxidation of 1,1,1-trichloroethane stimulated by thermally activated persulfate, *Ind. Eng. Chem. Res.* 50 (2011) 11029–11036, <https://doi.org/10.1021/ie201059x>.
- [47] H. Gao, J. Chen, Y. Zhang, X. Zhou, Sulfate radicals induced degradation of Triclosan in thermally activated persulfate system, *Chem. Eng. J.* 306 (2016) 522–530, <https://doi.org/10.1016/j.cej.2016.07.080>.
- [48] L. Zhou, C. Ferronato, J.M. Chovelon, M. Sleiman, C. Richard, Investigations of diazotriazole degradation by photo-activated persulfate, *Chem. Eng. J.* (2017), <https://doi.org/10.1016/j.cej.2016.11.066>.
- [49] Y. Gao, N. Gao, Y. Deng, D. Yin, Y. Zhang, Degradation of florfenicol in water by UV/Na₂S₂O₈ process, *Environ. Sci. Pollut. Res.* 22 (2015) 8693–8701, <https://doi.org/10.1007/s11356-014-4054-6>.
- [50] Y. Fan, Y. Ji, D. Kong, J. Lu, Q. Zhou, Kinetic and mechanistic investigations of the degradation of sulfamethazine in heat-activated persulfate oxidation process, *J. Hazard. Mater.* (2015), <https://doi.org/10.1016/j.jhazmat.2015.06.058>.
- [51] S. Norzaee, M. Taghavi, B. Djahed, F.K. Mostafapour, Degradation of Penicillin G by heat activated persulfate in aqueous solution, *J. Environ. Manage.* 215 (2018) 316–323, <https://doi.org/10.1016/j.jenvman.2018.03.038>.
- [52] S. Wang, J. Wu, X. Lu, W. Xu, Q. Gong, J. Ding, B. Dan, P. Xie, Removal of acetaminophen in the Fe²⁺/persulfate system: Kinetic model and degradation pathways, *Chem. Eng. J.* 358 (2019) 1091–1100, <https://doi.org/10.1016/j.cej.2018.09.145>.
- [53] C. Tan, N. Gao, Y. Deng, W. Rong, S. Zhou, N. Lu, Degradation of antipyrine by heat activated persulfate, *Sep. Purif. Technol.* 109 (2013) 122–128, <https://doi.org/10.1016/J.SEPUR.2013.03.003>.
- [54] D. Miao, J. Peng, X. Zhou, L. Qian, M. Wang, L. Zhai, S. Gao, Oxidative degradation of atenolol by heat-activated persulfate: Kinetics, degradation pathways and distribution of transformation intermediates, *Chemosphere* 207 (2018) 174–182, <https://doi.org/10.1016/j.chemosphere.2018.05.068>.
- [55] A. Ghauch, A.M. Tuqan, Oxidation of bisoprolol in heated persulfate/H₂O systems: kinetics and products, *Chem. Eng. J.* (2012), <https://doi.org/10.1016/j.cej.2011.12.048>.
- [56] C. Liang, Z.-S. Wang, N. Mohanty, Influences of carbonate and chloride ions on persulfate oxidation of trichloroethylene at 20 °C, *Sci. Total Environ.* 370 (2006)

- 271–277, <https://doi.org/10.1016/j.scitotenv.2006.08.028>.
- [57] K. Hasegawa, P. Neta, Rate constants and mechanisms of reaction of Cl₂-radicals, *J. Phys. Chem.* 82 (1978) 854–857.
- [58] D.A. Armstrong, R.E. Huie, S. Lyman, W.H. Koppenol, G. Merényi, P. Neta, D.M. Stanbury, S. Steenken, P. Wardman, Standard electrode potentials involving radicals in aqueous solution: Inorganic radicals, *Bioinorg. React. Mech.* (2013), <https://doi.org/10.1515/irm-2013-0005>.
- [59] J. Kiwi, A. Lopez, V. Nadochenko, Mechanism and kinetics of the OH-radical intervention during fenton oxidation in the presence of a significant amount of radical scavenger (Cl⁻), *Environ. Sci. Technol.* 34 (2000) 2162–2168, <https://doi.org/10.1021/es991406i>.
- [60] P.L. Brezonik, J. Fulkerson-Brekken, Nitrate-induced photolysis in natural waters: controls on concentrations of hydroxyl radical photo-intermediates by natural scavenging agents, *Environ. Sci. Technol.* 32 (1998) 3004–3010, <https://doi.org/10.1021/es9802908>.
- [61] D. Vione, S. Khanra, S.C. Man, P.R. Maddigapu, R. Das, C. Arsene, R.-I. Olariu, V. Maurino, C. Minero, Inhibition vs. enhancement of the nitrate-induced photo-transformation of organic substrates by the •OH scavengers bicarbonate and carbonate, *Water Res.* 43 (2009) 4718–4728, <https://doi.org/10.1016/j.watres.2009.07.032>.
- [62] G.-D. Fang, D.D. Dionysiou, S.R. Al-Abed, D.-M. Zhou, Superoxide radical driving the activation of persulfate by magnetite nanoparticles: Implications for the degradation of PCBs, *Appl. Catal. B Environ.* 129 (2013) 325–332, <https://doi.org/10.1016/j.apcatb.2012.09.042>.
- [63] Z.-H. Diao, J.-J. Liu, Y.-X. Hu, L.-J. Kong, D. Jiang, X.-R. Xu, Comparative study of Rhodamine B degradation by the systems pyrite/H₂O₂ and pyrite/persulfate: reactivity, stability, products and mechanism, *Sep. Purif. Technol.* 184 (2017) 374–383, <https://doi.org/10.1016/j.seppur.2017.05.016>.
- [64] D.B. Miklos, C. Remy, M. Jekel, K.G. Linden, J.E. Drewes, U. Hübner, Evaluation of advanced oxidation processes for water and wastewater treatment – a critical review, *Water Res.* 139 (2018) 118–131, <https://doi.org/10.1016/j.watres.2018.03.042>.
- [65] E. Lipczynska-Kochany, G. Sprah, S. Harms, Influence of some groundwater and surface waters constituents on the degradation of 4-chlorophenol by the Fenton reaction, *Chemosphere* 30 (1995) 9–20, [https://doi.org/10.1016/0045-6535\(94\)00371-Z](https://doi.org/10.1016/0045-6535(94)00371-Z).
- [66] J.H. Baxendale, J.A. Wilson, The photolysis of hydrogen peroxide at high light intensities, *Trans. Faraday Soc.* (1957), <https://doi.org/10.1039/TF9575300344>.
- [67] Y. Yang, X. Lu, J. Jiang, J. Ma, G. Liu, Y. Cao, W. Liu, J. Li, S. Pang, X. Kong, C. Luo, Degradation of sulfamethoxazole by UV, UV/H₂O₂ and UV/persulfate (PDS): formation of oxidation products and effect of bicarbonate, *Water Res.* (2017), <https://doi.org/10.1016/j.watres.2017.03.054>.
- [68] Z.X. Khoo, J.E.M. Teoh, Y. Liu, C.K. Chua, S. Yang, J. An, K.F. Leong, W.Y. Yeong, 3D printing of smart materials: a review on recent progresses in 4D printing, *Virtual Phys. Prototyp.* 10 (2015) 103–122, <https://doi.org/10.1080/17452759.2015.1097054>.
- [69] A. Darbi, T. Viraraghavan, Y.-C. Jin, L. Braul, D. Corkal, Sulfate removal from water, *Water Qual. Res. J. 38* (2003) 169–182, <https://doi.org/10.2166/wqrj.2003.011>.
- [70] D.R. Hitchcock, Biogenic contributions to atmospheric sulphate levels, in: Proc. Second Natl. Conf. Complet. Water Re-Use. Am. Inst. Chem. Eng. US Environ. Prot. Agency, Chicago, IL, May, 1975: p. 291.
- [71] S.Y. Oh, H.W. Kim, J.M. Park, H.S. Park, C. Yoon, Oxidation of polyvinyl alcohol by persulfate activated with heat, Fe²⁺, and zero-valent iron, *J. Hazard. Mater.* 168 (2009) 346–351, <https://doi.org/10.1016/j.jhazmat.2009.02.065>.
- [72] S.-Y. Oh, S.-G. Kang, P.C. Chiu, Degradation of 2, 4-dinitrotoluene by persulfate activated with zero-valent iron, *Sci. Total Environ.* 408 (2010) 3464–3468.
- [73] H. Zhang, Z. Wang, C. Liu, Y. Guo, N. Shan, C. Meng, L. Sun, Removal of COD from landfill leachate by an electro/Fe²⁺/peroxydisulfate process, *Chem. Eng. J.* 250 (2014) 76–82, <https://doi.org/10.1016/j.cej.2014.03.114>.
- [74] J. Yang, Z. Liu, Z. Zeng, Z. Huang, Y. Cui, A method for removing persulfate interference in the analysis of the chemical oxygen demand in wastewater, *Environ. Chem. Lett.* 17 (2019) 1085–1089, <https://doi.org/10.1007/s10311-018-00832-2>.
- [75] J.R. Bolton, K.G. Bircher, W. Tumas, C.A. Tolman, Figures-of-merit for the technical development and application of advanced oxidation technologies for both electric- and solar-driven systems (IUPAC Technical Report), *Pure Appl. Chem.* (2001), <https://doi.org/10.1351/pac200173040627>.
- [76] F. Fardoun, O. Ibrahim, R. Younes, H. Louahlia-Gualous, Electricity of Lebanon: problems and recommendations, *Energy Procedia* 19 (2012) 310–320, <https://doi.org/10.1016/j.egypro.2012.05.211>.
- [77] XE Currency Converter: LBP to USD, (n.d.). <https://www.xe.com/currencyconverter/convert/?Amount=225&From=LBP&To=USD> (accessed December 16, 2018).

**Degradation of theophylline in a UV₂₅₄/PS system: matrix effect and
application to a factory effluent**

Suha Al Hakim, Saly Jaber, Nagham Zein Eddine, Abbas Baalbaki, Antoine Ghauch^{*[1]}

¹American University of Beirut | Faculty of Arts and Sciences | Department of Chemistry

P.O. Box 11-0236 Riad El Solh – 1107-2020 Beirut – Lebanon

Prepared for Chemical Engineering Journal

June 2019

Supplementary Material

21 pages

Five tables, six texts, eight figures

¹ Corresponding Author: e mail antoine.ghauch@aub.edu.lb Phone: +961 1350 000 Fax: +961 1 365 217

Text S1

Theophylline calibration curve

Calibration curve obtained for [TP] presented in Fig. 1S exhibited high linearity ($R^2 = 0.999$) over a linear dynamic range of 0.02-50 mg L^{-1} with a limit of detection (LOD) amounting to 0.0176 mg L^{-1} (0.0977 μM). Error bars for calibration curve are calculated as $A = A_{\text{average}} \pm \frac{ts}{\sqrt{n}}$, where n is the number of replicates, t is student value for 95% confidence ($t = 4.303$ for 2 degrees of freedom) and s is the standard deviation of the three replicates tested. TP physical properties are summarized in Fig. 1S (c).

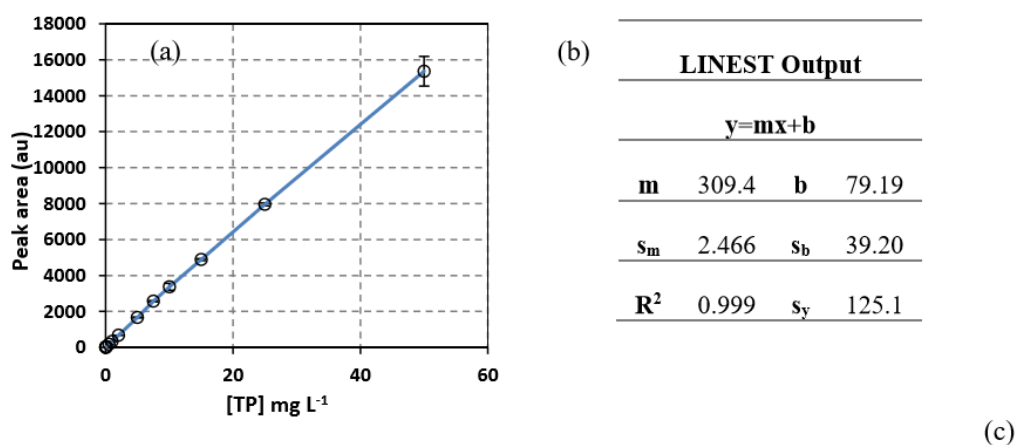


Fig. 1S. (a) Calibration curve of TP obtained using HPLC/DAD at wavelength of 270 nm, (b) LINEST output for TP calibration curve, and (c) selected TP characteristics.

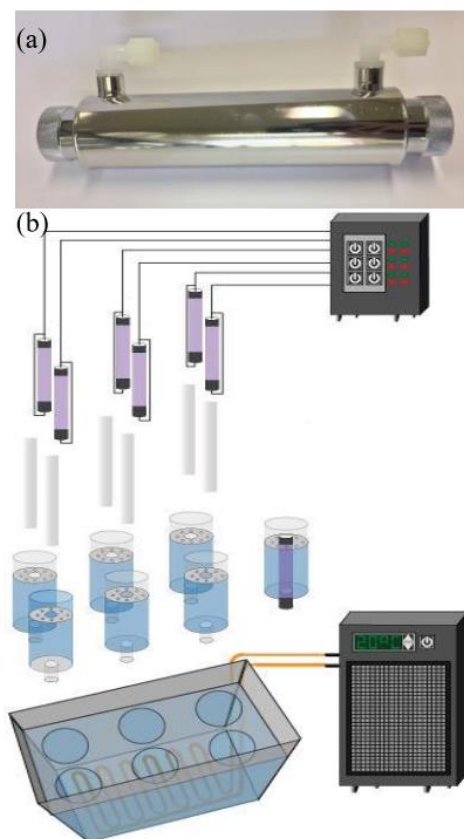


Fig. 2S. (a) Generic 1 gallon per minute UV continuous water disinfection element, and (b) an exploded diagram of the experimental setup.

Text S2

2.3 Experimental setup: UV reactors

A bench-scale experimental setup was used simulating the commercial UV water sterilization apparatus. Six units of a generic *1 gallon per minute* UV water disinfection element (Fig. 2S) were used in the construction of the experimental setup. The commercial units utilized originally consist of a UV 11-watt low-pressure mercury lamp (LPHgL) (Philips TUV 11W G11 T5, Poland), fitted in a quartz tube placed in a 280 mL 316 stainless steel casing that continuously intakes pre-filtered water. The UV lamps and their quartz fittings were utilized from the commercial product, and the stainless-steel casing was replaced by a 400 mL home-made borosilicate cylinder. The borosilicate used in the setup is as inert as the stainless-steel used in the commercial product, however the borosilicate allows easy handling and real-time

monitoring of reactors to assure no precipitates were formed. Our developed system (Fig.2S(b)) utilizes a temperature-controlled water bath (20 °C) by the aid of a PolyScience MM7 chiller. UV-254 nm intensity was $3.2 \text{ mWcm}^{-2} \pm 0.16$ measured using a radiometer (Model UVC-254 Lutron; Taipei, Taiwan) at a distance of 3cm, which is similar to the distance between the lamp and the termination part of the solution treated in the designed system. All experiments were done in triplicates, where two different experiments could be done at once.

Text S3

2.4. Experimental procedure

Stock solution of TP (0.555 mM) was prepared by dissolving 100 mg of dry TP powder in one liter of DI water, and that of Persulfate (PS) (100 mM) was prepared by dissolving 2.38 g of sodium persulfate in 100 mL of DI water. Both solutions were stored in dark at 4 °C for a maximum period of two weeks. For persulfate detection method potassium iodide solution (40 mM) was prepared by dissolving 6.64 g of KI and 5 g of NaHCO₃ in 1 L volumetric flask and left to stir overnight. Before every experiment LPHgLs (11 Watts) were stabilized for a period of 60 min. Monthly routine check of the LPHgL's UV-254 nm intensity was performed using a UVC radiometer (UVC-254 Lutron, Taiwan) to confirm that the power of the lamps is within $\pm 10 \%$ the original value, otherwise the lamps were replaced by new ones. The water chiller was turned on and set at 20 °C 60 minutes ahead of all experiments. Temperature of water in reaction medium was measured several times during the experiment to make sure it is within a range of 20 ± 2 °C. The order of addition of reagents was as follows: first Theophylline solution from stock was placed in the reactor, then DI was added, followed by additive matrix solutions (if any), finally, PS or H₂O₂, from stock solutions were added. Samples were withdrawn every 2 min using a separate syringe for each reactor and placed in 2 mL HPLC vials after filtration by a 0.45 μm PTFE 13 mm disc filters. Wastewater used in experiments was pre-filtered using a 1 μm ashless glass fiber filter.

Table S1

Degradation of $[TP]_0 = 10 \text{ mg L}^{-1}$ at $[PS]_0 = 0.01\text{-}0.5 \text{ mM}$. k_{obs} and linearity constant (R^2) obtained for plots of $\ln \frac{[TP]_t}{[TP]_0}$ versus time (min) for tested conditions upon first order fitting are presented.

[TP] ppm	[PS] ₀ mM	$k_{\text{obs}} \times 10^{-1} (\text{min}^{-1})$	R^2
10	0.01	0.04 (± 0.01)	0.9675
	0.1	0.49 (± 0.02)	0.9553
	0.25	1.74 (± 0.06)	0.9933
	0.5	3.7 (± 0.2)	0.955

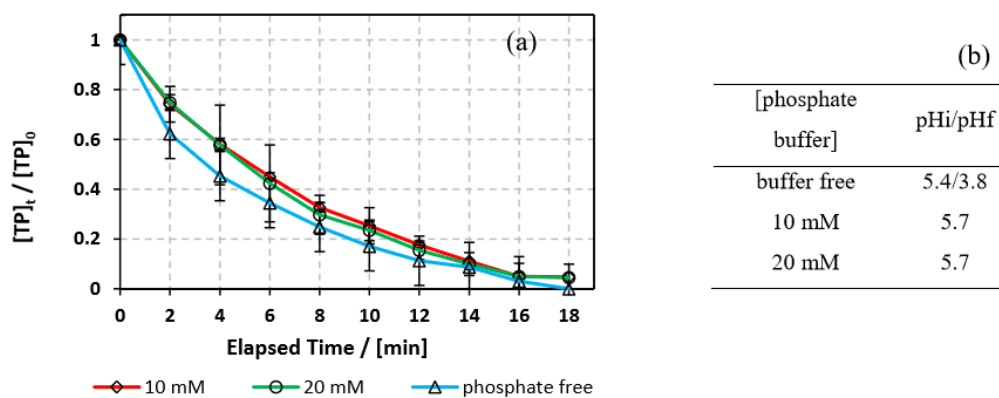


Fig. 3S. (a) Effect of phosphates (0, 10 and 20 mM) on TP degradation. (b) pH in buffered and non-buffered solutions. Experimental conditions: $[TP]_0 = 10 \text{ mg L}^{-1}$, $[PS]_0 = 0.25 \text{ mM}$. Error bars are calculated as $\frac{ts}{\sqrt{n}}$, where absent bars fall within the symbols.

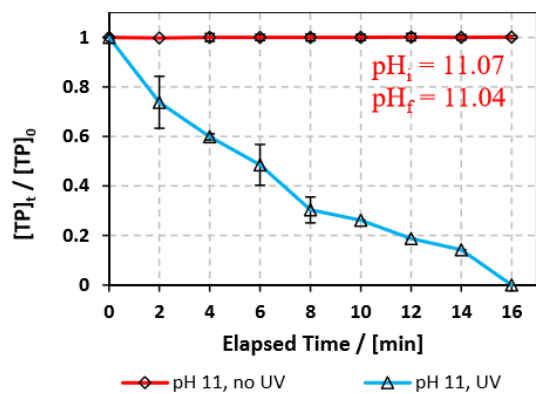
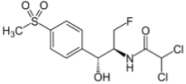
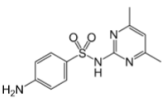
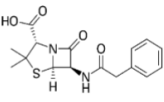
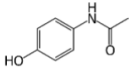


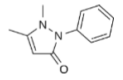
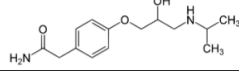
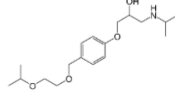
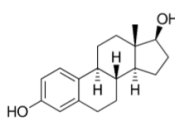
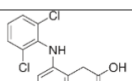
Fig. 4S. Comparison between UV and base activation of PS. Experimental conditions: $[TP]_0 = 10 \text{ mg L}^{-1}$, $[PS]_0 = 0.25 \text{ mM}$, and $[\text{phosphate buffer}] = 10 \text{ mM}$ of $\text{pH} = 11$ in both cases.

Error bars are calculated as $\frac{ts}{\sqrt{n}}$, where absent bars fall within the symbols.

Table S2

Review of the effect of chloride (Cl⁻) presence on the degradation of several organic probes in Persulfate activated systems. (+) and (-) represent an increase or a decrease in the degradation rate constant of the oxidation reaction, respectively.

Family	Probe	Structure	PS system used	[PS] ₀ mM	[Cl ⁻] (mM)	[NaCl] (mg L ⁻¹)	Effect on <i>k</i> _{obs}	Main reactive radical species	Reference
Antibiotic	Florfenicol		UV/PS	1	1, 10, 100	58.4, 584, 5844	-	No data	[2]
	Sulfamethazine		Heat/PS	2	5, 10	292, 584	Negligible effect	SO ₄ ^{-•}	[3]
					100, 200	5844, 11688	+		
Penicillin G		Heat/PS	0.5	0.171	10	-	SO ₄ ^{-•}	[4]	
				0.0943	5.51	-			
Antipyretic	Acetaminophen		Fe ²⁺ /PS	0.8	0.1	5.84	Negligible effect	SO ₄ ^{-•}	[5]
					2	116.9	-		
					5, 10	292, 584	+		

			UV/PS	0.132	2, 10, 20	117, 584, 1169	+	SO ₄ ^{-•}	[6]
					50, 100	2922, 5844	-		
	Antipyryne		Heat/PS	1.855	18.5	1081	+	SO ₄ ^{-•}	[7]
					1850	108114	-		
Beta blocker	Atenolol		Heat/PS	0.5	1, 5, 10, 50	58.4, 292, 584, 2922	Negligible effect	SO ₄ ^{-•}	[8]
	Bisoprolol		Heat/PS	1	0.0855	5	+	SO ₄ ^{-•} , OH [•]	[9]
Hormone	17β-estradiol		UV/PS	Slow-release flow through system	0.028, 0.282, 2.82	1.6, 16.5, 165	-	SO ₄ ^{-•}	[10]
					28.2, 42.3	1648, 2472	+		
					56.4, 564, 846, 1269	3256, 32960, 49440, 74160	-		
Nonsteroidal anti-inflammatory	Diclofenac		UV/PS	1	25, 50	1461, 2922	+	No data	[11]

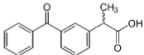
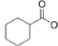
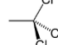
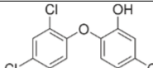
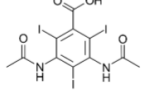
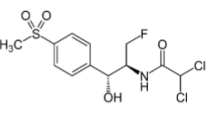
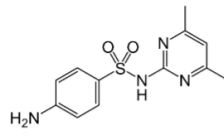
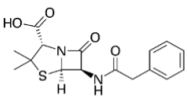
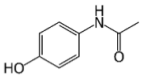
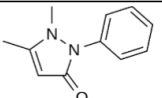
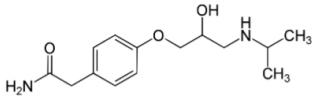
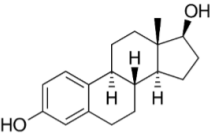
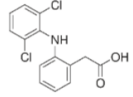
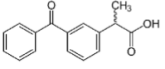
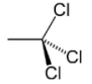
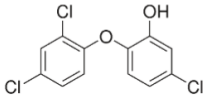
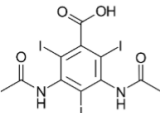
					100, 200	5844, 11688	-		
	Ketoprofen		Heat/PS	1	3.42	200	+	No data	[12]
34.2, 342					2000, 20000	-			
3.42			200	+					
			UV/PS	0.1	34.2, 342	2000, 20000	-		
			Fe ²⁺ /PS	0.5	3.42, 34.2, 342	200, 2000, 20000	-		
Persistent organic molecules	Cyclohexanoic acid		UV/PS	2	14.1	824	-	OH [*]	[13]
	1,1,1-Trichloroethane		Heat/PS	15	1	58.4	Negligible effect	No data	[14]
					10, 100	584.4, 5844	-		
Pesticides	Triclosan		Heat/PS	0.155	0.15, 1, 10	8.8, 58.4, 584.4	-	SO ₄ ⁻	[15]
					20, 50	1169, 2922	+		
	Diatrizoate		UV/PS	12	1, 10, 100	58.4, 584.4, 5844	Negligible effect	SO ₄ ⁻	[16]
500					29220	-			

Table S3

Review of the effect of bicarbonate (HCO₃⁻) presence on the degradation of several organic probes in Persulfate activated systems. (+) and (-) represent an increase or a decrease in the degradation rate constant of the oxidation reaction, respectively.

Family	Probe	Structure	PS system used	[PS] ₀ mM	[HCO ₃ ⁻] (mM)	Effect on k _{obs}	Main reactive radical species	Reference
Antibiotic	Florfenicol		UV/PS	1	1, 10, 100	-	No data	[2]
	Sulfamethazine		Heat/PS	2	5, 10, 50	+	SO ₄ ⁻	[3]

	Penicillin G		Heat/PS	0.5	0.0943	-	SO_4^{2-}	[4]
Antipyretic	Acetaminophen		UV/PS	0.132	2 10, 20, 50, 100	- +	SO_4^{2-}	[6]
	Antipyrine		Heat/PS	1.855	18.55, 92.75, 185.5, 927.5	-	SO_4^{2-}	[7]
Beta blocker	Atenolol		Heat/PS	0.5	1, 5, 10, 50	-	SO_4^{2-}	[8]
Hormone	17 β -estradiol		UV/PS	Slow-release flow through system	4.76	+	SO_4^{2-}	[10]
					11.9, 23.8	-		

Nonsteroidal anti-inflammatory	Diclofenac		UV/PS	1	25, 50, 100 and 200	+	No data	[11]
	Ketoprofen		Heat/PS	1	1, 50, 100 mM	-	No data	[12]
Persistent organic molecules	1,1,1-Trichloroethane		Heat/PS	15	1, 10, 100	-	No data	[14]
	Triclosan		Heat/PS	0.155	1 – 50	-	SO_4^{2-}	[15]
Pesticide	Diatrizoate		UV/PS	12	2.5, 5, 10, 20, 40	+	SO_4^{2-}	[16]

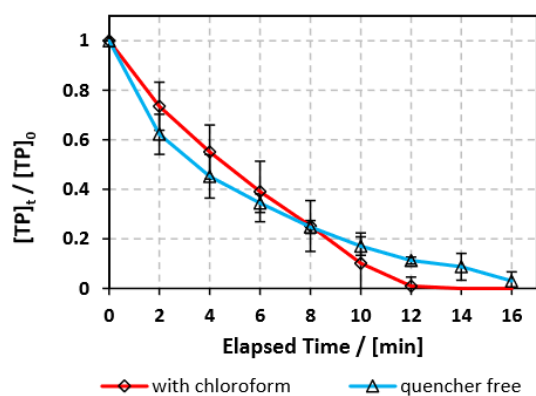
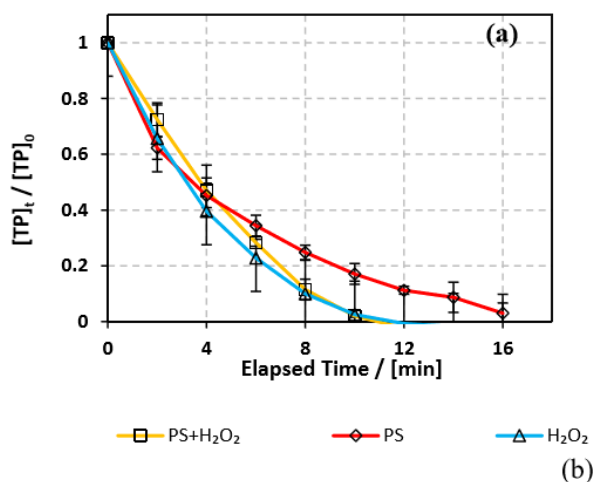


Fig. 5S. TP degradation in presence and absence of chloroform used as superoxide radical quencher. Solution is saturated with chloroform at 20 °C. Experimental conditions: $[TP]_0 = 10 \text{ mg L}^{-1}$ and $[PS]_0 = 0.25 \text{ mM}$.



System	pH _i	pH _f	k _{obs} (min ⁻¹)
PS	5.7	3.4	1.73 (± 0.04) x 10 ⁻¹
PS + H ₂ O ₂	5.2	5.5	3.6 (± 0.4) x 10 ⁻¹
H ₂ O ₂	5.4	4.4	3.5 (± 0.2) x 10 ⁻¹

Fig. 6S. Comparison of oxidation effectivity of H₂O₂ and PS toward TP. (a) [TP]_t/[TP]₀ for three different tested systems and (b) the corresponding pH at initial (t = 0 min) and final time (t = 16 min) with the calculated k_{obs}. Experimental conditions: [TP]₀ = 10 mg L⁻¹, [PS]₀ = 0.25 mM, [H₂O₂]₀ = 0.25 mM and [PS]₀ = [H₂O₂]₀ = 0.125 mM for the case of mixed oxidants.

Text S4

Determination of %contribution of SO₄^{•-} and HO[•]

It is known that MeOH quenches both SO₄^{•-} and HO[•] while TBA quenches HO[•] mainly.

The contribution of SO₄^{•-} is obtained from the TP degradation in the case of TBA as follows:

$$\text{contribution of } SO_4^{\bullet-} = 1 - \frac{[TP]}{[TP]_0} \text{ (case of TBA)}$$

Additionally, the contribution of HO[•] is estimated from the difference between TP degradation in cases of MeOH and TBA as follows:

$$\text{contribution of } HO^{\bullet} = \frac{[TP]}{[TP]_0}(\text{case of MeOH}) - \frac{[TP]}{[TP]_0}(\text{case of TBA})$$

Then, the contributions are added to obtain total contribution of the two mentioned radical species. %contribution at all reaction times is obtained as follows:

$$\% \text{ contribution} = \frac{\text{contribution of a single radical}}{\text{contribution of both radicals}} \times 100$$

The %contribution is obtained at different times of the reaction and an average is then obtained. To account for the fact that TBA quenches $SO_4^{\bullet-}$ slightly, the %contribution of $SO_4^{\bullet-}$ is expressed as $\geq 84\%$ (instead of = 84%).

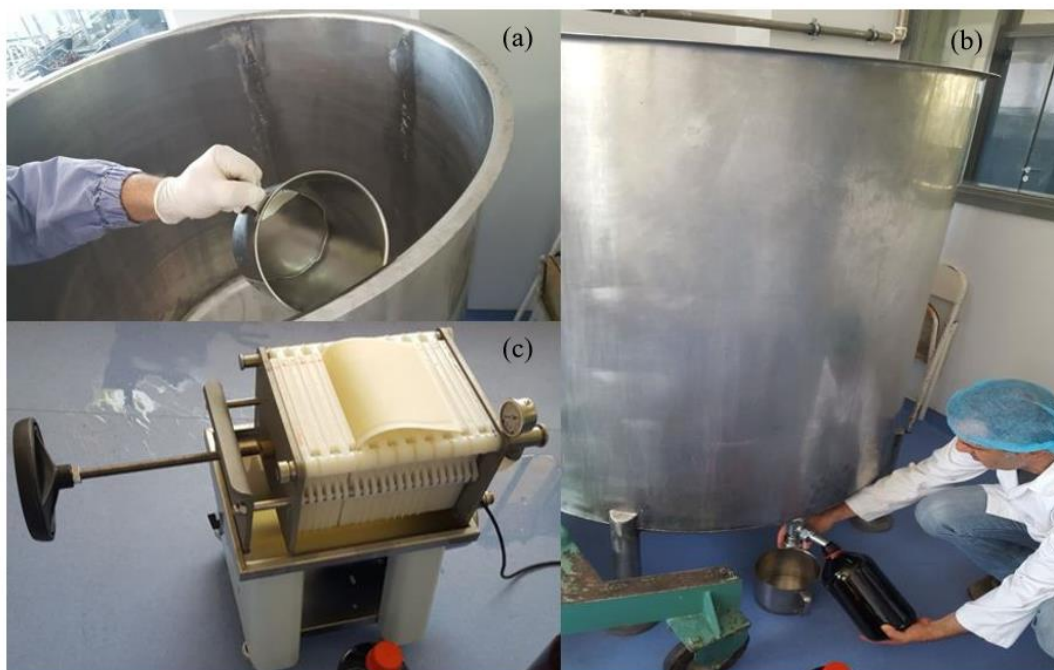


Fig. 7S. Wastewater samples containing TP collected from a local pharmaceutical production plant. (a) Washing of 1000 L 316 SS L mixing container, (b) collecting wastewater samples in amber bottles, and (c) filter press used in the manufacturing process.

Table S4

Masses and prices of reagents used based on available commercial prices

[PS] ¹	mol L ⁻¹	25
Reactor volume	L	0.4
n PS mol	mol	0.01
m Na ₂ S ₂ O ₈	g	2.38
Reagent price ²	\$/reactor	0.00476
Reagent price ²	\$/m ³	11.9

¹1 kg of PS costs 2 US \$.

²Based on price obtained from Jinan Shijitongda Chemical Co., Ltd

Text S5

Correction of COD values by calibration method

It is well known that PS causes overestimation in measuring COD values [17,18]. A method known as the calibration method is used to correct for this error [17]. The following equation is used:

$$COD_{corrected} = COD_{overestimated} - (30.52[PS] + 22.21)$$

With [PS] being the PS concentration remaining in g/L.

The PS was depleted, where it was below the detection limit, in the cases of $[PS]_0 = 25$ and 50 mM in treating pharmaceutical effluent and in all the cases of natural water media. Table S5 shows the calculations done to correct COD values in the cases where PS was still present at final reaction time.

Table S5

Correction of COD values by calibration method to reduce overestimation caused by PS

Condition	COD values	[PS] remained (g/L)	corrected COD values by calibration method
$[PS]_0 = 25$ mM/effluent	27390	0	-
$[PS]_0 = 50$ mM/effluent	27130	0	-
$[PS]_0 = 75$ mM/effluent	23850	0.12307	23824
$[PS]_0 = 100$ mM/effluent	22500	0.13653	22474
$[PS]_0 = 0.25$ mM/spring water	43	0	-
$[PS]_0 = 0.25$ mM/sea water	930	0	-
$[PS]_0 = 0.25$ mM/waste water	426	0	-

Text S6

3.9.3. Effect of successive PS spiking

To test the effect of successive additions of PS versus simultaneous addition at the initiation of the experiment, a trial was designed in which the initial $[PS]_0 = 25$ mM was equally divided (e.g. 5 mM) so that to cover five successive cycles of 36 min each Fig. 7Sa shows a comparison between successive and simultaneous addition of PS to the reaction medium. Results clearly show faster kinetics in the simultaneous addition in the first 80 min followed by slower kinetics; whereas successive additions showed more consistent slope for [TP] degradation. As for the final [TP] and [PS] in the reactor, both investigated cases showed similar results in which TP and PS were almost totally degraded and consumed, respectively

at 180 min of the reaction time (Fig. 7Sa). Moreover, one can notice from the current experiment that during the first cycle of the successive addition method, the % RSE, calculated for each cycle separately, was about 3.6%.; However, it dropped with every cycle to reach 0.6% in the fifth cycle, which can be explained by the competitive reactions between active radicals e.g. $SO_4^{\cdot-}$, HO^{\cdot} to degrade the accumulated by-products versus initial TP present in solution (Fig. 7Sa). The effectivity of successive versus simultaneous addition of PS in the treatment process was similar regarding the residual concentrations of TP and PS; however, one can deduce that successive additions of PS can provide more control and easier calculations for the operator of the treatment plant whereas simultaneous addition of PS showed almost linear [TP] decline similar to that of a zero order kinetic case.

3.9.4. Test of the system robustness

Robustness of the UV_{254}/PS system was studied upon spiking the reactor with varying amounts of concentrated effluent solution. Initial experimental conditions of $[PS]_0 = 25$ mM and $[TP]_0 = 160$ mg L^{-1} were adopted till $t = 60$ min, at which spiking with a concentrated effluent solution was done and resulted in $[TP]_{60} = 172$ mg L^{-1} . Then, at $t = 120$ min, a concentrated effluent solution was spiked again, with half the amount of TP previously spiked in order to stay within the same range of TP effluent concentration yielding $[TP]_{120} = 181$ mg L^{-1} . On the other hand, a monitoring of the residual concentration of PS in the medium showed that almost 90% of PS was consumed during the first cycle only (Fig. 7Sb). Therefore, the remaining PS was not enough to degrade the added amount along with the degradation by-products, and thus, the % RSE significantly dropped in the second (0.9%) and third (0.5%) cycles compared to the first one (4.5%) (Fig. 7Sb). In a comparative study, Ghauch et al. also noticed incomplete degradation of a pharmaceutical compound when successively spiking the reactor with CAP solution in a UV_{254}/PS system; In the first cycle 100% degradation of CAP was achieved however followed by a decrease in the % degradation rate for every cycle reaching only 47.1% by the end of the fifth cycle [19]. Oppositely, Amasha et al. showed sustainable degradation of Ketoprofen (KTP) upon UV activation of PS and successive KTP spiking which was endorsed by the direct photolysis of KTP under UV light [12]. Our results suggest that the system used is thus of low tolerance to major fluctuations in effluent concentration. Accordingly, one can deduce that in cases of varying and increasing effluent concentrations upon characterization, it is recommended that PS be spiked successively (section 3.9.3) with [PS] range consistent with that of [TP] fluctuation.

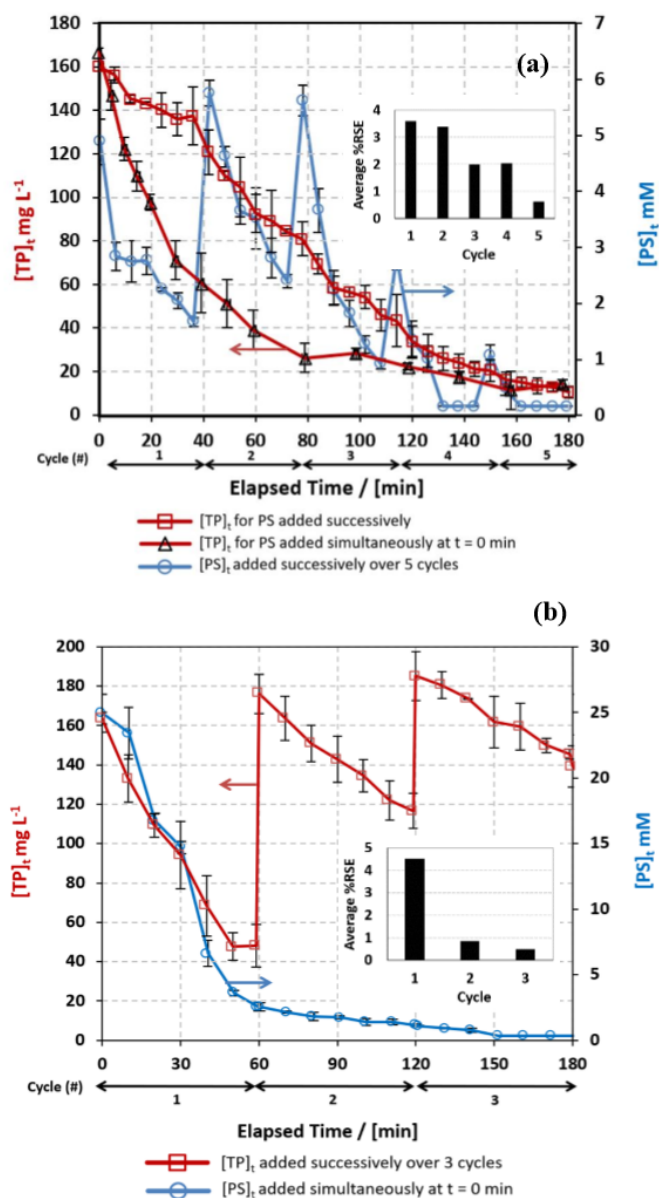


Fig. 8S. Degradation of TP in a real pharmaceutical effluent sample in UV₂₅₄/PS system. (a) PS is added either successively over 5 cycles ($[PS] = 5 \text{ mM / cycle}$) or simultaneously at $t = 0$ min ($[PS] = 25 \text{ mM}$) to TP effluent solution ($[TP]_0 \approx 160 \text{ mg L}^{-1}$). (b) Concentrated effluent solution spiked over 3 cycles of 1 h each starting at $[TP]_0 \approx 160 \text{ mg L}^{-1}$ and $[PS]_0 = 25 \text{ mM}$ added at $t = 0$ min. The insets correspond to the average % RSE calculated for every cycle. Error bars are calculated as $\frac{ts}{\sqrt{n}}$, where absent bars fall within the symbols.

References

- [1] Dissociation constants of organic acids in aqueous solution, *Pure Appl. Chem.* 1 (1960) 187. doi:10.1351/pac196001020187.
- [2] Y. Gao, N. Gao, Y. Deng, D. Yin, Y. Zhang, Degradation of florfenicol in water by UV/Na₂S₂O₈ process, *Environ. Sci. Pollut. Res.* 22 (2015) 8693–8701. doi:10.1007/s11356-014-4054-6.
- [3] Y. Fan, Y. Ji, D. Kong, J. Lu, Q. Zhou, Kinetic and mechanistic investigations of the degradation of sulfamethazine in heat-activated persulfate oxidation process, *J. Hazard. Mater.* (2015). doi:10.1016/j.jhazmat.2015.06.058.
- [4] S. Norzaee, M. Taghavi, B. Djahed, F.K. Mostafapour, Degradation of Penicillin G by heat activated persulfate in aqueous solution, *J. Environ. Manage.* 215 (2018) 316–323. doi:https://doi.org/10.1016/j.jenvman.2018.03.038.
- [5] S. Wang, J. Wu, X. Lu, W. Xu, Q. Gong, J. Ding, B. Dan, P. Xie, Removal of acetaminophen in the Fe²⁺/persulfate system: Kinetic model and degradation pathways, *Chem. Eng. J.* 358 (2019) 1091–1100. doi:https://doi.org/10.1016/j.cej.2018.09.145.
- [6] C. Tan, N. Gao, S. Zhou, Y. Xiao, Z. Zhuang, Kinetic study of acetaminophen degradation by UV-based advanced oxidation processes, *Chem. Eng. J.* (2014). doi:10.1016/j.cej.2014.05.013.
- [7] C. Tan, N. Gao, Y. Deng, W. Rong, S. Zhou, N. Lu, Degradation of antipyrine by heat activated persulfate, *Sep. Purif. Technol.* 109 (2013) 122–128. doi:10.1016/J.SEPPUR.2013.03.003.
- [8] D. Miao, J. Peng, X. Zhou, L. Qian, M. Wang, L. Zhai, S. Gao, Oxidative degradation of atenolol by heat-activated persulfate: Kinetics, degradation pathways and distribution of transformation intermediates, *Chemosphere.* 207 (2018) 174–182. doi:https://doi.org/10.1016/j.chemosphere.2018.05.068.
- [9] A. Ghauch, A.M. Tuqan, Oxidation of bisoprolol in heated persulfate/H₂O systems: Kinetics and products, *Chem. Eng. J.* (2012). doi:10.1016/j.cej.2011.12.048.
- [10] A. Angkaew, C. Sakulthaew, T. Satapanajaru, C. Chokejaroenrat, UV-activated persulfate oxidation of 17 β -estradiol: Implications for discharge water remediation, *J. Environ. Chem. Eng.* (2018) 102858. doi:https://doi.org/10.1016/j.jece.2018.102858.
- [11] X. Lu, Y. Shao, N. Gao, J. Chen, Y. Zhang, H. Xiang, Y. Guo, Degradation of diclofenac by UV-activated persulfate process: Kinetic studies, degradation pathways and toxicity assessments, *Ecotoxicol. Environ. Saf.* 141 (2017) 139–147. doi:https://doi.org/10.1016/j.ecoenv.2017.03.022.
- [12] M. Amasha, A. Baalbaki, A. Ghauch, A comparative study of the common persulfate activation techniques for the complete degradation of an NSAID: The case of ketoprofen, *Chem. Eng. J.* 350 (2018) 395–410. doi:https://doi.org/10.1016/j.cej.2018.05.118.

- [13] Z. Fang, P. Chelme-Ayala, Q. Shi, C. Xu, M. Gamal El-Din, Degradation of naphthenic acid model compounds in aqueous solution by UV activated persulfate: Influencing factors, kinetics and reaction mechanisms, *Chemosphere*. (2018). doi:10.1016/j.chemosphere.2018.07.132.
- [14] X. Gu, S. Lu, L. Li, Z. Qiu, Q. Sui, K. Lin, Q. Luo, Oxidation of 1,1,1-Trichloroethane Stimulated by Thermally Activated Persulfate, *Ind. Eng. Chem. Res.* 50 (2011) 11029–11036. doi:10.1021/ie201059x.
- [15] H. Gao, J. Chen, Y. Zhang, X. Zhou, Sulfate radicals induced degradation of Triclosan in thermally activated persulfate system, *Chem. Eng. J.* 306 (2016) 522–530. doi:https://doi.org/10.1016/j.cej.2016.07.080.
- [16] L. Zhou, C. Ferronato, J.M. Chovelon, M. Sleiman, C. Richard, Investigations of diatrizoate degradation by photo-activated persulfate, *Chem. Eng. J.* (2017). doi:10.1016/j.cej.2016.11.066.
- [17] H. Zhang, Z. Wang, C. Liu, Y. Guo, N. Shan, C. Meng, L. Sun, Removal of COD from landfill leachate by an electro/Fe²⁺/peroxydisulfate process, *Chem. Eng. J.* 250 (2014) 76–82. doi:https://doi.org/10.1016/j.cej.2014.03.114.
- [18] J. Yang, Z. Liu, Z. Zeng, Z. Huang, Y. Cui, A method for removing persulfate interference in the analysis of the chemical oxygen demand in wastewater, *Environ. Chem. Lett.* 17 (2019) 1085–1089. doi:10.1007/s10311-018-00832-2.
- [19] A. Ghauch, A. Baalbaki, M. Amasha, R. El Asmar, O. Tantawi, R. El Asmar, O. Tantawi, Contribution of persulfate in UV-254 nm activated systems for complete degradation of chloramphenicol antibiotic in water, *Chem. Eng. J.* 317 (2017) 1012–1025. doi:10.1016/j.cej.2017.02.133.

CHAPTER III

THEOPHYLLINE DEGRADATION BY THERMALLY AND CHEMICALLY ACTIVATED PERSULFATE

Since real-life applications might require a certain PS activation method over the other, additional PS activation techniques were thoroughly tested for the treatment of TP in an effluent solution. The degradation of TP was tested in systems of chemically and thermally activated persulfate. The two activation methods were tested separately as well as in combination, in order to optimize the system efficiency. Parameters including temperature, $[PS]_0$, $[PS]_0:[Fe^{2+}]_0$ ratio, in addition to different matrix elements were carefully studied. A real pharmaceutical factory effluent was collected and treated in a Fe^{2+} /heat/PS system.

Results of this project are presented below in the form of a research paper submitted to RSC Advances journal on July 13, 2019.



Chemically and thermally activated persulfate for theophylline degradation and application to a pharmaceutical factory effluent

Journal:	<i>RSC Advances</i>
Manuscript ID	RA-ART-07-2019-005362
Article Type:	Paper
Date Submitted by the Author:	13-Jul-2019
Complete List of Authors:	Al Hakim, Suha; American University of Beirut, Chemistry Baalbaki, Abbas; American University of Beirut, Chemistry Tantawi, Omar; American University of Beirut, Chemistry Ghauch, Antoine ; American University of Beirut, Chemistry
Subject area & keyword:	Remediation < Environmental

SCHOLARONE™
Manuscripts

RSC Advances

An international journal to further the chemical sciences



RSC Advances is an international open access, peer-reviewed, online journal covering all of the chemical sciences, including interdisciplinary fields.

The **criteria for publication** are that the experimental and/or theoretical work must be **high quality, well conducted** and **demonstrate a significant advance by adding to the development of the field**.

RSC Advances 2017 Impact Factor* = 2.936

Thank you for your assistance in evaluating this manuscript.

Guidelines to the reviewers

Reviewers have the [responsibility](#) to treat the manuscript as confidential; please be aware of our Ethical Guidelines for [reviewers](#) and [authors](#).

Only work which meets all the criteria for publication should be recommended for acceptance.

It is essential that all research work reported in RSC Advances is well-carried out and well-characterised. There should be enough supporting evidence for the claims made in the manuscript. (<http://www.rsc.org/journals-books-databases/about-journals/rsc-advances/>)

When preparing your report, please:

- comment on the originality and [scientific reliability](#) of the work;
- comment on the [characterisation of the compounds/materials reported](#) - has this been accurately interpreted and does it support the conclusions of the work; for theoretical works, please comment if enough supporting evidence has been provided;
- state clearly whether you would like to see the article accepted or rejected and give detailed comments (with references, as appropriate) that will both help the Editor to make a decision on the article and the authors to improve it.

Please inform the Editor if:

- there is a conflict of interest
- there is a significant part of the work which you are not able to referee with confidence
- the work, or a significant part of the work, has previously been published
- you believe the work, or a significant part of the work, is currently submitted elsewhere
- the work represents part of an unduly fragmented investigation.

For further information about RSC Advances, please visit: www.rsc.org/advances or contact us by email: advances@rsc.org.

*Data based on 2017 Journal Citation Reports®, (Clarivate Analytics, 2018).

ARTICLE

Chemically and thermally activated persulfate for theophylline degradation and application to a pharmaceutical factory effluent

Suha Al Hakim, Abbas Baalbaki, Omar Tantawi and Antoine Ghauch*

Received 00th January 20xx,
Accepted 00th January 20xx

DOI: 10.1039/x0xx00000x

PPCPs degradation by AOPs has gained a major interest in the past decade. In this work, theophylline (TP) oxidation was studied in thermally (TAP) and chemically (CAP) activated persulfate systems, separately and in combination (TCAP). For $[TP]_0 = 10 \text{ mg L}^{-1}$: (i) TAP resulted in 60% TP degradation at $[PS]_0 = 5 \text{ mM}$ and $T = 60^\circ\text{C}$ after 60 min of reaction, (ii) CAP showed slight degradation at room temperature, however (iii) TCAP resulted in complete TP degradation for $[PS]_0 = [Fe^{2+}]_0 = 2 \text{ mM}$ at $T = 60^\circ\text{C}$ following pseudo-first order reaction rate with calculated $k_{\text{obs}} = 5.6 (\pm 0.4) \times 10^{-2} \text{ min}^{-1}$. In TCAP system, $[PS]_0:[Fe^{2+}]_0$ ratio of 1:1 gave best results, and degradation rate increased with increasing temperature and $[PS]_0$. The degradation rate decreased with increasing pH. Chlorides as well as humic acids caused inhibition of the degradation process while nitrates showed slight enhancing effect. TP dissolved in spring, sea and waste water matrices showed lower degradation rate than in DI water, with the waste water causing the greatest inhibition ($k_{\text{obs}} = 2.6 (\pm 0.6) \times 10^{-4} \text{ min}^{-1}$). TCAP system was tested on a real factory effluent highly charged with TP e.g. $[TP]_0 = 160 \text{ mg L}^{-1}$. The results showed successful TP degradation at high concentration at 60°C and $[PS]_0 = [Fe^{2+}]_0 = 50 \text{ mM}$.

1. Introduction

Theophylline (TP), or 1,3-Dimethyl-7H-purine-2,6-dione, is a crystalline compound used in the treatment of respiratory diseases such as asthma and wheezing, and is found in trace amounts in a normal diet as in tea and cocoa beans^{1,2}. TP is part of pharmaceuticals and personal care products' (PPCPs) family, which has gained a global attention in the past few decades. This increased attention is attributed to PPCPs' discovery in ground and surface water aided by the advancements of analytical techniques that allowed their detection at previously undetected low concentrations³. PPCPs' presence in water, even at low concentrations, pose an environmental and a health risk: bioaccumulation, like the accumulation of lipophilic PPCPs in aquatic organisms^{4,5}, development of antibiotic resistance⁶, in addition to uncertain synergistic/antagonist effect of long term exposure to mixture of pharmaceuticals at low concentrations⁷. TP is introduced into nature by several pathways as from the untreated pharmaceutical production plants' wastewater effluents, in addition to the domestic wastewater that can contain TP from direct disposal of the drug and from urine excretion, which

contributes to pollution of water bodies by TP^{8,9}.

To solve the problem of water contamination by several pollutants, treatment water plants are integrated to treat wastewater discharges from domestic, agricultural and industrial sources. Conventional water treatment methods include, but are not limited to, carbon adsorption, chemical precipitation, evaporation and ion exchange¹⁰. It was shown that conventional methods do not treat PPCPs efficiently, where PPCPs were found to be resistant to such treatment and were detected in drinking water^{11–13}. One of the pharmaceuticals detected in water is TP, where it was found in spring water in Lebanon possibly caused by the discharge of untreated waste water¹⁴. TP degradation was studied during the past decades by several methods including degradation by means of Ferrate (VI)¹⁵, metal organic framework (Pd@MIL-100(Fe)) visible light ($\lambda \geq 420 \text{ nm}$)¹⁶, UV/H₂O₂^{17,18}, and UV/TiO₂ nanobelt¹⁹. Novel water treatment methods include advanced oxidation processes (AOPs) that were proved to be significantly efficient in removing persistent organic compounds. A wide variety of techniques involving different oxidants and different methods of activation is used in AOPs; examples include Fenton²⁰, photo-Fenton²¹, UV/PS^{22,23}, Fe/PS^{24,25}, heat/PS^{26–29}, in addition to alkaline/PS and alkaline/peroxymonosulfate³⁰ systems. Of the mentioned AOPs, activated PS was effective in degrading several pharmaceuticals^{31–34}, but to our knowledge, was not tested by other research groups to treat TP. The main PS activation methods are by UV, chemically, and by heat which generates highly reactive sulfate radicals (SRs) (Eqs. 1–3)^{22–29,34,35}. In this study TP degradation by thermally activated PS (TAP) and chemically activated PS (CAP) was studied, separately as well

American University of Beirut, Faculty of Arts and Sciences, Department of Chemistry

P.O. Box 11-0236 Riad El Solh – 1107-2020 Beirut – Lebanon

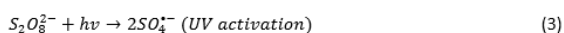
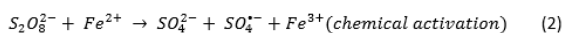
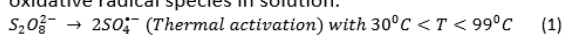
*Corresponding author. Tel/fax: +961 1350000/+961 1 365217 Email address:

antoine.ghauch@aub.edu.lb

† Footnotes relating to the title and/or authors should appear here.

Electronic Supplementary Information (ESI) available: [details of any supplementary information available should be included here]. See DOI: 10.1039/x0xx00000x

as combined in a thermally and chemically activated PS (TCAP) system. The combination of activation techniques was applied to a simulated and a real highly concentrated pharmaceutical effluent collected from a local pharmaceutical factory. The degradation process was optimized by testing several parameters in order to obtain efficient degradation within reasonable time at an affordable cost. Finally, a calculation of charge distribution and frontier orbitals was investigated in order to better elucidate TP degradation mechanism by oxidative radical species in solution.



2. Materials and Methods

2.1. Chemicals

Theophylline ($C_7H_8N_4O_2$) ($C_7H_8N_4O_2 \geq 99\%$) and sodium persulfate (PS) ($Na_2S_2O_8, \geq 99.0\%$), were obtained from Sigma-Aldrich (China and France respectively). Methanol (MeOH, CH_4O) of HPLC grade was purchased from Sigma-Aldrich (Germany) and used as mobile phase for chromatographic analysis in combination with deionized water (DI). Ferrrous chloride Tetrahydrate ($FeCl_2 \cdot 4H_2O$), used as chemical activator for PS, was obtained from Fluka (Switzerland). HCl (37%) was obtained from Fluka (Netherlands) and used to dissolve $FeCl_2$ in preparation of stock solutions. To evaluate the effect of ionic additives, sodium chloride (NaCl) was purchased from Fluka (Netherlands), and sodium nitrate ($NaNO_3$) was obtained from Sigma-Aldrich (Germany). DI water was used for the preparation of all solutions in this study.

2.2. Chemical analysis: TP quantification and identification

High performance liquid chromatography (HPLC, Agilent 1100 series) was used for TP quantification. The HPLC was equipped with a thermo-electrically cooled autosampler unit, a quaternary pump, a vacuum degasser, and a thermally controlled column. Separation of TP from other by-products was enabled by the use of a C-18 reverse phase column (Discovery[®] HS, 5 μ m; 4.6 mm internal diameter x 250 mm in length) connected to a guard column (HS C-18, 5 μ m; 4.0 mm internal diameter 20 mm long) (Pennsylvania, USA). The column was set at 30°C, while the autosampler compartment was set at 4°C. A column flow rate of 0.5 mL min^{-1} was used with a mobile phase consisting of water and MeOH (70:30 ratio) kept under isocratic mode. The injection volume was set at 80 μ L. A diode-array detector (DAD) for the quantification of TP was coupled to the HPLC. For the aforementioned conditions, TP retention time was observed at 12 min. All samples were filtered using 0.45 μ m PTFE 13 mm disc filters (Jaytee Biosciences Ltd., UK) before HPLC analysis. Selected TP chemical properties in addition to the calibration curve and the corresponding LINEST output are summarized in supporting information Fig. 1S(a-c). Identification of the degradation and transformation products of TP was performed

on an Ultimate 3000 RSLC Thermo Scientific HPLC-MS/MS connected to a Q Exactive Orbitrap. A Hypersil GOLD C18 150 column (100 x 2.1 mm, 1.9 μ m) was used for separation. The injection volume was set as 2 μ L and the elution process was performed at a flow rate of 0.3 mL min^{-1} using DI water (containing 0.1% formic acid) as eluent A and methanol as eluent B. The mass spectrometer was operated in positive ionization mode. The auxiliary gas heater temperature was set as 350°C and the capillary temperature was 320°C.

2.3. Experimental setup

The experimental setup consisted of 200 mL Erlenmeyer flasks used as reactors and immersed in a controlled-temperature water bath. The latter is equipped with an orbit shaker (Wise Bath WSB-30) and amended with a homemade Plexiglas cover plate with the capacity of holding all Erlenmeyer flasks by their necks in order to prevent reactors from falling (Fig. 2S). The experimental setup can accommodate up to 12 reactors at a time, where all experiments are done in triplicates. The reactors were efficiently submerged in the water bath to ensure that their temperature matches that of the surrounding water. This was further guaranteed by the measurement of the reactor's inner temperature using a thermometer. The temperatures tested were room temperature in addition to 40 - 75°C. To ensure proper homogenization and heat distribution, the orbit shaker was set at 70 revolutions per minute (RPM) throughout the whole experiments.

2.4. Experimental Procedure

The stock solutions were prepared as follows: TP (100 mg L^{-1}) was prepared by dissolving 100 mg of dry TP powder in 1 L of DI water; PS (100 mM) was prepared by dissolving 2.38 g of sodium persulfate in 100 mL of DI; $FeCl_2$ (80 mM) was prepared by dissolving 3.1808 g of $FeCl_2 \cdot 4H_2O$ in concentrated HCl (37%) followed by the addition of DI in a 250 mL volumetric flask. The stock solutions were prepared weekly and stored in dark at 4°C. The water bath was turned on ahead of the experiment so that the required temperature is attained. Reactors outside the water bath were each filled with predetermined amounts of prepared concentrated stock solutions of TP, matrix solution when required, in addition to DI water. The obtained solution was mixed and preheated in the water bath to reach the desired temperature. Finally, the experiment was initiated by adding $FeCl_2$ (20 mM) and PS (100 mM) stock solutions reaching a final reactor volume of 200 mL. Samples were withdrawn, using a clean 1 mL syringe for every reactor, then filtered using a 0.45 μ m PTFE 13 mm disc filter and stored in 2 mL HPLC vials. To quench any further oxidation reactions after sample withdrawal, vials were placed in an ice bath to prevent further thermal activation of PS²⁶ and spiked with 0.5 mL of methanol to prevent further chemical activation of PS³⁴. Waste water used in real water samples experiments was pre-filtered using a 1 μ m ashless glass fiber filter.

2.5. Calculation of charge distribution and frontier orbitals

The Theoretical calculations were done using Gaussian 09 program³⁶ with Density functional theory (DFT) method. The Becke, 3-parameter, Lee-Yang-Parr (B3LYP)^{37,38} functional was used with 6-311++(2d,2p) basis set. First, molecular

parameters of theophylline molecule were optimized using the mentioned level of theory. Second, at the same level of theory, the frontier electron densities and Mulliken charge distribution were obtained utilizing the optimized parameters.

3. Results and discussion

3.1. Thermal Activation of PS (TAP system)

3.1.1. Thermal stability of TP and effect of [PS]₀ To test the stability and behaviour of TP molecule upon thermal stress, control experiments were conducted in a PS-free medium with [TP]₀ = 10 mg L⁻¹ at different temperatures (40 - 75°C) for a total reaction time of 60 min. As it can be noticed from Fig. 3S, heat did not significantly affect TP stability in aqueous solutions. In fact, a slight decline in the concentration of TP was observed, with a maximum noticed of about 5% for T = 40 - 75°C demonstrating thermal stability of TP.

Thermal activation was tested by spiking a [TP]₀ = 10 mg L⁻¹ solution with different concentrations of PS at 60°C. Table 1 and Fig. 4S show that TP degradation increased from 3% to 60% upon [PS]₀ increase from 0.25 mM to 5 mM, respectively after a period of 60 min. This increase in the % degradation is attributed to the production of more SO₄^{•-} in the more PS concentrated solution as per Eq. 1.

3.1.2. Effect of temperature and determination of activation energy The temperature effect on TP degradation by TAP system was studied, with the following conditions adopted: [TP]₀ = 10 mg L⁻¹, [PS]₀ = 2 mM and T = 55 - 75°C. Fig. 1a shows that increasing the temperature resulted in improving TP degradation. For example, when temperature increased from

55°C to 75°C, the % TP degradation increased from 10% to 100% at t = 40 min. The observed trend is commonly found in several studies of TAP systems^{26,28}. This can be explained by the increase in the energy provided to the system upon heating which in its turn favors more and more the collision between the reacting TP and SRs.

The observed degradation rate constant (*k*_{obs}) was calculated according to pseudo-first order kinetics model following Eq. 4 which showed a good fitting (Text S2). Additionally, the activation energy (*E*_A) of the TP degradation reaction in TAP system was determined using the Arrhenius equation (Eq. 5), where *T* is the temperature in K, *k*_{obs} is the observed degradation rate constant calculated at different temperatures in min⁻¹, *A* is the Arrhenius constant, and *R* = 8.314 J mol⁻¹ K⁻¹ is the gas constant. Eq. 5 was plotted, and the slope obtained represents $\frac{E_A}{R}$ (Fig. 1b). *E*_A and ln(*A*) were determined to be 154 (±16) kJ mol⁻¹ and 50 (±5) kJ mol⁻¹, respectively. *E*_A value is close to that reported by Ghauch et al. for ibuprofen, *E*_A = 168 (±9) kJ mol⁻¹, and naproxen, *E*_A = 155.03 (±26.4) kJ mol⁻¹ both using TAP system however at half of the used [PS]₀ as compared to this work e.g. 1 mM^{26,28}. The uncertainties reported for ln(*A*) and *E*_A were determined using the LINEST function of Microsoft excel.

$$\ln \frac{[TP]}{[TP]_0} = -k_{obs}t \quad (4)$$

$$\ln(k_{obs}) = \ln(A) - \frac{E_A}{RT} \quad (5)$$

3.2. Chemical Activation of PS (CAP system)

Table 1

% TP degradation in TAP system at T = 55-75°C and different [PS]₀, and in CAP system at room temperature. Experimental conditions: [PS]₀ = 0.25-5 mM, [PS]₀:[Fe²⁺]₀ ratios = 1:10, 1:5 and 1:1, and [TP]₀ = 10 mg L⁻¹ for all studied cases

Activation method	[TP] ₀ (mg L ⁻¹)	T (°C)	[PS] ₀ (mM)	[Fe ²⁺] ₀ (mM)	%Degradation at t = 60 min	pH _i /pH _f
TA ^a	10	55	2	-	14	3.83/3.69
			0.25	-	3	4.30/4.56
		60	1	-	12	3.87/3.75
			2	-	28	3.83/3.58
		65	5	-	60	3.41/3.05
			2	-	45	3.57/3.46
		70	-	100	3.57/3.22	
75	-	100	3.50/3.22			
CA ^b	10	20	0.25	0.025	0.5	3.48/3.83
				0.125	-	2.97/2.84
			0.25	0.1	5	2.81/2.54
				0.05	4	2.96/3.18
			1	0.05	-	2.43/2.30
				1	2	2.23/2.12
			5	0.5	4	2.59/2.76
				0.25	1	1.84/1.79
5	2	1.65/1.54				

^a Check Fig. 4S, Fig. 1(a)

^b Check Fig. 5S

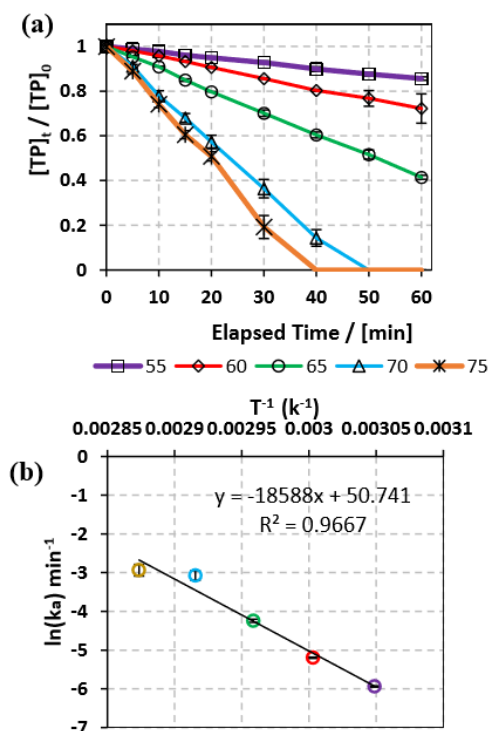
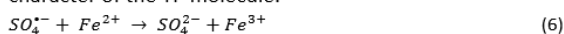


Fig. 1. (a) Effect of temperature on TP degradation in a TAP system. (b) The corresponding Arrhenius plot of $\ln(k_a)$ vs. $(1/T)$ showing equation for linear best fit. Experimental conditions: $[TP]_0 = 10 \text{ mg L}^{-1}$, $[PS]_0 = [Fe^{2+}]_0 = 2 \text{ mM}$ and $T = 55 - 75^\circ\text{C}$. Error bars are calculated as $\frac{ts}{\sqrt{n}}$, where absent bars fall within the symbols.

To test the effectiveness of CAP for TP degradation at room temperature, a solution of $[TP]_0 = 10 \text{ mg L}^{-1}$ was subjected to $[PS]_0 = 0.25, 1$ and 5 mM activated by Fe^{2+} having $[PS]_0:[Fe^{2+}]_0$ ratios of 10:1, 2:1 and 1:1 at favorable acidic pH to secure Fe^{2+} high solubility. Under all conditions tested, only negligible degradation of TP was observed (Fig. 5S), with a maximum of 5% TP degradation noticed at 60 min for the case of $[PS]_0 = 0.25 \text{ mM}$ and $[PS]_0:[Fe^{2+}]_0$ ratio of 1:1 as summarized in Table 1. Thus, TP is demonstrated to be relatively resistant to CAP system at room temperature compared to other organic contaminants. For example, Oh et al. obtained incomplete degradation of polyvinyl alcohol (PVA) utilizing Fe^{2+} -based CAP at room temperature and used higher reaction temperature to secure significant degradation of PVA³⁹ This can be explained by the common scavenging effect of $SO_4^{\bullet-}$ by Fe^{2+} to form the less effective Fe^{3+} ion (Eq. 6)⁴⁰ in addition to the recalcitrant character of the TP molecule.



3.3. Combined Thermal and Chemical activation of PS (TCAP system)

Since TAP and CAP systems showed low to negligible performance in degrading TP in aqueous solutions separately, both activation methods were combined into thermally and chemically activated PS (TCAP) system. This system was tested for different $[PS]_0:[Fe^{2+}]_0$ ratios, $[PS]_0$ and temperatures in order to confirm positively or negatively any synergistic effect that can be obtained upon combination of both PS activation techniques.

3.3.1. Effect of $[PS]_0:[Fe^{2+}]_0$ ratio and $[PS]_0$ TP degradation was studied at different $[PS]_0:[Fe^{2+}]_0$ ratios and $[PS]_0$. $[PS]_0:[Fe^{2+}]_0$ ratios of 10:1, 2:1 and 1:1 were tested at $[PS]_0 = 0.25, 1$ and 5 mM , $[TP]_0 = 10 \text{ mg L}^{-1}$ and $T = 60^\circ\text{C}$. k_{obs} was calculated for pseudo-first order kinetics model where Eq. 4 is followed (Text S3). As it can be depicted in Fig. 2 and Table 2, the 1:1 $[PS]_0:[Fe^{2+}]_0$ ratio showed the highest degradation rate, followed by 2:1 and 10:1 ratios in the three tested $[PS]_0$ conditions. Different studies showed effectivity of different $[PS]_0:[Fe^{2+}]_0$ ratios where the ratio varies depending on different parameters such as the target analyte, the method of iron addition, in addition to the state/morphology of the iron added⁴¹. For instance, a study by Oh et al. showed that a 1:1 $[PS]_0:[Fe^{2+}]_0$ is the optimum ratio for the degradation of polyvinyl alcohol by CAP³⁹. Also, Naim and Ghauch (2016) showed that 1:1 $[PS]_0:[Fe^{2+}]_0$ was the most effective ratio yielding full Ranitidine degradation in almost 10 min²⁴. On the other hand, Shang et al. obtained a 10:1 $[PS]_0:[Fe^{2+}]_0$ as the optimum ratio upon degrading diatrizoate in a CAP system⁴².

In order to study the effect of $[PS]_0$ on TP degradation, different $[PS]_0$ concentrations were used (0.25 - 5 mM) while keeping constant $[PS]_0:[Fe^{2+}]_0$ ratio of 1:1, $[TP]_0 = 10 \text{ mg L}^{-1}$ at $T = 60^\circ\text{C}$. Fig. 3 and Table 3 show that the higher the $[PS]_0$, the greater the observed rate constant k_{obs} . For example, k_{obs} increased by 32 folds when $[PS]_0$ increased from 0.25 mM to 5.0 mM following good correlation ($R^2 = 0.9879$) as shown in the inset of Fig. 3. This observation can be explained by the production of greater number of $SO_4^{\bullet-}$ obtained upon increasing $[PS]_0$ (Fig. 3).

3.3.2. Effect of temperature and determination of the activation energy To study the effect of the temperature on TP degradation in TCAP systems, the same conditions as before (section 3.3.1) were adopted however in addition to the temperature reaction variation: $[TP]_0 = 10 \text{ mg L}^{-1}$, $[PS]_0 = [Fe^{2+}]_0 = 2 \text{ mM}$ and $T = 55 - 75^\circ\text{C}$. As it can be noticed from Fig. 4a, complete TP degradation occurred in only 10 min at 75°C to last up to 50 min at 60°C . However, at 55°C only partial TP degradation, e.g. 83%, was obtained after 1 h of reaction. The results showed also that as the temperature increases from 55°C to 75°C , k_{obs} increased by 44 folds from $1.9 (\pm 0.1) \times 10^{-2} \text{ min}^{-1}$ to $8.3 (\pm 0.1) \times 10^{-1} \text{ min}^{-1}$.

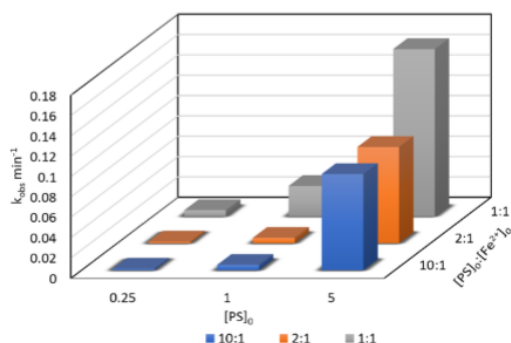


Fig 2. Effect of $[PS]_0:[Fe^{2+}]_0$ ratios on TP degradation in a TCAP system. Experimental conditions: $[PS]_0 = 0.25, 1$ and 5 mM, $[PS]_0:[Fe^{2+}]_0$ ratios of 1:1, 2:1 and 10:1, and $T = 60^\circ\text{C}$.

Table 2

Effect of $[PS]_0:[Fe^{2+}]_0$ ratios on TP degradation in a TCAP system. Initial and final pH values are presented for every case. Experimental conditions: $[PS]_0 = 0.25, 1$ and 5 mM, $[PS]_0:[Fe^{2+}]_0$ ratios of 1:1, 2:1 and 10:1, and $T = 60^\circ\text{C}$.

$[PS]_0:[Fe^{2+}]_0$	$[PS]_0$ mM	$[Fe^{2+}]_0$ mM	pH _i /pH _f
10:1	0.25	0.025	3.50/3.30
	1	0.1	2.79/2.7
	5	0.5	2.19/2.07
2:1	0.25	0.125	2.97/2.85
	1	0.5	2.53/2.9
	5	0.25	1.84/1.79
1:1	0.25	0.25	2.81/2.54
	1	1	2.23/2.12
	5	5	1.63/1.54

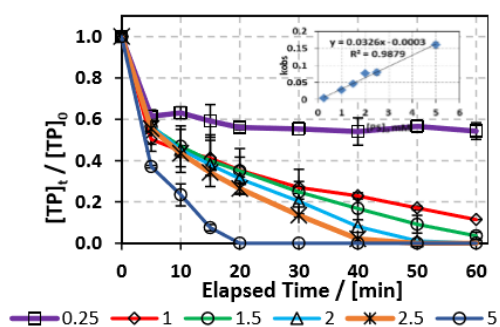


Fig. 3. Optimization of reaction conditions for the TCAP system: Effect of $[PS]_0 = 0.25 - 5$ mM on degradation of TP at $[PS]_0:[Fe^{2+}]_0$ ratio of 1:1. $[TP]_0 = 10$ mg L⁻¹ for all experiments and $T = 60^\circ\text{C}$. Error bars are calculated as $\frac{ts}{\sqrt{n}}$, where absent bars fall within the symbols.

Table 3

Optimization of $[PS]_0$ for the TCAP system. k_{obs} and linearity constant of the pseudo-first order equation plot are presented. $[TP]_0 = 10$ mg L⁻¹ for all experiments and $T = 60^\circ\text{C}$.

$[PS]_0$ (mM)	$[Fe^{2+}]_0$ (mM)	$k_{obs} \times 10^{-1}$ (min ⁻¹)	R ²
0.25	0.25	0.05 (±0.02)	0.41
1	1	0.29 (±0.02)	0.93
1.5	1.5	0.47 (±0.03)	0.96
2	2	0.56 (±0.04)	0.96
2.5	1.5	0.8 (±0.1)	0.93
5	5	1.6 (±0.1)	0.98

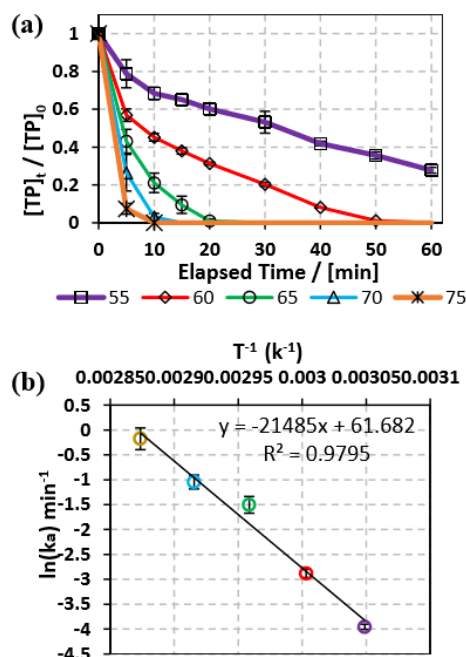


Fig 4. (a) Effect of temperature on TP degradation in a TCAP systems. (b) The corresponding Arrhenius plot of $\ln(k_a)$ vs $1/T$ showing equation for linear best fit. Experimental conditions: $[TP]_0 = 10$ mg L⁻¹, $[PS]_0 = [Fe^{2+}]_0 = 2$ mM and $T = 50 - 75$ °C. Error bars are calculated as $\frac{ts}{\sqrt{n}}$, where absent bars fall within the symbols.

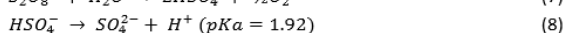
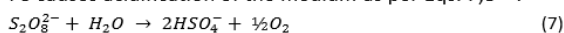
The TCAP system, as the TAP investigated system (section 3.1.2), showed also excellent fitting with the Arrhenius equation where the calculated $\ln(A)$ and the apparent activation energy E_A are greater than those calculated in the absence of Fe^{2+} e.g. $61 (\pm 5)$ kJ mol⁻¹ and $178 (\pm 14)$ kJ mol⁻¹, respectively (Fig. 4b). This should not be surprising as one might expect a lesser activation energy in the presence of Fe^{2+} . In fact, Fe^{2+} is not playing the role of a catalyst to decrease E_A neither involved in TP degradation reaction directly. It is rather playing a role in speeding up the production of $SO_4^{\bullet-}$ from PS upon chemical activation process (Eq. 2). Additional

experiments were carried out at 10:1 [PS]₀:[Fe²⁺]₀ ratio at different temperatures (40, 50 and 60°C) and the obtained results showed same outputs. For example, as the temperature reaction increased from 40, 50 to 60°C, the % degradation of TP improved from 29, 45 to 100%, respectively at 60 min for [PS]₀ = 5 mM (Fig. 6S). A similar trend was observed for aniline degradation, where [PS]₀ = 2.5 mM and zero valent iron [ZVI]₀ = 0.3 g L⁻¹ resulted in the total elimination of [Aniline]₀ = 0.05 mM in a period of 1 and 2 h at T = 80°C and 60°C, respectively⁴³.

3.4. Effect of pH adjustment in TCAP system

To study the effect of pH on TP degradation process in TCAP system, initial pH (pH_i) was adjusted to values of around 3, 5 and 7 using NaOH solution and before the addition of PS. The subsequent PS addition caused a further decrease in pH (pH_{ps}) (Fig. 5, Table 4). The use of a buffer solution was not possible since an organic buffer would compete with TP on the PS present in the solution and on the other hand an inorganic buffer, as phosphate buffer, would cause interference by complexing with Fe²⁺^{25,34}. The effect of initial pH is important to study in case the effluent to be treated contains traces of acid or base from the reactor cleaning process; however, most pharmaceutical production plants use deionized water for preliminary washing of the equipment and thus containing the highest [TP] at acidic pH.

It shall be noted that the drop in pH in the case of un-adjusted solution is due to two main factors. First, the Fe²⁺ solution added contains HCl that is used to aid in its solubility. Second, PS causes acidification of the medium as per Eqs. 7,8²⁵.



Results showed that the initial pH value significantly impacts the degradation process, where *k*_{obs} decreased with increasing pH_i, from 4.9 (±0.4) × 10⁻² min⁻¹ in case of pH_i = 2.48 to 6.0 (±0.3) × 10⁻³ min⁻¹ for pH_i = 7.07 (Fig. 5, Table 4). This can be explained by the fact that at increasing pH, e.g. pH above 4, free iron species in the solution decreases probably as a result of formation of Fe(II) complexes⁴⁴. This is proved experimentally by the formation of a visible precipitate upon pH increase e.g. formation of Fe(OH)₂ precipitate. As a result, a decrease in the amount of soluble Fe²⁺ occurs decreasing thereby the reaction rate between Fe²⁺ and PS for SO₄^{•-} production. This is further clarified by comparing the case of pH_i adjusted to pH 7 in the TCAP system to that of the TAP system at the same [PS]₀ = 2 mM. In fact, *k*_{obs} is 6.0 (±0.3) × 10⁻³ for the former and 5.52 (±0.08) × 10⁻³ min⁻¹ for the latter (Table 1S). These values can be explained by the insignificant effect of Fe²⁺ in the TCAP system adjusted initially to neutral pH. Thus, the studied TCAP system is very sensitive to pH variations. These results can be compared to a solar/Fe²⁺/PS system investigated by Nie et al.⁴⁵. In fact, the authors found a decrease in the degradation rate of chloramphenicol by around 70% when the reaction pH was increased from 3 to 9.

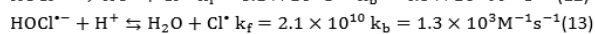
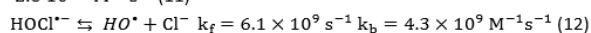
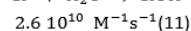
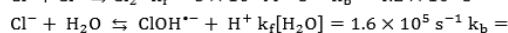
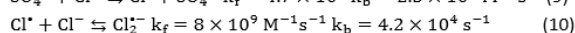
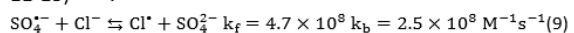
3.5. Additives and matrix effect in TCAP system

In order to test the effect of Cl⁻, NO₃⁻, and HA additives on the degradation rate of TP, experimental conditions yielding full TP

degradation in 1 h at 60°C were chosen as previously determined (Fig. 3).

3.5.1. Effect of sodium chloride Different concentrations of saline solutions spiked with TP were investigated in TCAP systems. The resulting TP solutions had NaCl concentrations of 0, 200, 2000 and 20000 mg L⁻¹ so as to mimic conditions of distilled, fresh, brackish and saline water, respectively and this according to Gorrell et al. and EPA data^{46,47}. It is noted that chloride is present in all solutions at a concentration of 4 mM from FeCl₂ (Fe²⁺ source), since FeCl₂ is used as a source of Fe²⁺. As it can be noticed from Fig. 6, the calculated *k*_{obs} for the cases of DI and fresh water were almost equal showing very slight positive effect of low [NaCl]₀ in solution. However, the results showed also that higher [NaCl]₀ caused inhibition of the degradation process, where *k*_{obs} decreased from 5.6 (±0.4) × 10⁻² min⁻¹ in the case of DI water to 3.0 (±0.2) × 10⁻² min⁻¹ and 8.0 (±0.5) × 10⁻³ min⁻¹ in the cases of brackish and saline water, respectively (Fig. 6a, Table 4). Moreover, although a decrease in *k*_{obs} was noticed for fresh water, almost full TP degradation was reached in 60 min. The decrease in *k*_{obs} is attributed to the quenching of SO₄^{•-} (E° = 2.437 (±0.019) V) by Cl⁻ to produce Cl[•] (E° = 2.432 (±0.018) V) which in turn reacts to produce Cl₂^{•-} (E° = 2.126 (±0.017) V) (Eqs. 9,10). The latter radical formed is of lower redox potential and thus less effective in terms of oxidation of TP and its transformation products compared to SO₄^{•-}⁴⁸⁻⁵⁰.

Different studies showed varied effect of Cl⁻ on the degradation processes. For instance, Fan et al. observed enhancement in the degradation of sulfamethazine⁵¹, whereas Norzaee et al. observed the inhibition of Penicillin G degradation⁵², both in TAP systems. Wang et al. observed inhibition in acetaminophen degradation at low chloride concentrations and enhancement at high concentrations, while Amasha et al. noticed inhibition in ketoprofen degradation, both in a Fe²⁺/PS systems^{34,53}. The increased degradation in the presence of Cl⁻ can be explained by the formation of Cl[•] which has a redox potential close to that of SO₄^{•-}, in addition to the formation of the reactive HO[•] (Eqs. 9, 11-13)^{49,50}.



3.5.2. Effect of nitrates Nitrates is one of the ions commonly present in different water bodies, as in groundwater due to the excessive use of fertilizers⁵⁴. Accordingly, the effect of [NO₃⁻] = 1, 10 and 100 mg L⁻¹ on TP degradation in TCAP system was tested. Results showed that reaction rate increased in the presence of [NO₃⁻], where *k*_{obs} increased by 6 folds from 5.6 (±0.4) × 10⁻² min⁻¹ to 1.0 (±0.1) × 10⁻¹ min⁻¹ in media of DI and [NO₃⁻] = 1 mg L⁻¹ respectively, and then slightly decreased for [NO₃⁻] = 10 and 100 mg L⁻¹ to values of 9.0 (±0.1) × 10⁻² min⁻¹ and 7.6 (±0.7) × 10⁻² min⁻¹, respectively (Fig. 6b, Table 5).

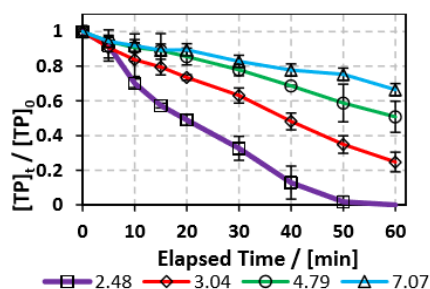


Fig. 5. Effect of pH adjustment on the degradation of TP in the TCAP system. pH adjusted before PS addition is presented. Experimental conditions: $[TP]_0 = 10 \text{ mg L}^{-1}$, $[PS]_0 = [Fe^{2+}]_0 = 2 \text{ mM}$ and $T = 60^\circ\text{C}$. Error bars are calculated as $\frac{ts}{\sqrt{n}}$, where absent bars fall within the symbols.

Table 4

Effect of pH adjustment on the degradation of TP in the TCAP system. pH_i represents pH adjusted before PS addition i.e. pH value of solution before treatment, pH_{PS} is pH after PS addition, and pH_f is final pH at $t = 60 \text{ min}$. k_{obs} is calculated from pseudo-first order equation plot. Experimental conditions: $[TP]_0 = 10 \text{ mg L}^{-1}$, $[PS]_0 = [Fe^{2+}]_0 = 2 \text{ mM}$ and $T = 60^\circ\text{C}$.

pH adjustment	pH_i^a	pH_{PS}^b	pH_f	k_{obs} (min^{-1})
-	2.48	2.01	2.20	$4.9 (\pm 0.4) \times 10^{-2}$
+	3.04	2.19	2.39	$1.7 (\pm 0.1) \times 10^{-2}$
+	4.79	2.23	2.93	$1.09 (\pm 0.6) \times 10^{-2}$
+	7.07	2.81	5.06	$6.0 (\pm 0.3) \times 10^{-2}$

^a pH_i is measured before PS addition

^b pH_{PS} is measured after PS addition

Table 5

Effect of $[\text{NaCl}] = 200 - 20,000 \text{ mg L}^{-1}$, $[\text{NO}_3^-] = 1 - 100 \text{ mg L}^{-1}$, and $[\text{HA}] = 0.5 - 20 \text{ mg L}^{-1}$ on TP degradation in a TCAP system. Experimental conditions: $[PS]_0 = [Fe^{2+}]_0 = 2 \text{ mM}$ and $[TP]_0 = 10 \text{ mg L}^{-1}$ for all conditions tested. k_{obs} is obtained as per pseudo-first order reaction rate model.

Matrix	Unit	$k_{obs} \times 10^{-2}$ (min^{-1})	pH_i/pH_f
No additive		$5.6 (\pm 0.4)$	1.85/1.53
$[\text{NaCl}] = 200$		$6.5 (\pm 0.5)$	1.85/1.56
$[\text{NaCl}] = 2000$		$3.0 (\pm 0.2)$	1.81/1.62
$[\text{NaCl}] = 20000$		$0.8 (\pm 0.05)$	1.78/1.56
$[\text{NO}_3^-] = 1$	mg L^{-1}	$10.0 (\pm 0.1)$	1.81/1.71
$[\text{NO}_3^-] = 10$		$9.0 (\pm 0.1)$	1.79/1.71
$[\text{NO}_3^-] = 100$		$7.6 (\pm 0.7)$	1.78/1.70
$[\text{HA}] = 0.5$		$1.68 (\pm 0.07)$	1.84/1.97
$[\text{HA}] = 5$		$2.1 (\pm 0.1)$	1.83/1.95
$[\text{HA}] = 20$		$2.2 (\pm 0.1)$	1.81/1.94

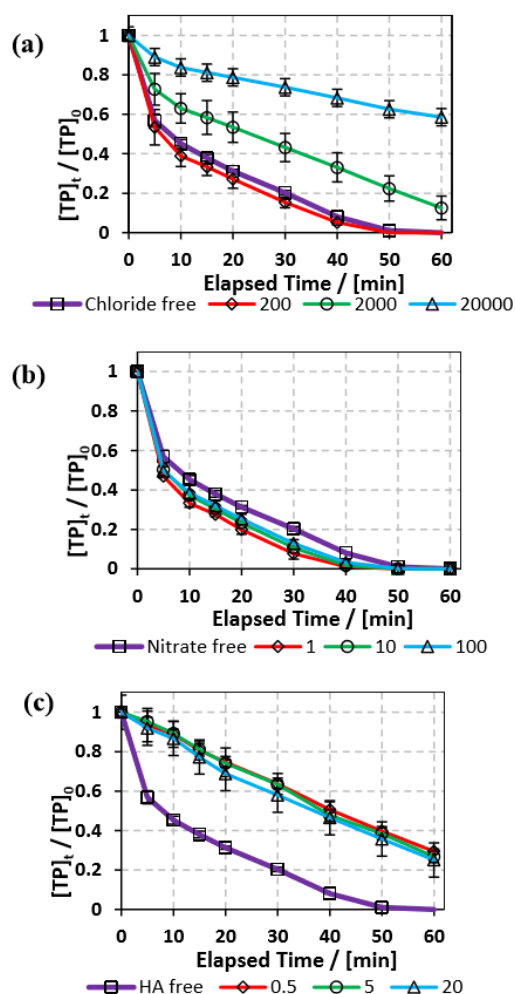
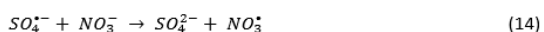


Fig. 6. Effect of (a) $[\text{NaCl}] = 200 - 20,000 \text{ mg L}^{-1}$, (b) $[\text{NO}_3^-] = 1 - 100 \text{ mg L}^{-1}$, and (c) $[\text{HA}] = 0.5 - 20 \text{ mg L}^{-1}$ on TP degradation in a TCAP system. Experimental conditions: $[PS]_0 = [Fe^{2+}]_0 = 2 \text{ mM}$ and $[TP]_0 = 10 \text{ mg L}^{-1}$ for all conditions tested. Error bars are calculated as $\frac{ts}{\sqrt{n}}$, where absent bars fall within the symbols.

The increase in TP degradation in the presence of nitrates can be attributed to the formation of NO_3^* that is considered of significant oxidation redox potential ($E_{1/2}^{red} = 2.50 \text{ V}$) which could react with TP²². So, although nitrates react with $\text{SO}_4^{\bullet-}$ and quenches them, the formation of NO_3^* seems to compensate for the decrease in $[\text{SO}_4^{\bullet-}]$ (Eq. 14). However, the increase in $[\text{NO}_3^-]$ results also in the increase of $[\text{NO}_3^*]$ where the latter can subsequently undergo self-quenching reactions, which decreases $[\text{NO}_3^*]$ and as a result decreases the degradation rate. Ghauch et al. also noticed an increase in nitrates degradation rate by 154.3% in the presence of $[\text{NO}_3^-] = 5 \text{ mg L}^{-1}$ in TAP system²⁶.



3.5.3. Effect of humic acid (HA) Of the widely present natural organic matter (NOM) is humic acid (HA) ⁴⁴. TP degradation in TCAP system was studied in the presence of $[HA]_0 = 0.5, 5$ and 20 mg L^{-1} , which is included in the typical naturally existing range ⁵⁵. Results show that HA caused inhibition in the degradation rate, where k_{obs} decreased by almost 3 folds when $[HA]_0 = 0.5 \text{ mg L}^{-1}$, compared to HA free medium. After that, the increase in $[HA]_0$ caused no significant change in k_{obs} (Fig. 6c, Table 5). The inhibition in TP degradation can be explained by the competitiveness of active radicals, where NOM quenches $SO_4^{\bullet-}$ due to the presence of electron-rich sites ⁵⁶. Liu et al. noticed a significant decrease in reaction rate with increasing $[HA]$ upon sulfachloropyridazine degradation in TAP system ⁵⁶. Amasha et al. noticed an enhancement in KTP degradation in CAP system at $[HA]_0 = 0.5$, which was explained by the possible reductive ability of HA towards transition metals which in the case of CAP system can regenerate Fe^{2+} from Fe^{3+} ^{34,57}. Thus, for the case of TP degradation in a TCAP system, the cease in decrease in k_{obs} with $[HA]_0$ increase, could be explained by the counter effects of HA where at higher concentrations, HA contributes more to re-generation of Fe^{2+} which counteracts its radical-quenching properties.

3.6. Case of natural water matrices: spring, sea, and waste water in TCAP system

The degradation of TP was studied in media of natural sea, spring and waste water (SW, SpW and WW) obtained from locations of coordinates $33^{\circ}44'17.9''N$ $35^{\circ}34'12.5''E$, $33^{\circ}54'11.1''N$ $35^{\circ}28'44.8''E$ and $33^{\circ}54'08.2''N$ $35^{\circ}29'05.0''E$, respectively. Experimental conditions are as follows: $[PS]_0 = 5 \text{ mM}$, $[Fe^{2+}]_0 = 0.5 \text{ mM}$, and TP was added in adequate amounts to each water medium such that $[TP]_0 = 10 \text{ mg L}^{-1}$. A $[PS]_0:[Fe^{2+}]_0$ ratio of 10:1 was used instead on the optimum ratio obtained of 1:1 in order to reduce the use of Fe^{2+} , e.g. to $Fe(OH)_2$ at neutral media ⁴⁴. These conditions are adopted since natural water matrices are buffered to around neutral pH (Table 6) because of the presence of bicarbonate mainly. Results showed that TP degradation was inhibited in the three tested cases compared to the DI matrix case where $k_{obs} = 1.5 (\pm 0.1) \times 10^{-1} \text{ min}^{-1}$, with WW showing ~ 570 folds inhibition in terms of $k_{obs} = 2.6 (\pm 0.6) \times 10^{-4} \text{ min}^{-1}$, followed by SpW ~ 14 folds and SW ~ 10 folds, $k_{obs} = 1.1 (\pm 0.1) \times 10^{-2}$ and $1.54 (\pm 0.09) \times 10^{-2} \text{ min}^{-1}$, respectively (Fig. 7).

One reason for the inhibition in the degradation of TP in the three investigated cases is the neutral to slightly basic pH (7–8.2), where such a pH causes the complexation and precipitation of Fe^{2+} , e.g. as $Fe(OH)_2$, where natural water media act as buffer solutions compared to DI medium that becomes acidic ($pH_i \approx 2$) right after addition of PS and Fe^{2+} solutions. Inhibition was the highest in the case of WW matrix, where WW possessed high values of total and fecal coliforms, chlorides, turbidity and total suspended and dissolved solids among the three studied matrices. The organic and inorganic material present in WW competes with TP on reacting with $SO_4^{\bullet-}$ thus inhibiting TP degradation. Additionally, chlorides act as a quencher in the studied TCAP system (Section 3.5.1) and WW showed the highest $[Cl^-]$. It is noted that total elimination

of coliforms was observed in WW and SW (Table 6) systems and is probably due to the heat factor, in addition to the activity of $SO_4^{\bullet-}$ present. Effluents of pharmaceutical production plants, after discharge, might be mixed with several water matrices of different properties. In addition, the water used for initial cleaning operations might be of natural origin and not DI water. Results presented in this section show that it is crucial to clean mixing reactors in pharmaceutical production facilities with distilled water whenever possible and to treat the effluent mixture before its release into the environment. A great decrease in the degradation rate in waste water was also observed by Ghauch research group upon degradation of chloramphenicol and ketoprofen in UV/PS systems ^{22,34}.

3.7. Case study: real factory effluent

3.7.1. Effect of $[PS]_0$ Efficiency of the TCAP system was tested on a real pharmaceutical factory effluent solution containing TP in addition to other excipients. The effluent samples were collected from a local production facility that produces a syrup containing TP. The production process consists of mixing TP and other excipients in a 1000 L 316 SS container, after which the mixture is pumped through a filter press into 100 L 316 SS containers. Waste water samples were collected from washing the SS reactor and the filter press with distilled water. The resulting factory effluent solution contained $[TP]_0 = 160 \text{ mg L}^{-1}$ (Fig. 8S). To account for the high $[TP]_0$ effluent content, $[PS]_0$ was tested at 25, 50, 75 and 100 mM utilizing the optimum $[PS]_0:[Fe^{2+}]_0$ ratio of 1:1, and $T = 60^{\circ}C$.

Results showed that higher $[PS]_0$ caused faster degradation, where total TP elimination was observed within 40 min in the case of $[PS]_0 = [Fe^{2+}]_0 = 100 \text{ mM}$, and within 180 min for $[PS]_0 = [Fe^{2+}]_0 = 25 \text{ mM}$ (Fig. 8, Table 7). To compare the degradation of TP in DI and in the factory effluent mixture, k_{obs} can be compared in cases of similar $[PS]_0/[TP]_0$ molar ratios. As such, for the case of $[TP]_0 = 10 \text{ mg L}^{-1}$ (0.0555 mM) and $[PS]_0 = [Fe^{2+}]_0 = 1.5 \text{ mM}$ in DI, $[PS]_0/[TP]_0 = 27$, while for the case of $[TP]_0 = 160 \text{ mg L}^{-1}$ and $[PS]_0 = [Fe^{2+}]_0 = 25 \text{ mM}$ in factory effluent, $[PS]_0/[TP]_0 = 28$. The corresponding k_{obs} decreased by 2 folds from $0.29 (\pm 0.02) 10^{-1}$ to $1.4 (\pm 0.1) \times 10^{-2} \text{ min}^{-1}$. Thus, TP degradation in the factory effluent is less efficient than in DI medium, which can be attributed to the presence of some excipients such as potassium sorbate, sorbitol, ethanol, vanillin and saccharine as provided by the manufacturer. Those can compete with TP in reacting with the active SRs. It is noted that the efficiency of the TCAP system would have been reduced if natural water was used to rinse the mixing reactor instead of DI water (Section 3.3.5), thus, it is crucial for industries to utilize adequate amounts of DI, or distilled, water in rinsing apparatuses and tools used during the syntheses and mixing processes for an efficient and cost effective effluent treatment.

3.7.2. Economic study The cost for factory effluent treatment utilizing the TCAP system was estimated. Electric energy required to heat the solution in addition to reagent price are considered the main contributors to the total cost of operation (Eq. 15).

ARTICLE

Table 6

Physical parameters of the natural water matrices used before and after treatment in a TCAP system. Experimental conditions: $[TP]_0 = 10 \text{ mg L}^{-1}$, $[PS]_0 = 5 \text{ mM}$ and $[Fe^{2+}]_0 = 0.5 \text{ mM}$.

Parameters	Units	Spring Water		Sea Water		Waste Water	
		Before treatment	After treatment	Before treatment	After treatment	Before treatment	After treatment
pH	-	7	3.14	8	2.84	8.2	4.12
Total Coliforms	CFU ^a	NA	NA	76	NA	TNTC ^c	NA
Fecal Coliforms		NA	NA	4	NA	TNTC	NA
Turbidity	NTU ^b	0.63	8.52	1	6.9	9.5	4.68
TSS		9	3	88	125	425	15
TDS		350	1460	32500	32400	4400	6140
Sulfate	mg/L	16	300	3500	3300	420	590
Chloride		42.6	450	25250	21500	3375	2265

^a Colony forming unit

^b Nephelometric turbidity unit

^c Too numerous to count

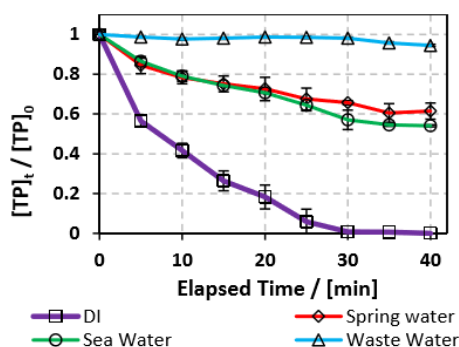


Fig. 7. Degradation of TP in real water samples: in spring, sea and waste water. Experimental conditions: $[TP]_0 = 10 \text{ mg L}^{-1}$, $[PS]_0 = 5 \text{ mM}$ and $[Fe^{2+}]_0 = 0.5 \text{ mM}$. Error bars are calculated as $\frac{ts}{\sqrt{n}}$, where absent bars fall within the symbols.

Table 7

Degradation of TP by TCAP in a real pharmaceutical effluent having $[TP]_0 = 160 \text{ mg L}^{-1}$. Experimental conditions: $[PS]_0 = 25 - 100 \text{ mM}$, $[PS]_0:[Fe^{2+}]_0$ ratio of 1:1, and $T = 60 \text{ }^\circ\text{C}$. k_{obs} is calculated for pseudo-first order reaction rate

$[PS]_0 \text{ mM}$	$[Fe^{2+}]_0 \text{ mM}$	$T \text{ }^\circ\text{C}$	$k_{obs} \text{ min}^{-1}$	pH_i/pH_f
25	25	60	$1.4 (\pm 0.1) \times 10^{-2}$	1.17/1.08
50	50		$4.5 (\pm 0.2) \times 10^{-2}$	0.85/0.78
75	75		$1.16 (\pm 0.05) \times 10^{-1}$	0.67/0.60
100	100		$1.65 (\pm 0.09) \times 10^{-1}$	0.58/0.48

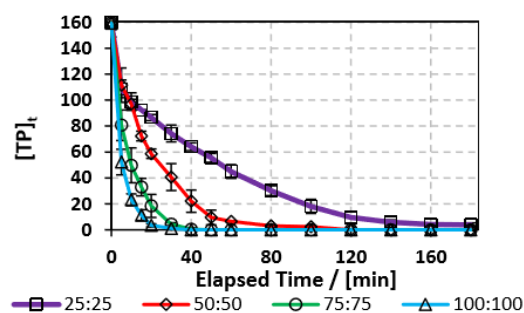


Fig. 8. Degradation of TP by TCAP in a real pharmaceutical effluent having $[TP]_0 = 160 \text{ mg L}^{-1}$. Experimental conditions: $[PS]_0 = 25, 50, 75$ and 100 mM , $[PS]_0:[Fe^{2+}]_0$ ratio of 1:1, and $T = 60 \text{ }^\circ\text{C}$. Error bars are calculated as $\frac{ts}{\sqrt{n}}$, where absent bars fall within the symbols.

$$\text{Total system cost } (\$ \text{ m}^{-3}) = \text{Electrical Energy Cost} + \text{Reagent Cost} \quad (15)$$

Electric energy per order (E_{EO}) defined as the electric energy required to degrade contaminants by one order of magnitude, for instance from 10 mg L^{-1} to 1 mg L^{-1} , in one cubic meter of contaminated water or air, was calculated using Eq. 16 for a batch system⁵⁸.

$$E_{EO} = \frac{P \times t \times 1000}{V \times \log(C_i/C_f)} \quad (16)$$

Where P is the power supplied to the system in kW, t is the duration of the treatment in hour, V is the volume treated in L, C_i and C_f are the initial and final concentrations respectively, and 1000 is a conversion factor from L to m^3 . Thus, E_{EO} is obtained in $\text{kWh m}^{-3} \text{ order}^{-1}$. Additionally, Eq. 16 is simplified by substituting the first-order reaction rate Eq. 17 in Eq. 16 and changing unit of time. Thus, the following simplification is done (Eqs. 16-19).

$$\log \frac{C_i}{C_f} = 0.4343 \times k_{\text{obs}} \times t \quad (17)$$

$$E_{\text{EO}} = \frac{P \times t \times 1000}{V \times 0.4343 \times k_{\text{obs}} \times t \times 60} \quad (18)$$

$$E_{\text{EO}} = \frac{38.4 \times P}{V \times k_{\text{obs}}} \quad (19)$$

The resulting simplified Eq. 19 shows P in kW, V in L, and k_{obs} in min^{-1} .⁵⁸ Power is calculated based on the energy and time needed to heat the reactors. The energy required for this heating is calculated using Eq. 20, where Q is the energy in J, m is the mass of water in g (200 g), C is the specific heat capacity of water (4.186 J/g°C), and ΔT (35°C) is the temperature difference for heating from 25 to 60°C. Q was found to be 29.3 kJ.

$$Q = m C \Delta T \quad (20)$$

Power was calculated utilizing Eq. 21, where t is the time in seconds needed to heat the solution to the desired temperature. Experimentally, it took 12 min to heat up the 200 mL reactor from room temperature to 60°C. Thus, P = 0.122 kW.

$$P = \frac{Q}{t} \quad (21)$$

The E_{EO} is calculated for each of the four different $[\text{PS}]_0$ and presented in Table 8. The electrical energy cost is estimated utilizing electricity cost rates in Lebanon, with Electricité du Liban (EDL) average rate of 255 LBP/kWh equivalent to 0.169 \$/kWh at the current conversion rate^{59,60}, as well as in the US, where the average electricity cost rate for the industrial sector is 0.0709 \$/kWh. Cost of reagents is calculated using wholesale prices for every case (Table S1). The total system cost can thus be obtained (Eq. 15) and is presented in details in Fig. 9. It is observed that as $[\text{PS}]_0$ increases, reagent cost increases, while electric cost, due to heating, decreases. Consequently, the choice of $[\text{PS}]_0$ for the treatment of the factory effluent can be based on the estimated total cost where the case of $[\text{PS}]_0 = 50$ mM gave the lowest total cost of 56.8 and 73.8 \$ m^{-3} based on electricity prices in the US and in Lebanon, respectively (Fig. 9, Table 8). Amasha et al. obtained a total cost of 44.414 \$ m^{-3} upon degradation of ketoprofen (KTP) in TAP system, with $[\text{KTP}]_0 = 7.87 \mu\text{M}$ (2.00 mg L^{-1}), $[\text{PS}]_0 = 1$ mM and $T = 60^\circ\text{C}$.³⁴ The lower total cost obtained by the mentioned study can be attributed to the fact that no Fe^{2+} was used, and thus lower reagent price, in addition to the fact that degradation was done in DI and not in a factory effluent where in the latter competitive reactions take place between $\text{SO}_4^{\bullet-}$ and excipients present (Section 3.7.1).

3.8. Suggested degradation pathway

Theoretical study of degradation pathway utilizing frontier orbitals and charge distribution was conducted. Frontier molecular orbital (FMO) theory shows that electrophilic reactions are more likely to occur at atoms with higher values of the highest occupied molecular orbital (HOMO) while nucleophilic reactions are prone to occur for atoms with higher values of the lowest unoccupied molecular orbital (LUMO).⁶¹ Consequently, several studies suggest that atoms with a higher $2\text{FED}_{\text{HOMO}}^2$ are more easily oxidized, and those with a higher

$\text{FED}_{\text{HOMO}}^2 + \text{FED}_{\text{LUMO}}^2$ are more susceptible to addition reactions^{62–64}. The $2\text{FED}_{\text{HOMO}}^2$, $2\text{FED}_{\text{LUMO}}^2$, and Mulliken charge distribution were calculated for TP and are presented along with the atom numbering and the isodensity surfaces of FMO in Fig. 10 and Table 9. For TP, 1C showed highest $2\text{FED}_{\text{HOMO}}^2$, followed by 9N, 8O, 2C, 19C, 3C and 7O. So, attack of oxidants is expected to occur readily on 1C, 9N and 8O. Also, 3C showed highest $\text{FED}_{\text{HOMO}}^2 + \text{FED}_{\text{LUMO}}^2$, followed by 19C, 1C, 9N, 2C, 7O and 4N. Thus, addition reactions will mostly take place at 1C, 19C and 3C; however, it is noted that 19C is the least sterically hindered of the three atoms, thus, addition reactions are expected to occur more readily at 19C as the formation of hydroxylated products at this site. It is known that HO^\bullet performs H abstraction, and $\text{SO}_4^{\bullet-}$ acts selectively as an electron transfer reactant⁶⁵. According to Mulliken charge distributions obtained, electron is mostly abstracted from 7O and 8O, as they show the most negative charges (Table 9).

LC/MS/MS was used to identify by-products of TP degradation. Fig. 8S shows two identified by-products termed BP1 (molecular weight 126.12 g mol^{-1}) and BP2 (molecular weight 156.14 g mol^{-1}). The extracted ion chromatograms of BP1 and BP2 showed the intensity of their peaks constantly increasing with time which proves that these by-products are formed throughout the degradation reaction (Fig. 8S). It is noted that the intensity of BP1 is higher, which suggests that it is more prevalent than BP2.

Fig. 11 presents the suggested degradation pathway, based on results obtained from theoretical study and LC/MS/MS results. Electron abstraction is expected on the oxygen group (8O, Fig. 10) by $\text{SO}_4^{\bullet-}$. Attack of $\text{SO}_4^{\bullet-}$ and HO^\bullet are expected on the 6-membered ring where ring opening occurs with formation of carboxylic group. This is followed by loss of CO_2 and demethylation on 5N and 9N sites. As a result, BP1 is obtained.

Demethylation is initiated by hydrogen abstraction at 10C and 14C which is followed by HO^\bullet attack. BP2 is formed through demethylation and saturation of double bonds. Ultimately, mineralization is expected, which was obtained in similar AOP studies^{66,67}.

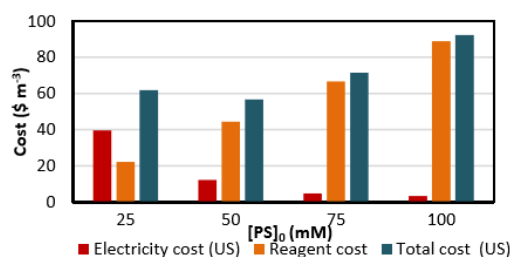


Fig. 9. Treatment cost of a pharmaceutical effluent contaminated by TP using a TCAP system. The electricity, reagent and total cost are presented (based on US electricity cost). Experimental conditions: $[\text{TP}]_0 = 160$ mg L^{-1} , $[\text{PS}]_0 = 25 - 100$ mM, $[\text{PS}]_0 : [\text{Fe}^{2+}]_0$ ratio of 1:1 and $T = 60^\circ\text{C}$.

Table 8

Treatment cost of a pharmaceutical effluent contaminated by TP using a TCAP system. Calculation of total system cost for different TP degradation conditions in pharmaceutical effluent based on electricity price rates in the US and in Lebanon is presented. Experimental conditions: $[TP]_0 = 160 \text{ mg L}^{-1}$, $[PS]_0 = 25, 50, 75 \text{ and } 100 \text{ mM}$, $[PS]_0:[Fe^{2+}]_0$ ratio of 1:1, and $T = 60^\circ\text{C}$.

$[PS]_0 \text{ mM}$	$k_{obs} \text{ min}^{-1}$	EEO $\text{kWh m}^{-3} \text{ order}^{-1}$	Electricity cost (US) $\$ \text{ m}^{-3} \text{ order}^{-1}$	Electricity cost (Lebanon) $\$ \text{ m}^{-3} \text{ order}^{-1}$	Reagent cost $\$ \text{ m}^{-3}$	Total cost (US) $\$ \text{ m}^{-3}$	Total cost (Lebanon) $\$ \text{ m}^{-3}$
25	$1.4 (\pm 0.1) \times 10^{-2}$	558	39.6	94.4	22.2	61.8	116.6
50	$4.5 (\pm 0.2) \times 10^{-2}$	174	12.3	29.4	44.5	56.8	73.8
75	$1.16 (\pm 0.05) \times 10^{-1}$	67.4	4.8	11.4	66.7	71.5	78.1
100	$1.65 (\pm 0.09) \times 10^{-1}$	47.4	3.4	8.0	88.9	92.3	96.9

Check Table 15

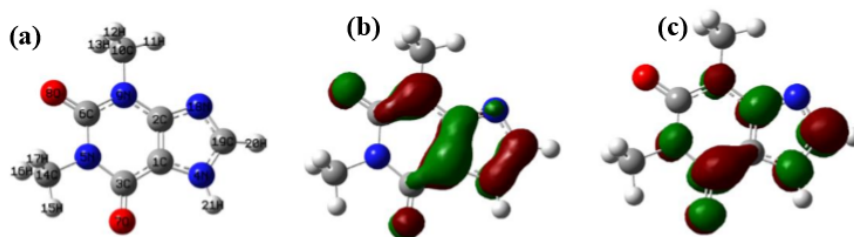


Fig. 10. (a) TP atomic labeling and numbering. Isodensity surfaces of (b) HOMO and (c) LUMO with isovalues of 0.05.

Table 9

The computed values of FEDs for HOMO and LUMO in addition to Mulliken charge distribution.

Atom	$FED_{HOMO}^2 + FED_{LUMO}^2$	$2FED_{HOMO}^2$	$2FED_{LUMO}^2$	Mulliken charge
1C	0.27	0.45	0.08	0.35
2C	0.23	0.19	0.27	0.11
3C	0.38	0.17	0.58	0.25
4N	0.17	0.13	0.21	-0.21
5N	0.05	0.01	0.10	-0.25
6C	0.02	0.04	0.01	0.56
7O	0.18	0.17	0.19	-0.66
8O	0.10	0.20	0.00	-0.67
9N	0.25	0.38	0.11	-0.26
10C	0.01	0.01	0.01	-0.21
11H	0.00	0.00	0.00	0.14
12H	0.01	0.02	0.00	0.14
13H	0.01	0.02	0.00	0.14
14C	0.00	0.00	0.00	-0.15
15H	0.00	0.00	0.00	0.15
16H	0.01	0.00	0.02	0.14
17H	0.01	0.00	0.02	0.14
18N	0.01	0.01	0.01	-0.47
19C	0.28	0.19	0.36	0.29
20H	0.00	0.00	0.00	0.23
21H	0.00	0.00	0.00	0.25
22H	-	-	-	-

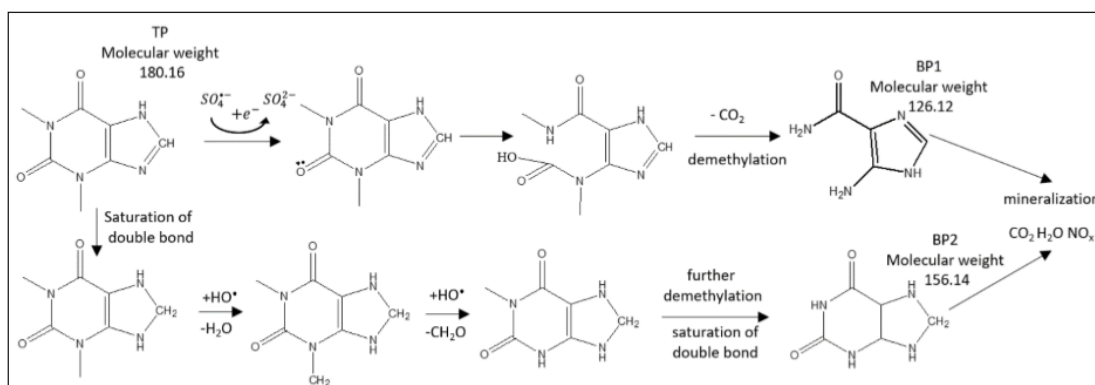


Fig. 11. Suggested TP degradation pathway by $SO_4^{\bullet-}$ and HO^{\bullet} . Two detected by-products BP1 and BP2 are included.

Conclusions

In this study TP degradation was tested in systems of TAP, CAP and TCAP. TAP resulted in incomplete (60%) TP degradation at $t = 60$ min for $[PS]_0 = 5$ mM and $T = 60^\circ\text{C}$. CAP system was not effective at room temperature, where a maximum of 5% TP degradation was observed at $t = 60$ min for $[PS]_0 = [Fe^{2+}]_0 = 0.25$ mM. To gain better efficiency, the two methods of PS activation were combined in a TCAP system which resulted in complete TP degradation at $T = 60^\circ\text{C}$ and for $[PS]_0 = [Fe^{2+}]_0 = 2$ mM. The reaction followed pseudo-first order reaction rate with $k_{obs} = 5.6 (\pm 0.4) 10^{-2} \text{ min}^{-1}$. The effect of $[PS]_0/[Fe^{2+}]_0$ ratio, $[PS]_0$ and temperature were tested, where a 1:1 ratio gave optimum results, and degradation rate increased with increasing $[PS]_0$ and temperature. Salinity caused inhibition in the degradation process while nitrates slightly enhanced the process. The presence of HAs caused inhibition in TP degradation. TP was dissolved in real water samples of spring, sea and waste water which showed lower degradation rate in comparison with DI water medium. A real factory effluent containing TP was obtained and showed total degradation of $[TP]_0 = 160 \text{ mg L}^{-1}$ within 180 and 40 min for $[PS]_0 = [Fe^{2+}]_0 = 25$ and 100 mM, respectively. The degradation cost was estimated to $53.0 \text{ \$ m}^{-3}$, for electricity price rates in the US, at $[PS]_0 = [Fe^{2+}]_0 = 50$ mM. A degradation mechanism involving in-situ evolved reactive oxidative species, mainly sulfate and hydroxyl radicals, was also suggested based on LC/MS/MS HRAM analyses supported by Frontier molecular orbital (FMO) theory calculation.

Conflicts of interest

There are no conflicts to declare.

Acknowledgements

This research was funded in part by the Lebanese National Council for Scientific Research (Award Number 103250), the K.

Shair CRSL fund (Award Number 103599), and the University Research Board (Award Number 103603) of the American University of Beirut and USAID-Lebanon through The National Academy of Sciences under PEER project 5-18 (Award number 103262). The author is thankful to Prof. Faraj Hasanayn for his kind assistance in obtaining the theoretical study data. Additionally, the author is thankful to Eng. Joan Younes, senior technician Simon Al-Ghawi and the glass blower at the chemistry department Boutros Sawaya for their technical assistance and the personnel of the K. Shair CRSL for their kind help.

References

- 1 I. American Society of Health-System Pharmacists, Theophylline, <https://medlineplus.gov/druginfo/meds/a681006.html>.
- 2 C. A. Shively and S. M. Tarka, *Prog. Clin. Biol. Res.*, 1984, **158**, 149–178.
- 3 K. Noguera-Oviedo and D. S. Aga, *J. Hazard. Mater.*, 2016, **316**, 242–251.
- 4 A. Wennmalm and S. C. Council, in *Encyclopedia of Environmental Health*, 2011, pp. 462–471.
- 5 A. Zenker, M. R. Cicero, F. Prestinaci, P. Bottoni and M. Carere, *J. Environ. Manage.*, 2014.
- 6 T. U. Berendonk, C. M. Manaia, C. Merlin, D. Fatta-Kassinos, E. Cytryn, F. Walsh, H. Bürgmann, H. Sørum, M. Norström, M. N. Pons, N. Kreuzinger, P. Huovinen, S. Stefani, T. Schwartz, V. Kisand, F. Baquero and J. L. Martinez, *Nat. Rev. Microbiol.*, 2015.
- 7 O. A. Jones, J. N. Lester and N. Voulvoulis, *Trends Biotechnol.*, 2005.
- 8 T. Heberer, *Toxicol. Lett.*, 2002, **131**, 5–17.
- 9 M. E. Rybak, M. R. Sternberg, C.-I. Pao, N. Ahluwalia and C. M. Pfeiffer, *J. Nutr.*, 2015, **145**, 766–774.
- 10 P. Rajasulochana and V. Preethy, *Resour. Technol.*, 2016, **2**, 175–184.
- 11 Y. Luo, W. Guo, H. H. Ngo, L. D. Nghiem, F. I. Hai, J. Zhang, S. Liang and X. C. Wang, *Sci. Total Environ.*, 2014, 473–474, 619–641.

Journal Name

ARTICLE

- 12 Y. Yang, Y. S. Ok, K.-H. Kim, E. E. Kwon and Y. F. Tsang, *Sci. Total Environ.*, 2017, **596–597**, 303–320.
- 13 S. A. Snyder, in *Ozone: Science and Engineering*, 2008, vol. 30, pp. 65–69.
- 14 J. DOUMMAR, K. NÖDLER, T. GEYER and M. SAUTER, *Assessment and Analysis of Micropollutants (2010–2011)*, .
- 15 S. Sun, J. Jiang, S. Pang, J. Ma, M. Xue, J. Li, Y. Liu and Y. Yuan, *Sep. Purif. Technol.*, 2018, **201**, 283–290.
- 16 R. Liang, S. Luo, F. Jing, L. Shen, N. Qin and L. Wu, *Appl. Catal. B Environ.*, 2015, **176–177**, 240–248.
- 17 M. M. Sunil Paul, U. K. Aravind, G. Pramod, A. Saha and C. T. Aravindakumar, *Org. Biomol. Chem.*, 2014, **12**, 5611–5620.
- 18 I. Kim, N. Yamashita and H. Tanaka, *Chemosphere*, 2009, **77**, 518–525.
- 19 R. Liang, A. Hu, W. Li and Y. N. Zhou, *J. Nanoparticle Res.*, 2013, **15**, 1990.
- 20 N. S. Shah, A. D. Rizwan, J. A. Khan, M. Sayed, Z. U. H. Khan, B. Murtaza, J. Iqbal, S. U. Din, M. Imran, M. Nadeem, A. H. Al-Muhtaseb, N. Muhammad, H. M. Khan, M. Ghauri and G. Zaman, *Process Saf. Environ. Prot.*, 2018, **117**, 473–482.
- 21 F. Ali, J. A. Khan, N. S. Shah, M. Sayed and H. M. Khan, *Process Saf. Environ. Prot.*, , DOI:10.1016/j.psep.2018.05.004.
- 22 A. Ghauch, A. Baalbaki, M. Amasha, R. El Asmar, O. Tantawi, R. El Asmar and O. Tantawi, *Chem. Eng. J.*, 2017, **317**, 1012–1025.
- 23 M. Amasha, A. Baalbaki, S. Al Hakim, R. El Asmar and A. Ghauch, *J. Adv. Oxid. Technol.*, 21, 261–273.
- 24 S. Naim and A. Ghauch, *Chem. Eng. J.*, , DOI:10.1016/j.cej.2015.11.101.
- 25 A. Ghauch, G. Ayoub and S. Naim, *Chem. Eng. J.*, , DOI:10.1016/j.cej.2013.05.045.
- 26 A. Ghauch, A. M. Tuqan and N. Kibbi, *Chem. Eng. J.*, 2015, **279**, 861–873.
- 27 A. Ghauch, A. M. Tuqan, N. Kibbi and S. Geryes, *Chem. Eng. J.*, 2012, **213**, 259–271.
- 28 A. Ghauch, A. M. Tuqan and N. Kibbi, *Chem. Eng. J.*, 2012, **197**, 483–492.
- 29 A. Ghauch and A. M. Tuqan, *Chem. Eng. J.*, , DOI:10.1016/j.cej.2011.12.048.
- 30 A. Fernandes, P. Makoś and G. Boczkaj, *J. Clean. Prod.*, 2018, **195**, 374–384.
- 31 Y. Gao, N. Gao, Y. Deng, Y. Yang and Y. Ma, *Chem. Eng. J.*, 2012, **195**, 248–253.
- 32 L. Bu, S. Zhou, Z. Shi, L. Deng, G. Li, Q. Yi and N. Gao, *Environ. Sci. Pollut. Res.*, 2016, **23**, 2848–2855.
- 33 C. Tan, N. Gao, S. Zhou, Y. Xiao and Z. Zhuang, *Chem. Eng. J.*, , DOI:10.1016/j.cej.2014.05.013.
- 34 M. Amasha, A. Baalbaki and A. Ghauch, *Chem. Eng. J.*, 2018, **350**, 395–410.
- 35 G. Mark, M. N. Schuchmann, H. P. Schuchmann and C. von Sonntag, *J. Photochem. Photobiol. A Chem.*, , DOI:10.1016/1010-6030(90)80028-V.
- 36 M. J. Frisch, G. W. Trucks, H. B. Schlegel, G. E. Scuseria, M. A. Robb, J. R. Cheeseman, G. Scalmani, V. Barone, B. Mennucci, G. A. Petersson, H. Nakatsuji, M. Caricato, X. Li, H. P. Hratchian, A. F. Izmaylov, J. Bloino, G. Zheng, J. L. Sonnenberg, M. Hada, M. Ehara, K. Toyota, R. Fukuda, J. Hasegawa, M. Ishida, T. Nakajima, Y. Honda, O. Kitao, H. Nakai, T. Vreven, J. A. Montgomery Jr., J. E. Peralta, F. Ogliaro, M. Bearpark, J. J. Heyd, E. Brothers, K. N. Kudin, V. N. Staroverov, R. Kobayashi, J. Normand, K. Raghavachari, A. Rendell, J. C. Burant, S. S. Iyengar, J. Tomasi, M. Cossi, N. Rega, J. M. Millam, M. Klene, J. E. Knox, J. B. Cross, V. Bakken, C. Adamo, J. Jaramillo, R. Gomperts, R. E. Stratmann, O. Yazyev, A. J. Austin, R. Cammi, C. Pomelli, J. W. Ochterski, R. L. Martin, K. Morokuma, V. G. Zakrzewski, G. A. Voth, P. Salvador, J. J. Dannenberg, S. Dapprich, A. D. Daniels, Ö. Farkas, J. B. Foresman, J. V. Ortiz, J. Cioslowski and D. J. Fox, *Gaussian, Inc., Wallingford CT*, 2013.
- 37 C. Lee, W. Yang and R. G. Parr, *Phys. Rev. B*, 1988, **37**, 785–789.
- 38 A. D. Becke, *Phys. Rev. A*, 1988, **38**, 3098–3100.
- 39 S. Y. Oh, H. W. Kim, J. M. Park, H. S. Park and C. Yoon, *J. Hazard. Mater.*, 2009, **168**, 346–351.
- 40 I. M. Kolthoff, A. I. Medalia and H. P. Raaen, *J. Am. Chem. Soc.*, 1951, **73**, 1733–1739.
- 41 L. W. Matzek and K. E. Carter, *Chemosphere*, 2016, **151**, 178–188.
- 42 W. Shang, Z. Dong, M. Li, X. Song, M. Zhang, C. Jiang and S. Feiyun, *Chem. Eng. J.*, 2019, **361**, 1333–1344.
- 43 I. Hussain, Y. Zhang and S. Huang, *RSC Adv.*, , DOI:10.1039/c3ra43364a.
- 44 D. Wu, X. Li, J. Zhang, W. Chen, P. Lu, Y. Tang and L. Li, *Sep. Purif. Technol.*, , DOI:10.1016/j.seppur.2018.06.059.
- 45 M. Nie, C. Yan, X. Xiong, X. Wen, X. Yang, Z. Lv and W. Dong, *Chem. Eng. J.*, 2018, **348**, 455–463.
- 46 H. A. Gorrell, *Am. Assoc. Pet. Geol. Bull.*, 1958, **42**, 2513.
- 47 Environment Protection Authority (EPA) in South Australia, Salinity, http://www.epa.sa.gov.au/environmental_info/water_quality/threats/salinity, (accessed 15 June 2017).
- 48 D. A. Armstronga, R. E. Huie, S. Lyman, W. H. Koppenol, G. Merényi, P. Neta, D. M. Stanbury, S. Steenken and P. Wardman, *Bioinorg. React. Mech.*, , DOI:10.1515/irm-2013-0005.
- 49 C. Liang, Z.-S. Wang and N. Mohanty, *Sci. Total Environ.*, 2006, **370**, 271–277.
- 50 K., Hasegawa, P. and Neta, *J. Phys. Chem.*, 1978, **82**, 854–857.
- 51 Y. Fan, Y. Ji, D. Kong, J. Lu and Q. Zhou, *J. Hazard. Mater.*, , DOI:10.1016/j.jhazmat.2015.06.058.
- 52 S. Norzaee, M. Taghavi, B. Djahed and F. K. Mostafapour, *J. Environ. Manage.*, 2018, **215**, 316–323.
- 53 S. Wang, J. Wu, X. Lu, W. Xu, Q. Gong, J. Ding, B. Dan and P. Xie, *Chem. Eng. J.*, 2019, **358**, 1091–1100.
- 54 D. Keeney and R. A. Olson, *Crit. Rev. Environ. Control*, 1986, **16**, 257–304.
- 55 S. J. Boggs, D. Livermore and M. G. Seitz, *Humic substances in natural waters and their complexation with trace metals and radionuclides: a review. [129 references]*, 1985.
- 56 L. Liu, S. Lin, W. Zhang, U. Farooq, G. Shen and S. Hu, *Chem. Eng. J.*, , DOI:10.1016/j.cej.2018.04.068.

ARTICLE

Journal Name

- 57 M. D. Paciolla, S. Kolla and S. A. Jansen, *Adv. Environ. Res.*, , DOI:10.1016/S1093-0191(01)00129-0.
- 58 J. R. Bolton, K. G. Bircher, W. Tumas and C. A. Tolman, *Pure Appl. Chem.*, , DOI:10.1351/pac200173040627.
- 59 F. Fardoun, O. Ibrahim, R. Younes and H. Louahlia-Gualous, *Energy Procedia*, 2012, **19**, 310–320.
- 60 XE Currency Converter: LBP to USD, <https://www.xe.com/currencyconverter/convert/?Amount=225&From=LBP&To=USD>, (accessed 16 December 2018).
- 61 K. Fukui, T. Yonezawa and H. Shingu, *J. Chem. Phys.*, , DOI:10.1063/1.1700523.
- 62 H. Yang, S. Zhou, H. Liu, W. Yan, L. Yang and B. Yi, *J. Environ. Sci. (China)*, , DOI:10.1016/S1001-0742(12)60217-4.
- 63 D. Miao, J. Peng, X. Zhou, L. Qian, M. Wang, L. Zhai and S. Gao, *Chemosphere*, 2018, **207**, 174–182.
- 64 H. Liu, P. Sun, M. Feng, H. Liu, S. Yang, L. Wang and Z. Wang, *Appl. Catal. B Environ.*, , DOI:10.1016/j.apcatb.2016.01.036.
- 65 E. Lipczynska-Kochany, G. Sprah and S. Harms, *Chemosphere*, 1995, **30**, 9–20.
- 66 J. M. Monteagudo, A. Durán, J. Latorre and A. J. Expósito, *J. Hazard. Mater.*, 2016, **306**, 77–86.
- 67 X. Xu, G. Pliego, J. A. Zazo, J. A. Casas and J. J. Rodriguez, *J. Hazard. Mater.*, 2016, **318**, 355–362.

- S1 -

Chemically and thermally activated persulfate for theophylline degradation and application to a pharmaceutical factory effluent

Suha Al Hakim, Abbas Baalbaki, Omar Tantawi and Antoine Ghauch*

American University of Beirut, Faculty of Arts and Sciences, Department of Chemistry

P.O. Box 11-0236 Riad El Solh – 1107-2020 Beirut – Lebanon

**Corresponding author. Tel/fax: +961 1350000/+961 1 365217 Email address: antoine.ghauch@aub.edu.lb*

Prepared for RSC

July 2019

Electronic supplementary information

9 Pages, 3 Texts, 8 Figures, 2 Tables

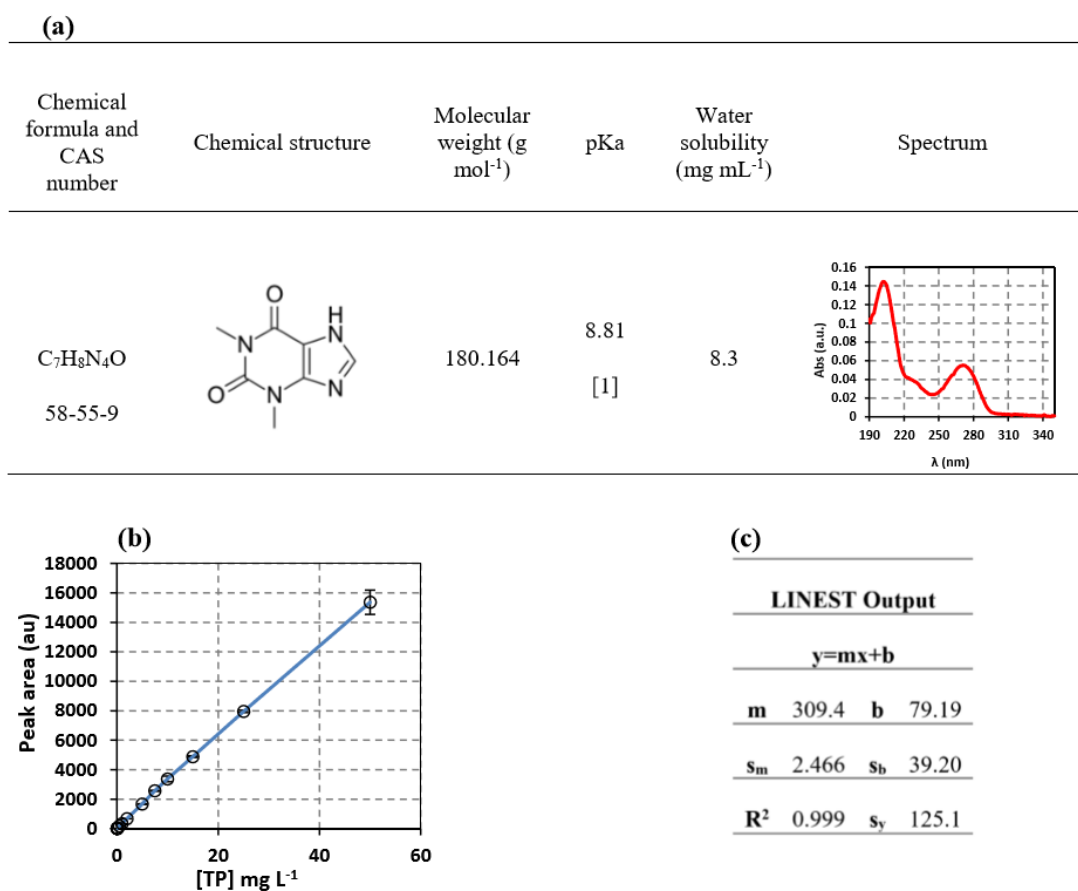


Fig. 1S. (a) Table showing selected TP chemical and physical properties. (b) Calibration curve of TP obtained using HPLC/DAD instrument at a wavelength of 270 nm, over a linear dynamic range of 0.02-50 mg L⁻¹ with a detection limit = 0.0176 mg L⁻¹ and quantification limit = 0.0586 mg L⁻¹. (c) LINEST output for TP calibration curve.

Text S1

Theophylline calibration curve

Selected TP physical properties are summarized in Fig. 1S (a). Calibration curve obtained for TP at a wavelength of 270 nm is presented in Fig. 1S(b). High linearity ($R^2 = 0.999$) is obtained over a linear dynamic range of 0.02-50 mg L⁻¹ with a detection limit = 0.0176 mg L⁻¹ and quantification limit = 0.0586 mg L⁻¹. Error bars for calibration curve are calculated as

- S3 -

$A = A_{average} \pm \frac{ts}{\sqrt{n}}$, where n is the number of replicates, t is student value for 95% confidence ($t = 4.303$ for 2 degrees of freedom) and s is the standard deviation of the three replicates tested.

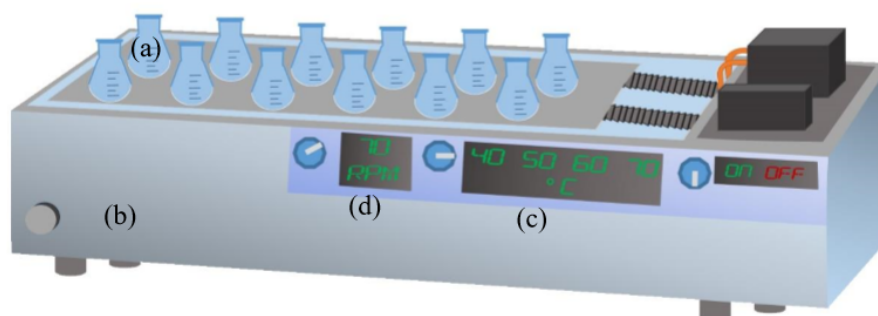


Fig. 2S. Experimental setup showing (a) reactors in (b) water bath equipped with (c) temperature control, and (d) automatic shaker. Temperature is displayed in °C and shaker in revolutions per minute (RPM).

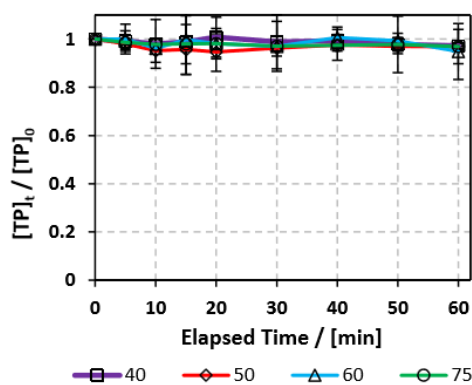


Fig. 3S. Stability of TP under heat stress. Experimental conditions: $[TP]_0 = 10 \text{ mg L}^{-1}$, Temperature = 40, 50, 60 and 75°C.

- S4 -

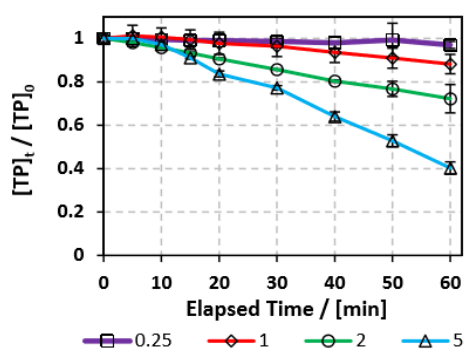


Fig. 4S. Effect of $[PS]_0$ on TP degradation in TAP systems. Experimental conditions: $[TP]_0 = 10 \text{ mg L}^{-1}$, $[PS]_0 = 0.25\text{-}5 \text{ mM}$ and $T = 55 - 75^\circ\text{C}$. Error bars are calculated as $\frac{ts}{\sqrt{n}}$, where absent bars fall within the symbols.

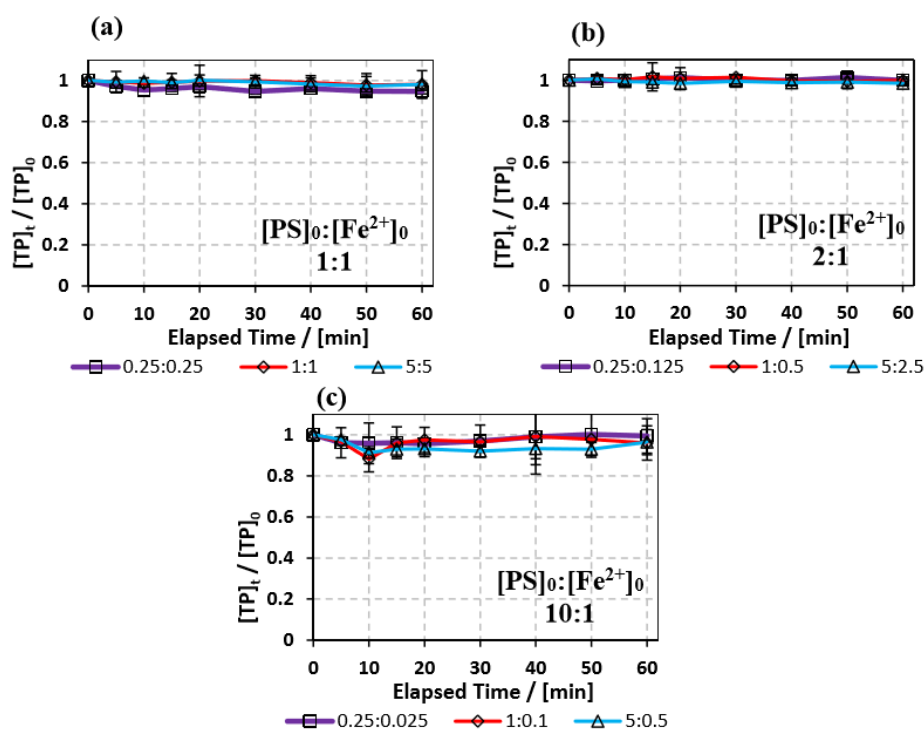


Fig. 5S. Effect of $[PS]_0:[Fe^{2+}]_0$ ratio on TP degradation in CAP system. Experimental conditions: $[TP]_0 = 10 \text{ mg L}^{-1}$, $[PS]_0 = 0.25, 1 \text{ and } 5 \text{ mM}$, $T = 20^\circ\text{C}$, and $[PS]_0:[Fe^{2+}]_0$ ratio is (a) 1:1 (b) 2:1 and (c) 10:1. Error bars are calculated as $\frac{ts}{\sqrt{n}}$, where absent bars fall within the symbols.

Text S2**Kinetics study in TAP system**

Kinetics study was done in TAP system, for $T = 55\text{-}60^\circ\text{C}$, $[\text{PS}]_0 = 0.25\text{-}5\text{ mM}$ and $[\text{TP}]_0 = 10\text{ mg L}^{-1}$. Eq. (1) presents the pseudo-first order rate equation, with k_{obs} representing the pseudo-first-order rate constant (min^{-1}), and t representing time (min). Table S1 shows the calculated observed rate constant (k_{obs}) for the different conditions, with the corresponding linearity constant for each plot of $\ln \frac{[\text{TP}]}{[\text{TP}_0]}$ versus time. The high linearity frequently obtained proves that the reaction follows a pseudo-first order rate. Pseudo-first order kinetics is frequently considered for degradation reactions of organic contaminants by activated PS [2–6].

Table 1S.

TP degradation in TAP system at $T = 55\text{-}60^\circ\text{C}$, $[\text{PS}]_0 = 0.25\text{-}5\text{ mM}$ and $[\text{TP}]_0 = 10\text{ mg L}^{-1}$ for all studied cases. k_{obs} is calculated for pseudo-first order reaction rate and the corresponding linearity constant (R^2) and reaction half-life ($t_{1/2}$) are presented.

$[\text{TP}]_0$ mg L^{-1}	T $^\circ\text{C}$	$[\text{PS}]_0$ mM	k_{obs} min^{-1}	R^2	$t_{1/2}$ min		
10	55	2	$2.63 (\pm 0.04) \times 10^{-3}$	0.998	263		
		0.25	$3.8 (\pm 0.1) \times 10^{-4}$	0.680	17×10^2		
	60	1	$2.2 (\pm 0.1) \times 10^{-3}$	0.959	30×10^1		
		2	$5.52 (\pm 0.08) \times 10^{-3}$	0.998	125		
	65	5	1.5	$1.5 (\pm 0.1) \times 10^{-2}$	0.956	46	
			2	$1.43 (\pm 0.05) \times 10^{-2}$	0.988	48.2	
		70	2	4.6	$4.6 (\pm 0.5) \times 10^{-2}$	0.928	15
				5.3	$5.3 (\pm 0.7) \times 10^{-2}$	0.918	13

$$\ln \frac{[\text{TP}]}{[\text{TP}_0]} = -k_{\text{obs}}t \quad (1)$$

Text S3

Kinetics study in TCAP system

Kinetics study was done in TCAP system at $[PS]_0 = 0.25 - 5$ mM, $[PS]_0:[Fe^{2+}]_0$ ratio of 1:1, and $T = 60^\circ\text{C}$. Eq. (1) presenting the pseudo-first order rate was fitted. Fig 3b shows the calculated observed rate constant (k_{obs}) for the different $[PS]_0$, with the corresponding linearity constant for each plot of $\ln \frac{[TP]}{[TP]_0}$ versus time. The high linearity frequently obtained proves that the reaction follows a pseudo-first order rate.

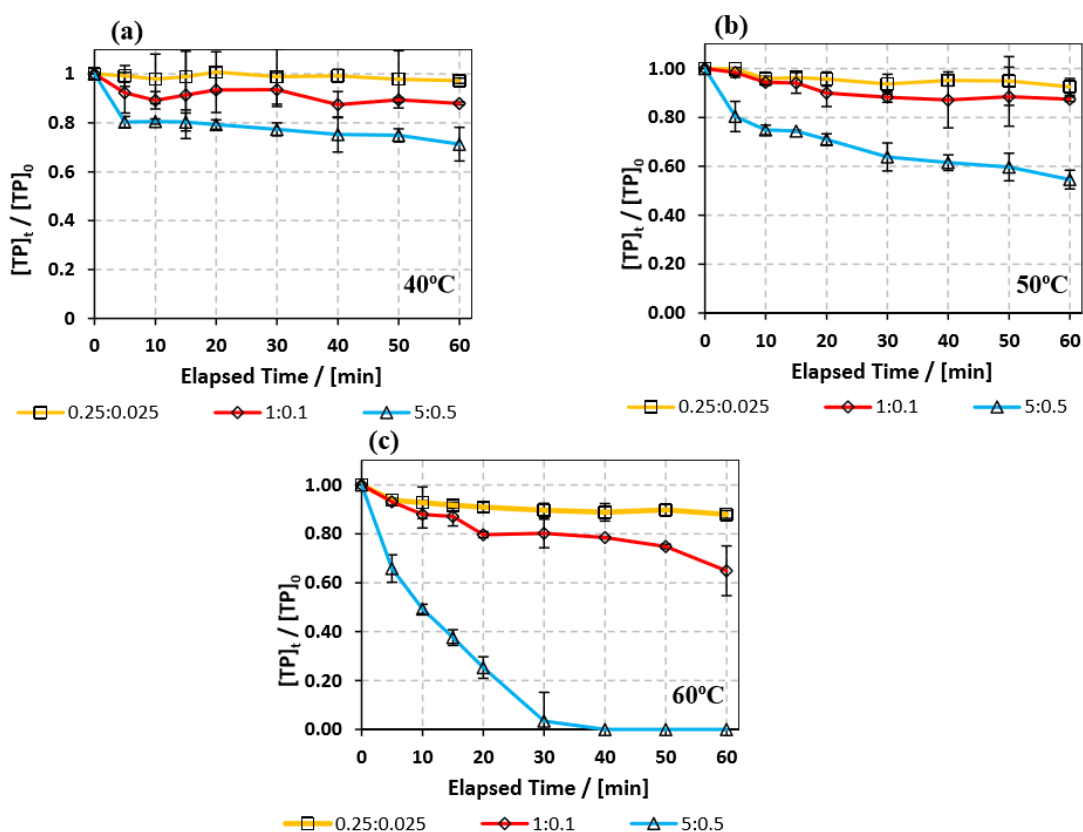


Fig. 6S. Effect of temperature on the degradation of TP in TCAP system. Experimental conditions: $[TP]_0 = 10$ mg L⁻¹, $[PS]_0 = 0.25, 1$ and 5 mM, $[PS]_0:[Fe^{2+}]_0$ ratio is 10:1, and temperature is (a) 40°C (b) 50°C and (c) 60°C. Error bars are calculated as $\frac{ts}{\sqrt{n}}$, where absent bars fall within the symbols.

- S7 -

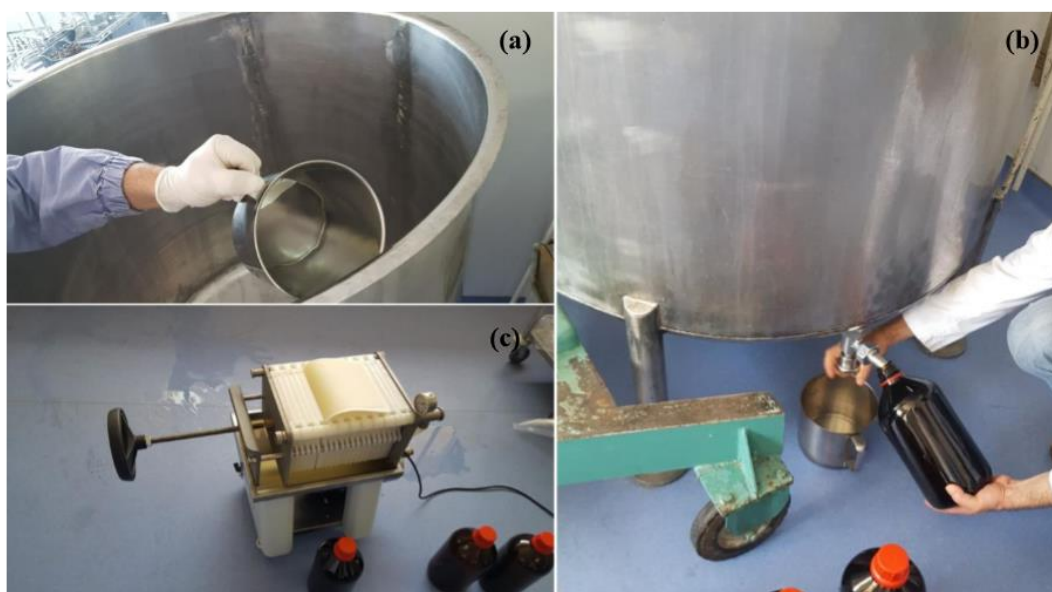


Fig. 7S. Collecting pharmaceutical water effluent. (a) Washing of the 1000 L 316 SS L mixing container, (b) water collected from the container, and (c) the filter press used in the manufacturing process.

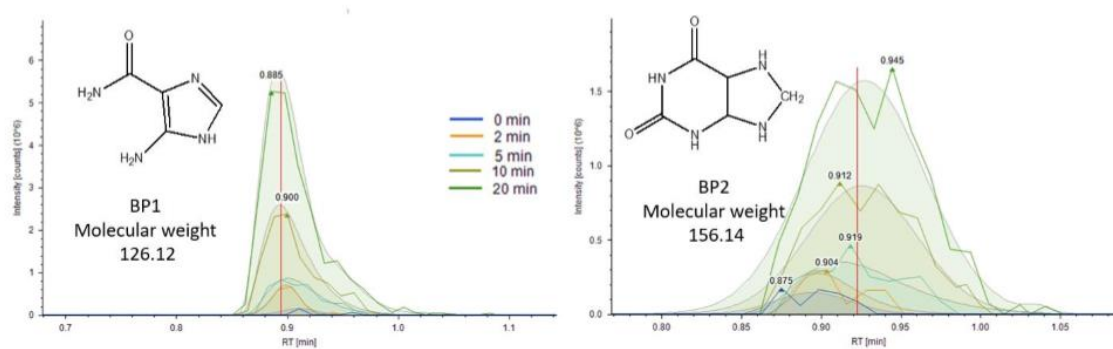


Fig. 8S. Extracted chromatograms of two by-products detected by LC/MS/MS. Intensity of peaks is displayed at reaction time 0 – 20 min.

Table 2S.

Masses and prices of reagents used based on commercial prices where 1 kg of PS costs 2 US \$^a, 1 Kg of FeCl₂.4H₂O costs 1.7 US \$^b, and 1 L of HCl (37%), used to dissolve the iron salt, costs 0.3 US \$^c.

[PS] ₀ mM	25	50	75	100
[Fe ²⁺] ₀ mM	25	50	75	100
Reactor volume L	0.2	0.2	0.2	0.2
n PS mol	0.005	0.01	0.015	0.02
n Fe mol	0.005	0.01	0.015	0.02
m Na ₂ S ₂ O ₈ g	1.19	2.38	3.57	4.76
m FeCl ₂ .4H ₂ O g	0.994	1.99	2.98	3.98
v HCl (37%) mL	1.25	2.50	3.75	5.00
Total cost \$ reactor ⁻¹	0.00445	0.00889	0.0133	0.0178
Total cost \$ m ⁻³	22.2	44.5	66.7	88.9

^a Based on price obtained from Jinan Shijitongda Chemical Co., Ltd.

^b Based on price obtained from Gemhold (SJZ) Trading Co., Ltd.

^c Based on price obtained from Hangzhou Focus Corporation.

References

- [1] Dissociation constants of organic acids in aqueous solution, *Pure Appl. Chem.* 1 (1960) 187. doi:10.1351/pac196001020187.
- [2] C. Qi, X. Liu, C. Lin, X. Zhang, J. Ma, H. Tan, W. Ye, Degradation of sulfamethoxazole by microwave-activated persulfate: Kinetics, mechanism and acute toxicity, *Chem. Eng. J.* 249 (2014) 6–14. doi:https://doi.org/10.1016/j.cej.2014.03.086.
- [3] X. Lu, Y. Shao, N. Gao, J. Chen, Y. Zhang, H. Xiang, Y. Guo, Degradation of diclofenac by UV-activated persulfate process: Kinetic studies, degradation pathways and toxicity assessments, *Ecotoxicol. Environ. Saf.* 141 (2017) 139–147. doi:https://doi.org/10.1016/j.ecoenv.2017.03.022.
- [4] S. Dhaka, R. Kumar, M.A. Khan, K.-J. Paeng, M.B. Kurade, S.-J. Kim, B.-H. Jeon, Aqueous phase degradation of methyl paraben using UV-activated persulfate method, *Chem. Eng. J.* 321 (2017) 11–19. doi:https://doi.org/10.1016/j.cej.2017.03.085.
- [5] C. Tan, N. Gao, S. Zhou, Y. Xiao, Z. Zhuang, Kinetic study of acetaminophen degradation by UV-based advanced oxidation processes, *Chem. Eng. J.* (2014). doi:10.1016/j.cej.2014.05.013.
- [6] L. Zhao, H. Hou, A. Fujii, M. Hosomi, F. Li, Degradation of 1,4-dioxane in water with heat and Fe²⁺ activated persulfate oxidation, *Environ. Sci. Pollut. Res.* 21 (2014) 7457–7465. doi:10.1007/s11356-014-2668-3.

CHAPTER IV CONCLUSION

This work demonstrated the applicability of a UV₂₅₄/PS system and a Fe²⁺/heat/PS system for TP degradation in a simulated and a real pharmaceutical factory effluent.

TP UV₂₅₄/PS lab scale batch system allowed total [TP]₀ = 10 mg L⁻¹ degradation within 20 min for [PS]₀ = 0.25 mM. The effect of different experimental parameters on the degradation process was studied.

Both heat/PS and Fe²⁺/PS systems tested separately showed low to negligible efficiency. Accordingly, they were combined into Fe²⁺/heat/PS system. The combined system allowed total [TP]₀ = 10 mg L⁻¹ degradation within 60 min for [PS]₀ = [Fe²⁺]₀ = 2 mM and T = 60°C.

In the UV₂₅₄/PS, the degradation process was hindered in acidic and basic media, while neutral pH showed improved degradation rate. However, the Fe²⁺/heat/PS system performed best at acidic pH, while increasing pH greatly hindered TP degradation.

Pseudo-first order reaction kinetics was observed in the two tested systems. Also, in both systems, degradation was hindered in natural water media, with waste water causing the major hindrance. Chloride presence had negligible effect on UV₂₅₄/PS system, while it had an inhibiting effect in Fe²⁺/heat/PS system. For treating a pharmaceutical factory effluent, total TP degradation in the former system occurred within 180 min and for the latter within 120 min.

This study demonstrated the importance of treating pharmaceutical factory effluents independently before mixing them with natural water matrices. Also, this work has reported the applicability of the UV₂₅₄/PS and Fe²⁺/heat/PS systems in degrading TP in a highly concentrated pharmaceutical effluent mixture in a batch system.

The UV₂₅₄/PS system compared to Fe²⁺/heat/PS system, was of lower cost in treating a highly concentrated pharmaceutical effluent. Additionally, the effectivity of the UV₂₅₄/PS system was better than the latter system in media of neutral pH and high chloride content. Thus, in general, the UV₂₅₄/PS system was shown to be superior over the Fe²⁺/heat/PS system.

This opens the way towards testing the studied AOP methods in a continuous system. Furthermore, the results of this study could be used to develop a plan for the treatment of pharmaceutical factory effluents in Lebanon.

Currently, Metal-Organic Frameworks (MOFs) are being studied in our laboratory, without or with UV light, as activators for PS and/or hydrogen peroxide oxidants as a novel AOP method, which showed so far promising results.